PREDICTABILITY AND ATTRIBUTION OF THE SOUTH AFRICAN SEASONAL CLIMATE

Report to the
Water Research Commission
on a Project entitled *The Limits of Predictability of the South African Seasonal Climate*

by

Kamoru Lawal, Piotr Wolski, Chris Lennard, Mark Tadross, Babatunde Abiodun
Department of Environmental and Geographical Sciences, University of Cape Town, Rondebosch, South Africa

Oliver Angélil
Institute for Atmospheric and Climate Science, Eidgenössische Technische Hochschule Zürich, Zurich, Switzerland

Ruth Cerezo Mota
Ciencias Atmosféricas, Universidad Veracruzana, Veracruz, Mexico and
Department of Environmental and Geographical Sciences, University of Cape Town, Rondebosch, South Africa

Dáithí Stone
Lawrence Berkeley National Laboratory, Berkeley, California, U.S.A. and
Department of Environmental and Geographical Sciences, University of Cape Town, Rondebosch, South Africa

WRC Report No 2067/1/15
ISBN 978-1-4312-0633-9

April 2015

Obtainable from
Water Research Commission
Private Bag X03
GEZINA, 0031

orders@wrc.org.za or download from www.wrc.org.za

EXECUTIVE SUMMARY

This report details various accomplishments and findings of the project entitled "The Limits of Predictability of the South African Seasonal Climate" funded by the South African Water Research Commission from 2010 to 2014. The project has two main goals concerning South African seasonal climate: to characterize the degree to which the predictability of seasonal forecasts varies from year to year, and to identify causes of such variations; and to characterize the degree to which anthropogenic greenhouse gas emissions have altered the chance of extreme months. In addition, the project includes a case study extending the predictability and attribution methods to a hydrological case study: the stream flow discharge into the Okavango Delta, Botswana.

The first part of this project examines the degree to which seasonal predictability, and thus the confidence in our forecasts, may be inherently changing through time. Seasonal forecasts are probabilitistic in nature, consisting of a range of plausible outcomes. While the skill of seasonal forecasts in estimating the resultant real-world realization of seasonal weather has been, and continues to be, extensively investigated, not much attention has been given to whether the range of forecast plausible outcomes varies with time, and whether knowledge of that uncertainty would be a useful addition to seasonal forecast products. This project has three aims with regard to characterizing the potential for information content in variations in the forecast range of seasonal outcomes. [Sections 1 and 3]

To determine the limits of the predictability of the South African seasonal climate state and how these limits depend on the season and on the ocean and land surface forcing

Most analyses in this project addressing this aim use a unique climate model resource, the weather@home/SAF project, which included a large number of "hindcast" (like forecasts but with perfect knowledge of the boundary conditions) simulations covering the 1960-2009 period, using a similar modeling system to that used by the operational seasonal forecast service issued by the University of Cape Town. The ranges of simulations exhibit a strong east-west gradient in the case of precipitation, and a strong coastal-inland gradient in the case of temperature. Interannual variations in the spread of the simulations are larger than expected purely by chance given the number of simulations. While the occurrence of El Niño and La Niña events in the tropical Pacific (known to strongly influence South African climate) are linked to variations in the spread of the simulations, robust relationships are not found for other areas of the ocean that are also considered to strongly influence South African climate. While some suggestions of interannual variations in the spread of forecasts of stream flow in a major hydrological system, the Okavango River, are found, the evidence for a relationship is not conclusive. [Sections 2, 4, 5, and 8]

To estimate the contribution of anthropogenic emissions to forecast predictability

The spread of model simulations shows long-term narrowing and widening trends for both monthly rainfall and temperature, with the nature of the trends varying as a function of location and season. A narrowing of the width of precipitation spread occurs over inland

provinces from late austral spring to summer. Trends in temperature spread exhibit narrowing tendencies along the coasts from spring to early summer. These long-term trends are larger than expected due to sampling considerations, and in some cases amount to an appreciable fraction of the average spread of the simulations. While a formal analysis linking the trends to anthropogenic emissions is not conducted, anthropogenic emissions are the major long-term driver of climate change, especially for temperature, and thus the narrowing and widening trends indicate the potential that anthropogenic emissions are substantially altering the nature of South African seasonal forecasts. [Section 4]

To characterise the relevance of the limits of predictability in the operational forecast setting
The analyses of the variations in the spread of the simulations described above indicate some potential for added-value in the addition of a measure of confidence to seasonal forecast products. The variations in simulation spread found in this project are reflected in variations in model forecast skill, indicating that the variations in simulation spread do indeed reflect real-world variations in seasonal predictability. Furthermore, some long-term trends in spread amounted to a substantial fraction of the averaged simulation spread. However, how effectively such a measure of confidence can be implemented depends strongly on how seasonal forecasts are presented. When described as an anomaly with respect to some baseline climatology, skill and confidence in the forecast may be increasing through time as a result of anthropogenic climate change, a somewhat artificial apparent increase in confidence that may overwhelm any real increases along the lines of those studied in this project. [Sections 4, 5, 8, 9]

The second part of this project examines the degree to which anthropogenic emissions may be altering the chance of unusual monthly events. As the climate warms in response to anthropogenic emissions, many of the largest impacts are expected to be manifest through changes in the frequency and intensity of extreme weather events. There has been much attention in the media over the question of whether anthropogenic emissions are "to blame" for specific recent damaging weather events, and the question of liability may be emerging as a major component of a "loss and damage" mechanism for distributing international climate change adaptation funding. This project has one aims with regard to characterizing the relation between anthropogenic emissions and extreme weather. [Sections 1, 6, 7, and 8]

To estimate the attribution of the risk of extreme weather events to anthropogenic emissions
The project included further development of the Weather Risk Attribution Forecast (WRAF) service, a regular monthly assessment of the degree to which anthropogenic greenhouse gas emissions have altered the chance of weather events around the world (frequently termed "event attribution"). Using simulations generated through the WRAF system, it is found that event attribution estimates are neither sensitive to the choice of climate model used, nor to downscaling methods when examining the chance of flooding events in a hydrological system. According to the analyses in this project, anthropogenic greenhouse gas emissions have at least doubled the chance of unusually hot months over South Africa during all times of the year, and similarly at least halved the chance of cold months. Changes in the chance of

unusual rainfall events are less strong, but there does appear to be at least a decrease in the chance of unusually wet months during the onset and cessation of the wet season, with a concomitant increase in the chance of dry events. Despite recent tendencies toward higher floods in the Okavango Delta, analyses in this report indicate that anthropogenic emissions have decreased the chance of higher floods as a result of increased evaporation in a warmer climate. [Sections 6, 7, 8]

Part of this project comprised the Ph.D. research of K. Lawal at the University of Cape Town (UCT). Analysis of simulations generated under this project was also carried out by O. Angélil, a South African, as part of his M.Sc. studies at ETH Zurich, Switzerland. Finally, output from simulations from this project have been published online through the data portal of the International CLIVAR C20C+ Detection and Attribution Project (C20C+ D&A; accessible at http://esg.nersc.gov; project "c20c") and were distributed by USB stick to 22 African researchers in October 2013. [Section 10]

Work is nearly complete on setting up a new version of the UCT seasonal forecast using a more realistic modeling setup and using a much larger number of simulations. The larger number of simulations, in particular, is a necessary condition for adding confidence guidance into the forecast product. Nevertheless, the forecast system still does not include dynamical interaction between the atmosphere and ocean: thus whether the ocean dynamics themselves exhibit variations in predictability is something that has not yet been examined with respect to the South African seasonal climate. While the results of this project indicate the potential for added information content with the addition of confidence guidance on seasonal forecasts, the potential for effective implementation in an operational seasonal forecast depends strongly on the framework used for communicating the forecasts, as noted above. The larger number of simulations, in particular, is a necessary condition for adding confidence guidance into the forecast product. Further investigation of how confidence guidance can potentially fit within different communication strategies would thus be the next obvious step. [Section 9]

The attribution component of this project served as a trial experiment for the World Climate Research Programme's International CLIVAR C20C+ Detection and Attribution Project, both in terms of developing a template and for testing various aspects of the planned experimental protocols. Lessons from this trial experiment are being applied in the fulfillment of the C20C+ D&A Project's core experiment, now underway; the University of Cape Town is contributing to that core experiment with simulations now underway, which will be published on the C20C+ D&A data portal. Lessons for development and operation of the Weather Risk Attribution Forecast, a globally unique product, are similarly informing development of comparable services in the U.K. and U.S.A. [Section 9]

The event attribution capacity now existing at the University of Cape Town, with extensions to hydrological impacts, is especially relevant given recent concern that Africa should be developing an attribution capacity to inform climate change adaptation funding mechanisms. Facilitation of further development of African capacity for attribution analysis, such as the

workshop and fellowship programme being planned with the African Center of Meteorological Application for Development (ACMAD) and other institutions outside Africa, could thus form a major development in availability of scientific information supporting climate change adaptation activities. [Section 9]

ACKNOWLEDGEMENTS

A number of people and institutions external to this project have provided useful and, in some cases, crucial contributions. The project team is grateful for their roles.

- Thousands of volunteers from around the world ran the weather@home/SAF simulations on their home computers. The output from theses simulations formed a unique data set analysed under this project.
- The University of Oxford operates the climateprediction.net facility under which the weather@home/SAF simulations were performed.
- Pennsylvania State University hosted the data server to which results of the weather@home/SAF simulations were uploaded.
- Lawrence Berkeley National Laboratory paid for D. Stone's involvement in the project starting in October 2011.
- Michael Wehner and Lawrence Berkeley National Laboratory contributed simulations of the CAM5.1-2degree climate model which following the same experimental design as the UCT simulations generated under this project, thus providing the opportunity to examine the sensitivity of results to the selection of climate model.
- The National Energy Research Scientific Computing Center, U.S.A., is providing data portal services for the International CLIVAR C20C+ Detection and Attribution Project, including for simulations produced under this deliverable.
- The University of Botswana partially supported the Okavango Basin study through employment of P. Wolski until December 2011.
- Travel funding for attendance of conferences and workshops was received from:
  - Japan Agency for Marine-Earth Science and Technology (JAMSTEC)
  - Applied Center for Climate and Earth Systems Science (ACCESS)
  - South African Department of Science and Technology
  - World Climate Research Programme
  - Organisers of the "Attribution of Climate and Weather Extremes: Assessing, Anticipating and Communicating Climate Risks" workshop in Oxford, United Kingdom

Finally, this project would not have been possible without funding from the South African Water Research Commission and the guidance and assistance of Dr. Willem Landman and Prof. Geoff Pegram. The project team is sincerely grateful for these contributions.

REFERENCE GROUP (STEERING COMMITTEE)

Mr MC Moseki	:	Water Research Commission (Chairman)
Dr DA Stone	:	Lawrence Berkeley Laboratory (Project Leader)
Prof BC Hewitson	:	University of Cape Town
Prof G Pegram	:	Pegram and Associates
Dr BJ Abiodun	:	University of Cape Town
Dr WA Landman	:	CSIR
Mr KA Lawal	:	University of Cape Town
Dr C Lennard	:	University of Cape Town
Dr JD Daron	:	University of Cape Town
Mr N Kroese	:	South African Weather Services
Mr Z Maswuma	:	
Mrs S Barnard	:	University of Cape Town (Committee Secretary)

TABLE OF CONTENTS

LIST OF TABLES

LIST OF FIGURES

LIST OF ABBREVIATIONS AND ACRONYMS USED IN THIS STUDY

AAO	AntArctic Oscillation
ACCESS	Applied Center for Climate and Earth Systems Science
ACMAD	African Center of Meteorological Application for Development
C20C	Climate of the 20th Century
CAM	Community Atmospheric Model
CLIVAR	Climate Variability and Prediction (Predictability)
CORDEX	Coordinated Regional Downscaling Experiment
CSAG	Climate Systems Analysis Group
CSIR	Council for Scientific and Industrial Research
D&A	Detection and Attribution Project
DJF	Austral Summer (December-January-February)
ECP	Eastern Cape Province
ENSO	El Nino-Southern Oscillation
ERA-INTERIM	ECMWF (European Centre for Medium-Range Weather Forecasts) Re-Analysis
ETH	Swiss Federal Institute of Technology, Zurich, Switzerland
FADR	Fraction of Attributable Risk
FAR	Fraction of Decrease in Attributable Risk
FSP	Free State Province
GGP	Gauteng Province
GHG	Greenhouse gases
GPCC	Global Precipitation Climatology Centre
HadAM3P	Hadley Atmospheric Model version 3p
HadRM3P	Hadley Regional Model version 3p
IOD	Indian Ocean Dipole
JAMSTEC	Japan Agency for Marine-Earth Science and Technology
JJA	Austral Winter (June-July-August)
KZP	KwaZulu-Natal Province
LBNL	Lawrence Berkeley National Laboratory, California, Los Angelis
LMP	Limpopo Province
MAM	Austral Autumn (March-April-May)
MEI	Multivariate ENSO Index
MLP	Mpumalanga Province
NCEP	National Centers for Environmental Predictions
NCP	Northern Cape Province
NERSC	National Energy Research Scientific Computing Center, U.S.A.
NOAA	National Oceanic and Atmospheric Administration
NWP	North West Province
PET	Potential Evapotranspiration
PRECIS	A U. K. Met Office Hadley Centre's regional climate modeling system (pronounced as in the French précis – "PRAY-sea").
RoP	Range of Possibility

SAF	Southern Africa
SON	Austral Spring (September-October-November)
SST	Sea Surface Temperature
StdDev	Standard deviation
TRMM	Tropical Rainfall Measuring Mission
TSA	Tropical Southern Atlantic
UCLA	University of California, Los Angelis
UCT	University of Cape Town, Cape Town, South Africa
U. K.	United Kingdom
U. S. A.	United States of America
USB	Universal Serial Bus
WCP	Western Cape Province
WCRP	World Climate Research Programme
WRAF	Weather Risk Attribution Forecast
WRC	Water Research Commission (South African)

1 Introduction

1.1 Motivation

The prospect of future improvement in seasonal forecasting underpins much of the development in frameworks for managing water resources. Yet against that prospect, recent progress in forecasting the seasonal climate state has been incremental at best. In this light, there is an urgent need to determine how predictable the seasonal climate state is over South Africa, given the knowledge of the ocean state, land surface state, and atmospheric composition that provide the conditions for predictions. The summer wet season, accompanied with a strong El Niño event, is considered the case with the highest predictability for a seasonal forecast, but beyond this little is known about the dependence of predictability as a function of the external conditions. Is there any predictability in seasons of weak hemispheric forcing anomalies, for instance? Some skill in forecasting seasonal temperature and temperature-derivatives derives from the fact we are in a changing climate, with a reference during a cooler period making a “warmer than normal” forecast increasingly likely to be accurate. How does the contribution from this long-term trend compare to those from year-to-year variability in the ocean and land state? It is imperative that these fundamental questions be addressed in order to confidently move forward with management activities which depend on seasonal forecasting.

This report presents results of a first examination of how South African seasonal predictability varies from year-to-year and why it does so. It also examines the degree to which anthropogenic emissions may have altered the chance of extreme weather events, with implications on increasing predictability of the chance of these events under a changing climate. This is a climate-model-based study, using a variety of novel climate model data products tailored for attacking the aims of the project (Figure 1.1). Overall, the project has four main aims as listed in Table 1.1.

1.2 Theoretical basis

Forecasts of the seasonal climate state depend on three factors: the state of the ocean surface, the state of the land surface, and the chemical composition of the atmosphere. The atmosphere evolves rapidly from any given initial state, so information on the physical state of the atmosphere provides no discernible impact on a forecast months in advance. The ocean and land surface, on the other hand, vary more slowly, so their state can be reliably forecast months into the future. The influence of the slowly varying anomalies in the state of the ocean and land surface on the atmosphere thus provides the principle underlying seasonal forecasting. However, the atmosphere still provides plenty of "noise" on top of any predictable signal. Understanding of the fundamental limit this imposes on the predictability of seasonal forecasts for South Africa remains weak.

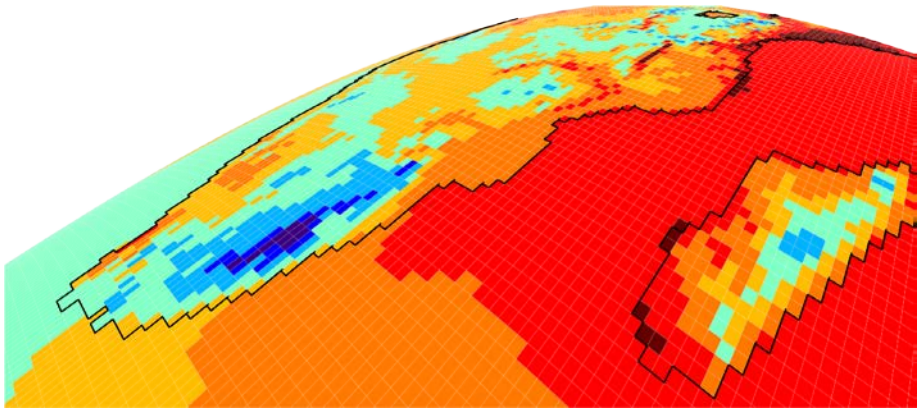

Figure 1.1 A snapshot of surface air temperature from a simulation of the HadRM3P-50km atmospheric model analyzed in this project (Section 2.2). The regional HadRM3P-50km regional atmospheric model was run at a spatial resolution of 50 km, embedded within a global atmospheric model running at 150 km resolution. Using thousands of home computers volunteered by people around the globe, this modeling pair was run for tens of thousands of years' worth of simulations.

Table 1.1 List of project aims

Number	Description	Sections
1	To determine the limits of the predictability of the South African seasonal climate state and how these limits depend on the season and on the ocean and land surface forcing	3, 4, 5, 8
2	To estimate the contribution of anthropogenic emissions to forecast predictability	4
3	To estimate the attribution of the risk of extreme weather events to anthropogenic emissions	7, 8
4	To characterize the relevance of the limits of predictability in the operational forecast setting	4, 5, 8, 9

Beyond this, the atmosphere is a highly nonlinear dynamical system. This complicates our understanding of the predictability of the seasonal forecast – the degree to which an accurate prediction is possible.

The predictability is undoubtedly itself also a function of the ocean and land surface states. For example, in conditions with weak anomalous surface forcing, there may be little scope for an accurate prediction, whereas in conditions with strong forcing, such as an El Niño event, the atmospheric state may be highly constrained. There remains little understanding of how predictability varies as a function of the surface state, other than the existence of a

relatively higher predictability in summer wet seasons during El Niño events in the tropical Pacific. Thus, at the moment it is unknown whether management strategies should require the flexibility to focus on strong preparatory measures during some seasons and forecast conditions but more open, responsive measures during other cases.

Seasonal forecasts are frequently expressed as anomalies from a historical reference, both due to climate model limitations and user relevance. In a changing climate, however, that historical reference may be biased and thus may be providing "artificial" (yet relevant and useful) skill. In particular, forecasts of warmer-than-normal seasons are more frequent these days than forecasts for cooler-than-normal seasons, because "normal" is defined with relevance to a cooler past climate (Liniger et al., 2007). It is currently unknown how much changes in atmospheric composition, such as increasing greenhouse gas concentrations, are contributing to the predictability of seasonal forecasts for South Africa. This contribution is highly relevant, though, in understanding the potential usefulness of seasonal forecasting. First, if predictability is a strong function of atmospheric composition, then the future accuracy and relevance of seasonal forecasting will depend explicitly on international activities to reduce emissions of greenhouse gas and various aerosol precursors. Second, it provides a connection between forecasting and longer term climate change. This is highly relevant in Africa, where adaptation in the near-future is the priority climate change issue. In particular, the ability to tap international funding mechanisms for climate change adaptation activities will likely depend in part on there being a demonstrable impact on current climate risks (Huggel et al., 2013). Current climate risk is generally estimated through seasonal forecasting, but as yet there has been little study of the climate change contribution through the seasonal forecasting framework.

1.3 Outline

This report starts by describing the various climate model data sets used in the first part of this project examining the limits of predictability of seasonal forecasts (Section 2). It then contains three chapters dealing specifically with whether predictability varies from year-to-year over South Africa and why this is the case. Section 3 comprises a discussion of the theory behind predictability and presents the two measures of predictability, based on the spread of a large ensemble of climate model simulations that will be used in the analysis report in the following two sections. Analyses of long-term trends in these two predictability measures are presented in Section 4, with analyses of relationships between various large-scale global climate indices and year-to-year variations in predictability over South Africa presented in Section 5.

The report switches to the second part of the project with Section 6, investigating the degree to which anthropogenic emissions have altered the chance of unusual weather events. The climate model data used in this analysis, some generated as part of this project and some obtained from other institutions, is described in Section 6. Section 7 comprises analyses of how anthropogenic emissions have altered the chance of extreme monthly weather events over South Africa and elsewhere, including application of such analyses in an operational

setting.

Section 8 presents a case study which combines the predictability and attribution analyses in a hydrological setting, specifically stream flow into the Okavango Delta. Further discussions of possible implications of the results of this project are discussed in Section 9, while lists of project outputs are included in Section 10.

2 Climate model simulations for predictability analysis

2.1 Objectives for simulations in this project

This project required climate model simulations for analysis. Requirement for these simulations varied, and thus the simulations used were a combination of some generated at UCT as part of this project as well as simulations received from other institutions. These various simulations are described in this section and in Section 6. This section describes the simulations used in the analyses of the limits of predictability reported in the first part of the report, while Section 6 describes the simulations used in the attribution analyses reported in the second part of the report. The various sets of simulations, along with their special properties relevant for analyses in this project, are listed in Table 2.1. The simulations, for the limits of predictability analysis, reported in this section are also discussed in Lawal et al. (2014a, b) and Cerezo-Mota et al. ("Impacts of land-scheme and integration domains on African precipitation", in preparation).

2.2 Experimental design of the weather@home/SAF simulations

The primary data source indicated in the proposal for this project was an unprecedentedly large number of simulations run using the weather@home/SAF effort (http://weatherathome.org) through the climateprediction.net facility. The project generating these simulations was in collaboration between UCT, the University of Oxford, the U.K. Met Office Hadley Centre, and Pennsylvania State University, performed under a separate funding source.

This project involved running the HadAM3P-N96 global atmospheric model, simulating weather around the globe at approximately 150km resolution. The HadRM3P regional model, simulating regional weather, was run in parallel to the global model, receiving input from the global model along its regional boundaries and simulating the regional weather at approximately 50km resolution (Jones et al., 2004). The regional domain covered the southern half of the African continent (Figures 1.1 and 2.1), but in this project we only analyzed data over South Africa.

The novel aspect of the weather@home/SAF project was that it used distributed computing to produce unprecedentedly large numbers of simulations. In particular, thousands of volunteers around the world ran the model in the background on their home desktop computers, quite probably including some from South Africa (Figure 2.2 and Table 2.2). Volunteers downloaded the model and simulation parameters, ran the model for one year of model time, and uploaded results to a central results server.

One year of simulation typically took one week on current desktops given their normal workload. A subsequent simulation on another computer may have started from the final weather state of the original simulation, meaning that it is possible to assemble sequences of one-year simulation segments into a multi-year simulation. Given this, the strategy was chosen to start sequences every five years, starting with December 1964 (U.K. Met Office

models have an odd preference for starting in December), in order to economize with first-year "spin-ups".

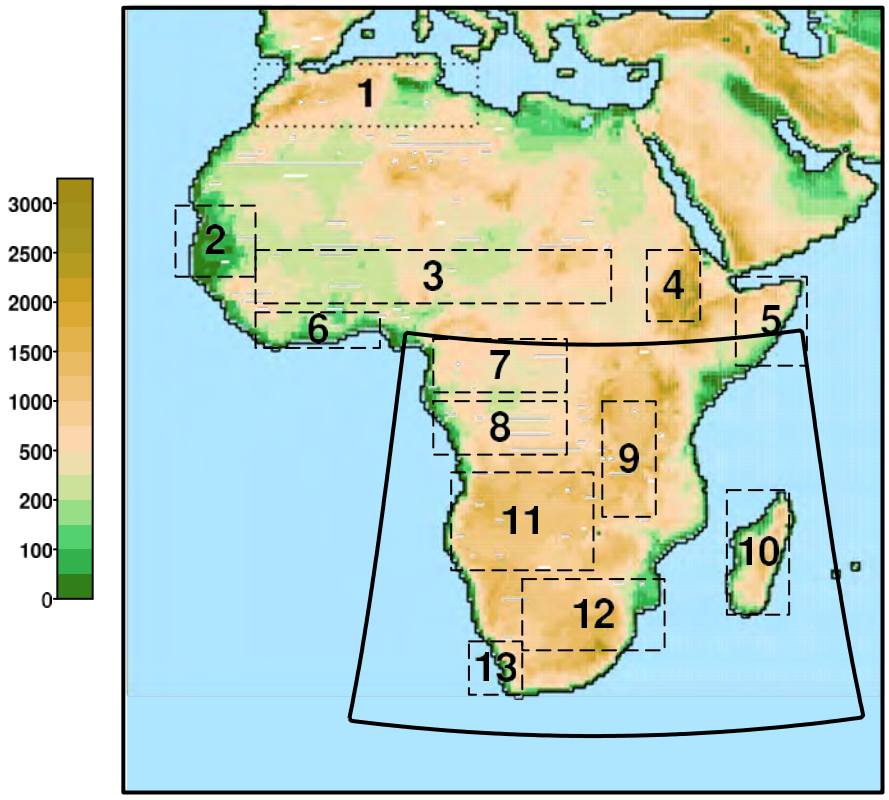

Figure 2.1 The spatial domain covered by the HadRM3P-50km regional model, denoted by the box covering Africa south of 10°N. The full map indicates the CORDEX-Africa spatial domain used by the benchmark simulations. The dotted rectangles denote diagnostic regions, some of which are used in Section 2.5.

The operation of the simulation-sequence feature was not as smooth as anticipated, and so while earlier years in each 5-year sequence were well sampled (~1000), later simulations in the sequences were less so (minimum 30) (Figure 2.3). Following discovery of faulty aerosol forcing in the post-1999 simulations, a new batch of post-1999 simulation were conducted with higher priority and an every-year sampling strategy, producing a jump in numbers post-1999. Not all simulations counted in this figure were included in the analyses in this project. In particular:

- Careful examination revealed that a small number of simulations had returned months with corrupt data. These simulations were removed.
- Simulations were only retained if they had results for all twelve months.

Table 2.1 List of the various sets of model simulations used in this project, whether generated as part of the project or received from other institutions. The sections of this report in which results of analyses of the simulations are reported are also indicated.

Institution	Model	Property	Section
Lawrence Berkeley National Laboratory (LBNL)	CAM5.1-2degree	Large ensembles; multiple decades; includes shorter simulations for a natural historical world; same experimental design as UCT-CSAG/HadAM3P -N96 simulations	6, 7, 8
University of Cape Town (UCT-CSAG)	HadAM3P-N96	Large ensembles; multiple decades; includes shorter simulations for a natural historical world; same experimental design as LBNL/CAM5.1-2degree simulations; updated monthly	6, 7, 8
University of Cape Town (UCT-CSAG)	HadRM3P-50km	Same experimental design as weather@home/SAF simulations; large number of output variables	2.4, 2.5
weather@home/SAF (University of Oxford, University of Cape Town, U.K. Met Office, Pennsylvania State University, public volunteers)	HadAM3P-N96/ HadRM3P-50km	Very large ensembles; multiple decades; high spatial resolution	2.2, 2.3, 3.3, 4, 5

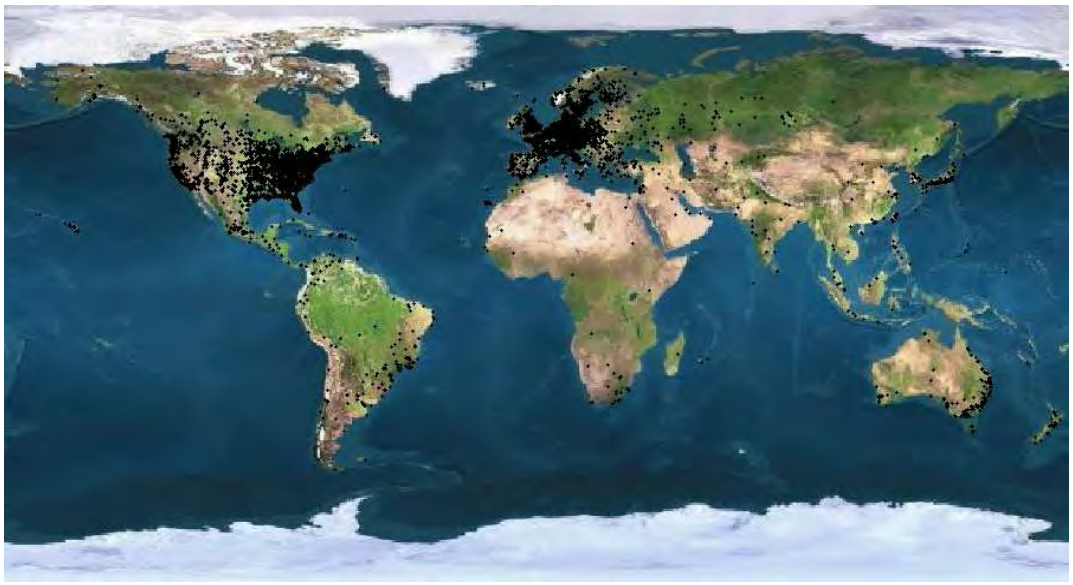

Figure 2.2 Map showing locations of the 96 457 volunteers in 138 countries around the world running climateprediction.net on their home computers, as of 7 March 2012. Separate statistics are not available, but a large fraction of these volunteers were running weather@home/SAF simulations.

Table 2.2 List of volunteers in southern African countries running climateprediction.net on their home computers, as of 7 March 2012. Separate statistics are not available, but a large fraction of these volunteers were probably running weather@home/SAF simulations.

Country	Volunteers
Earth (138 countries)	96 457
Angola	2
Botswana	5
Kenya	2
Madagascar	1
Mauritius	3
Namibia	6
South Africa	433

- To help increase the probability of completion of a given simulation-year, continuation simulations were sent out multiple times. This often meant that two copies of the simulation-year were completed with results returned to the central results server. Sometimes these two copies differ in results because of differences in computer hardware or software, but they could also have ended up being identical. Rather than trawl through all these multiple realizations to search for duplicates, we simply retained one of the realizations.

2.3 Characteristics of output of the weather@home/SAF simulations

The annual mean precipitation values for each province from these simulations are shown in Figures 2.4 and 2.5. While the number of simulations differs between years, the data is clearly sufficient for revealing certain features. Most relevant, the locations of the spread of simulations shift between drier and wetter states. This represents predictability in the annual totals based on boundary condition information, mostly from variations in sea surface temperatures.

Thus according to this modeling system sea surface conditions were strongly favorable for a wet 1995 in all provinces except the Western Cape, for example. The spread of the simulations then represents the unpredictable component of the variability, and this spread also varies from year to year. Further analysis of the spread of these simulations is reported in Sections 4 and 5.

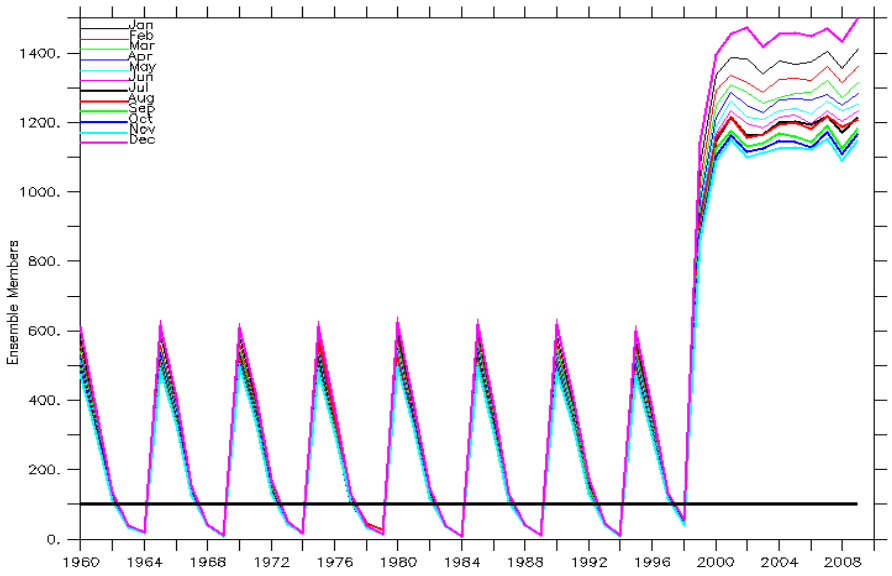

Figure 2.3 The number of weather@home/SAF simulations with results recorded on the central results server for each month in the 1960-2009 periods. Time series are shown separately for each calendar month. Sequences of simulations during the 20th century were started at 5-year intervals, and due to technical problems in running later years of simulation sequences these later years were not as well sampled. Each one-year simulation started in December and ended in November; with some volunteers discontinuing the simulations, earlier months in this December-November year are thus better sampled than later months.

2.4 weather@home/SAF benchmark simulations

The weather@home/SAF project uses a regional atmospheric model nested within a global atmospheric model. There are some aspects of this arrangement that could constrain model behavior. To diagnose the relevance of such factors, a number of simulations were performed at UCT using the HadRM3P-50km regional model, as used by weather@home/SAF, under different setups following the benchmarking protocols of the Coordinated Regional Climate

Downscaling Experiment's African project (CORDEX-Africa), an international activity downscaling global climate model output to better characterize possible future climate change (Nikulin et al., 2012). These protocols include driving the model with ERA-INTERIM reanalysis data at the side boundaries of the domain, and performing the simulations over the 1989-2008 periods. ERA-Interim is considered an improvement over earlier reanalysis for driving regional climate models over Southern Africa (Sylla et al., 2012).

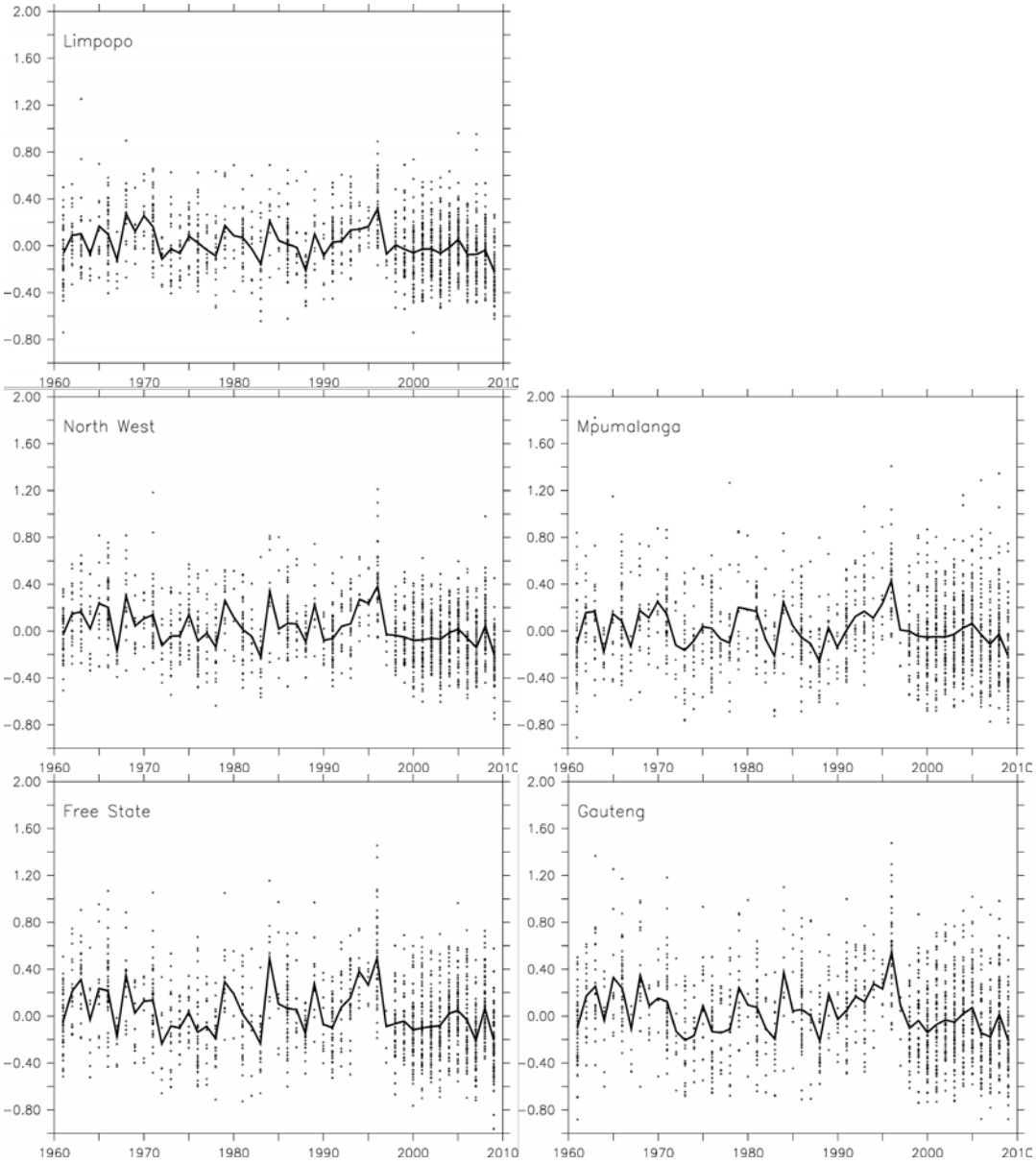

Figure 2.4 The anomalies of annual average precipitation rate for the inland provinces (the Free State, Gauteng, Limpopo, Mpumalanga, and North West province) from the weather@home/SAF simulations analyzed in later sections. The solid line denotes the ensemble annual mean. In unit of mm day^{-1}. A 1 mm day^{-1} anomaly in precipitation rate corresponds to an annual total anomaly of 360 mm (because the climate models run on a 360-day calendar).

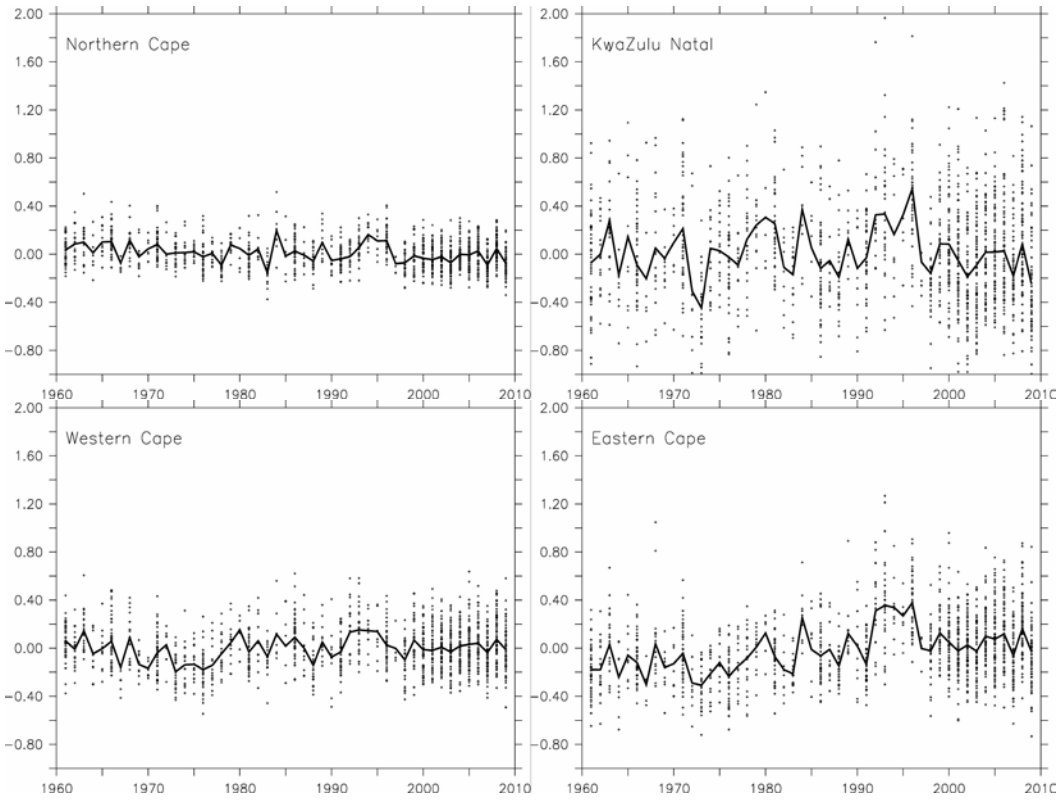

Figure 2.5 The anomalies of annual average precipitation rate for the coastal provinces (Eastern Cape, KwaZulu-Natal, the Northern Cape, and the Western Cape) from the weather@home/SAF simulations analyzed in later sections. The solid line denotes the ensemble annual mean. In unit of mm day^{-1}. A 1 mm day^{-1} anomaly in precipitation rate corresponds to an annual total anomaly of 360 mm (because the climate models run on a 360-day calendar).

The four different configurations investigated are listed in Table 2.3. The experimental design examined two specific aspects of the model configuration: the spatial domain; and the land surface scheme. Two domains were examined: the weather@home/SAF domain covering southern Africa; and the CORDEX-Africa domain covering the entire African continent (Figure 2.1). Comparison of these two domains serves to ascertain how the weather@home/SAF simulations fit within the context of the CORDEX-Africa. Two schemes were used for representing land surface properties: MOSES and MOSES2. Unlike MOSES, which does not consider sub-grid-scale heterogeneity, MOSES2 treats each grid box as a mixture of five plant functional types (broadleaf trees, needleleaf trees, C3 grass, C4 grass and shrubs) and four non-vegetated surface types (urban, inland, water, soil and ice) (Essery et al. 2001). By doing this MOSES2 considers a sub-grid within a grid cell and surface temperature, short and long wave radiation, radiative and turbulent fluxes, ground heat fluxes, canopy moisture content, snow mass and snow melt rate are calculated for each surface type in a grid box. MOSES2 also includes a prescribed annual cycle in vegetative properties, notably the leaf area index, whereas the parameters in MOSES do not vary in

time. Neither scheme includes a dynamic representation of vegetative processes. The "wm1" simulation, using the weather@home/SAF domain and MOSES land surface scheme, matches the setup used in the weather@home/SAF project. Further details on these simulations are given in Cerezo-Mota et al. (2014).

Table 2.3 Description of various setups used for the benchmarking simulations using the HadRM3P-50km model run at UCT. The spatial domains are shown in Figure 2.1.

Label	Spatial domain	Land surface component
cm1	CORDEX-Africa	MOSES1
cm2	CORDEX-Africa	MOSES1
wm1	weather@home/SAF	MOSES2
wm2	weather@home/SAF	MOSES2

2.5 Benchmarking the weather@home/SAF simulations

There is little difference in the annual cycle of precipitation over the northeastern half of South Africa ("Region 12") between the four configurations of the HadRM3P-50km regional model that were examined (Figure 2.6). All four configurations overestimate average precipitation during the wet season over that region relative to a variety of observationally-based data products (Figure 2.6). For the Western Cape area ("Region 13"), while the annual precipitation totals are comparable between the HadRM3P-50km simulations and observationally-based datasets, the HadRM3P-50km simulations have a wet peak that is several months early. An important reason for this is visible in plots of the annual cycle at the model's grid resolution (Figure 2.7). While the simulations have a properly timed (but usually lower magnitude) peak in the southwestern coastal areas, this winter peak does not propagate far enough inland before transitioning to the summer rainfall peak prevalent over the rest of the country. When aggregated over the area, this inland discrepancy dominates.

The simulations using the weather@home/SAF domain also result in substantially less precipitation than do the simulations using the CORDEX-Africa domain during the March-April period, which is the wettest in the simulations. This difference is most visible in the southern parts of the region (Figure 2.7). Further analysis (not shown) has indicated that this results from the phase shift of the different grids used. While both the weather@home/SAF and CORDEX-Africa grids are 50×50 km in size, the grids are shifted with respect to one another and the alignment of the grids with local topography is such that in the weather@home/SAF grid there is a more progressive slope in southern areas of the region toward the high-altitude interior, meaning that orographically induced precipitation is lower.

The annual cycle of surface air temperature is comparable between the observations and the model simulations (Figure 2.6), although the simulations tend to be 1-2^{o}C cooler over the northeastern half of the country ("Region 13").

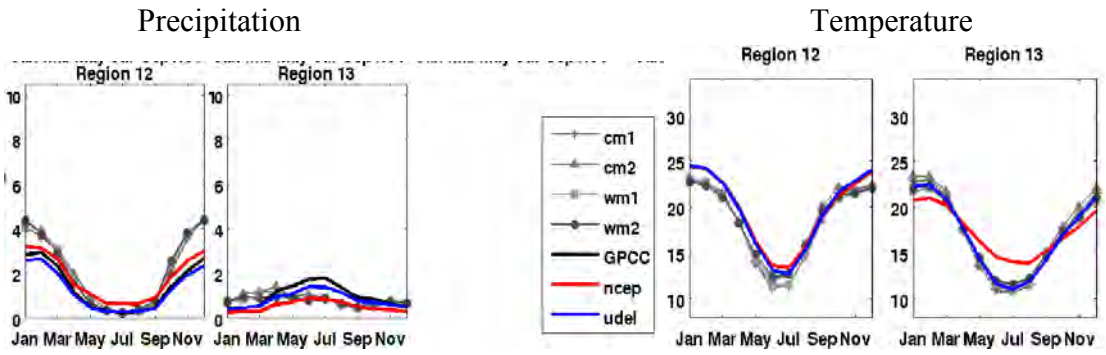

Figure 2.6 The annual cycle in precipitation and temperature in simulations of the HadRM3P-50km model run under different configurations. Region 12 corresponds to the northeastern half of South Africa while Region 13 corresponds to the Western Cape area; the exact regional specifications are shown in Figure 2.1. The grey and black lines show the results for the different model configurations listed in Table 2.3. Data are also shown from the GPCC (Rudolf et al., 2010) and University of Delaware (UDel; Willmott and Matsuura, 1995) observationally-based data products and from the NCEP2 reanalysis (Kanamitsu et al., 2002).

The month-to-month anomalous variability in precipitation closely matches the GPCC and UDel observational datasets over both regions, but the NCEP2 reanalysis product is completely uncorrelated (Figure 2.8). Temporal correlations between the simulations and observations can be considered something of a hindcast test, with the regional model being driven by reanalysis (i.e. an hindcast estimate of the weather that was actually experienced) surface boundary conditions and along the side boundaries of the domain. Not surprisingly, the simulations using the weather@home/SAF domain have a substantially higher correlation with both observational datasets than do those using the CORDEX-Africa domain, as the closer regional boundaries can exert more control over the weather simulated in the interior of the domain. The temperature time series from the weather@home/SAF-domain simulations also have a higher correlation with the observational and reanalysis datasets, in this case sharing at least two thirds of the variance. Further details on these and other analyses are given in Cerezo-Mota et al. (2014).

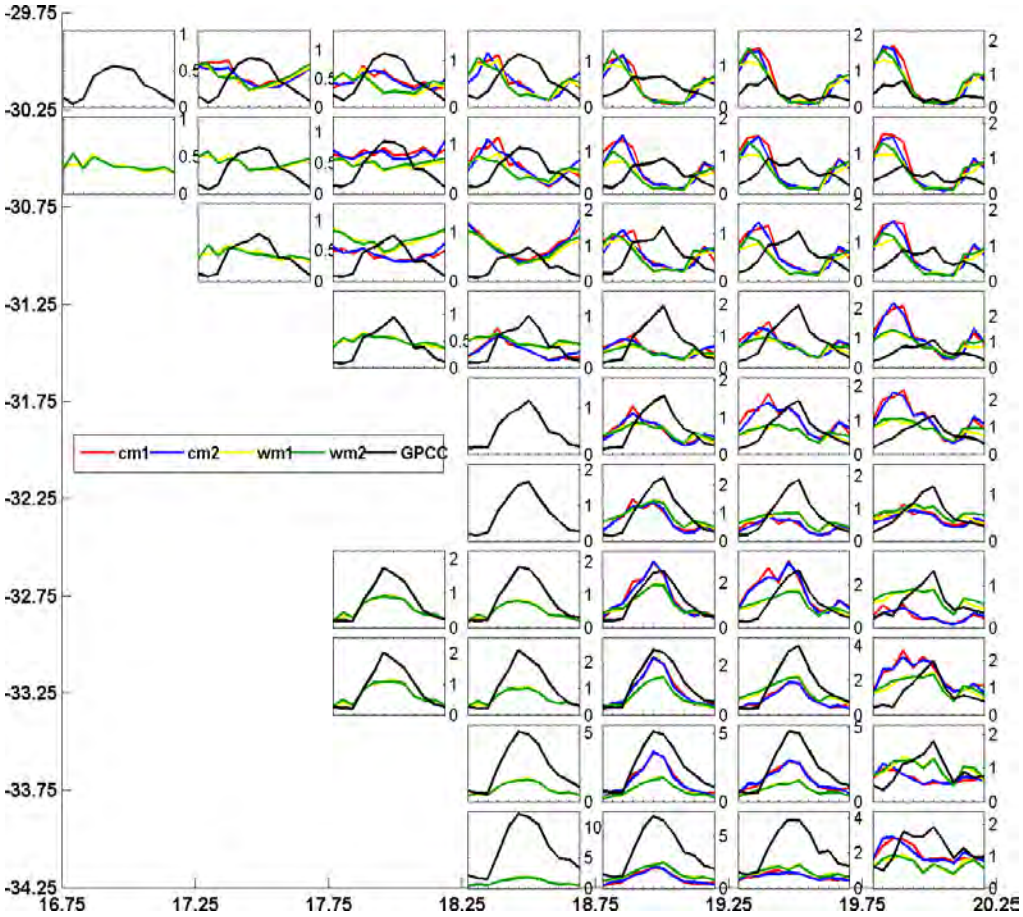

Figure 2.7 The mean annual cycle of precipitation over each grid cell of the GPCC observationally-based data product (Rudolf et al., 2010) in the Western Cape area, from the GPCC product and from simulations of the HadRM3P-50km model run under different configurations. The location of this region within the South African context is visible in Figure 2.1 as "Region 13". The colored lines show the results for the different model configurations listed in Table 2.3. Differences between annual cycles between the "cm" and "wm" simulations result from differences in the alignment of their spatial grids with local topography. Model data have been interpolated to the GPCC spatial grid.

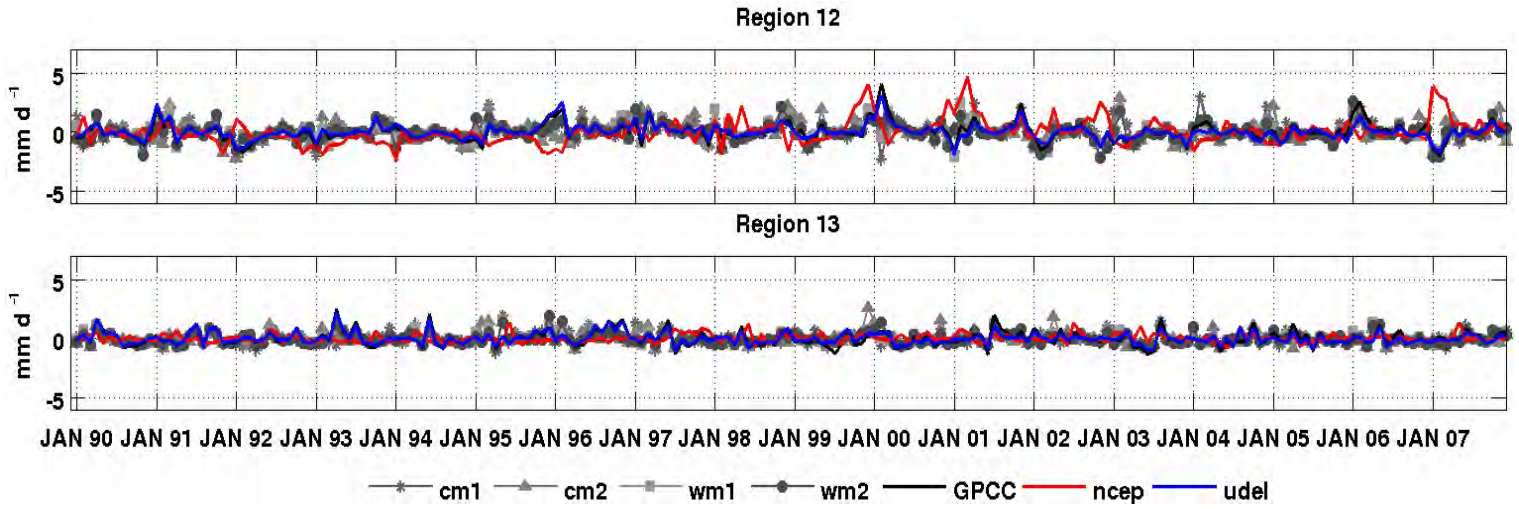

Figure 2.8 Time series of monthly precipitation anomalies from simulations of the HadRM3P-50km model run under different configurations. Region 12 corresponds to the northeastern half of South Africa while Region 13 corresponds to the Western Cape area; the exact regional specifications are shown in Figure 2.1. The lines with symbols show the results for the different model configurations listed in Table 2.3. Data are also shown from the GPCC (Rudolf et al., 2010) and University of Delaware (UDel; Willmott and Matsuura, 1995) observationally-based data products and from the NCEP2 reanalysis (Kanamitsu et al., 2002). Values are anomalies from the mean annual cycle.

3 Prediction, descriptions and measures of the limits of predictability

3.1 Prediction

This section describes some of the theoretical and methodological background behind the analyses of the limits of predictability reported in Sections 4, 5, and 8. It is derived from discussions in Lawal et al. (2014a, b).

Prediction, a statement of anticipated weather in a particular area during a stated time period, can be short-, medium-, or long-range (Buckle, 1996). Short-range predictions, generally for one, two, or three days in advance, are typically the most detailed. Forecasts for three to six days are medium-range, while those for weeks, a month or more in advance are known as long-range forecasts. Temperature and precipitation are the main climate variables communicated in medium- and long-range forecasts, and are usually expressed as departures from the climatic mean i.e. anomalies. Long-range prediction, synonymous with seasonal climate forecasting, is an attempt to provide useful and reliable information about the outlooks of weather that can be expected in the coming months. It is always a probabilistic forecast of the climatic anomalies on the seasonal time-scale.

The importance of a timely and reliable prediction of seasonal climate over South Africa cannot be ignored. The information from seasonal climate forecasts, expressed as anomalies from a historical reference period, is needed for planning and risk management in various socio-economic sectors such as agricultural activities, health, water resources management, environmental management, engineering, etc. (Johnston et al., 2004). Timely and reliable prediction of seasonal climate can help reduce the damages from extreme climate events. Its usefulness also extends to insurance markets where it assists in the operational task of preparing for major pay-outs. Therefore, a forecast is only useful if it is reliable because a wrong forecast can lead to wrong decisions and also can reduce the trust of the public in using forecast information for planning.

However, there are limits to predictability, the extent to which a skilful forecast is possible, of seasonal climate. Suspected reasons for these are: (1) complexities in the interactions of land, ocean and atmosphere; (2) knowledge of the initial states of ocean, land and atmosphere; and, (3) variations in chemical composition of the atmosphere.

Climate over any region, especially South Africa where climate variability is high, is determined by complex interaction between the land, ocean and atmospheric processes. Most of these interactions are yet to be fully understood (Houghton, 1991; Pennell and Reichler, 2010). For instance, seasonal forecasting over South Africa tends to be more reliable during the El-Niño years than the non El-Niño years when the main processes that dominate atmospheric circulations are not well known (Tyson and Preston-Whyte, 2000; Johnston et al., 2004; Landman and Beraki, 2010).

Nonlinearities in the atmosphere complicate our understanding of the atmospheric physics and predictability of the seasonal climate as timely and reliable seasonal climate predictions depend on knowing the initial states of the ocean surface, land surface and that of the atmosphere (Pielke et al., 2006). The ocean and land surface vary more slowly than the atmosphere, therefore, their state can be predicted, to some degree of accuracy, months into the future. In sharp contrast to these slow variations, the atmosphere can always diverge rapidly from an initial state, resulting in little added value of knowledge of the initial state when forecasting months ahead. Therefore, influences of the slowly varying anomalies in the state of the ocean and land surfaces on the atmosphere provide the principle underlying seasonal forecasting. Despite this, atmosphere still produces plenty of noise on top of any predictable signal. Tyson and Preston-Whyte (2000) define noise as random fluctuation in a parameter caused by effects other than the one being studied. Understanding of the fundamental limits this noise imposes on the predictability of seasonal climate over South Africa remains weak.

Any change in the chemical composition of the atmosphere can significantly alter its predictability. Variations in the atmospheric chemical compositions, such as dust and gas contents, may influence climate by altering the transparency of the atmosphere for incoming and outgoing radiations (Buckle, 1996). Studies such as Hegerl et al. (2007) and Stott et al. (2010) have shown that an increase in atmospheric green-house gases (GHG), since the pre-industrial era, has led to global warming over the last century. Since this will alter the long-time climatology, the baseline for calculating seasonal climate anomalies, it will limit the predictability of the seasonal climate. How much changes in atmospheric chemical composition, such as increasing anthropogenic greenhouse gases (GHG) concentration, contribute to the predictability of seasonal climate over South Africa is currently unknown.

3.2 Descriptions of the limits of predictability

There are on-going debates about the extent to which the atmosphere is predictable beyond a few days, that the uncertainties in weather predictions are primarily an initial value problem, and that errors in the initial conditions are the dominant source of error in weather forecasting. Studies such as Lorenz (1975), Molteni et al. (1996) and Luo et al. (2011) argue that these errors grow rapidly and limit the weather predictability horizon to the order of a week or less. When model errors are ignored, predictability of weather events a few days in advance is essentially limited by the accuracy of atmospheric initial value conditions (Rowell, 1998; Luo et al., 2011). Therefore, seasonal climate predictions and inter-annual climate projections face boundary conditions problems because the atmosphere cannot on its own produce predictable random variations that can persist for months Zwiers (1996). The sources of these boundary conditions are obtainable from predictable but slow processes such as changes in ocean circulation. The ocean, which is highly viscous, is not mixing rapidly, is vertically stable (i.e. the heating is at the top), and has a large heat capacity, provides the climate with a memory of the system. This memory results in atmospheric deviations that can last for months, or years. While it is not something we examine in this project, variations in land cover may also be an important source of boundary conditions Boer (2000).

Rowell (1998), Kumar et al. (2003) and Reichler and Roads (2004) have made attempts at investigating the temporal-spatial distribution of atmospheric predictability. They based their studies primarily on theoretical, statistical, and numerical models and gave qualitative estimates of atmospheric predictability, such as information on regions with either higher or lower predictability. It is noted that model deficiencies strongly influence their estimates of atmospheric predictability. Nevertheless, some studies have quantified the limits of atmospheric predictability. Luo et al. (2005, 2007 and 2008) and Keenlyside et al. (2008) showed that tropical climate signals have some degree of predictability from on the order of a few seasons to 1-2 years based on current state-of-the-art fully coupled models. For instance, Luo et al. (2011) showed that with a perfect warming trend and/or a perfect model, global surface air temperature and precipitation could be predicted beyond two years in advance with an anomaly correlation skill above 0.6. Furthermore, Li and Ding (2011) used a nonlinear local Lyapunov exponent (NLLE) algorithm to investigate temporal spatial distributions of predictability limits of the daily geopotential height and wind fields. While there has been some dispute on the relevance of the Lorenz (1975) two-dimensional vorticity equation that they analyzed (Straus and Shukla 2005; Rotunno and Synder 2008), Li and Ding (2011) nevertheless noted that limits on atmospheric predictability varies widely with region, altitude, and season; and concluded that limits on noticeable predictability of the daily geopotential height and wind fields are generally less than 3 weeks in the troposphere and approximately 1 month in the lower stratosphere. These imply that a three-dimensional structure of predictability limit exists in the atmosphere. See also González-Miranda (1997), Kumar et al. (2003) and Reichler and Roads (2004).

This project aims to estimate what the theoretical range of forecasts is for a variety of seasons and ocean states, in the context of a single forecasting model system, and thus establish the theoretical limits as to how much we may be able to improve seasonal forecasts. This knowledge gap will be filled by examining the spread of output from a regional climate model, specifically the regional component of the Hadley Centre Atmospheric / Regional Model version 3 (HadAM3P-N96/HadRM3P-50km) modeling system, run in a hindcast framework. Many simulations of this regional model, with slightly different initial conditions, will be employed to investigate the characteristics of the measures of the limits of predictability of seasonal forecasts over South Africa (see Section 2.2 for details on the simulations).

3.3 Measures of the limits of predictability

Ensemble spreads of many simulations of the HadAM3P-N96/HadRM3-50km modeling system, with slightly different initial conditions, are utilized to represent the theoretical range of forecasts for various climatic seasons over South Africa. The range is quantified using two measures: the Standard Deviation (StdDev) and the “Range of Possibility” (RoP). The StdDev describe all of the data and can be estimated accurately from small samples, but it is also very sensitive to outliers. RoP, the 10-90th percentile range, can essentially be considered the opposite of StdDev in all these three aspects. With these differences, the two

measures are complementary and thus give an indication of the sensitivity of conclusions to the particulars of how ensemble spread is measured. Therefore, analyses of spreads of ensembles of many simulations from the regional model as depicted in Figure 3.1 are carried out.

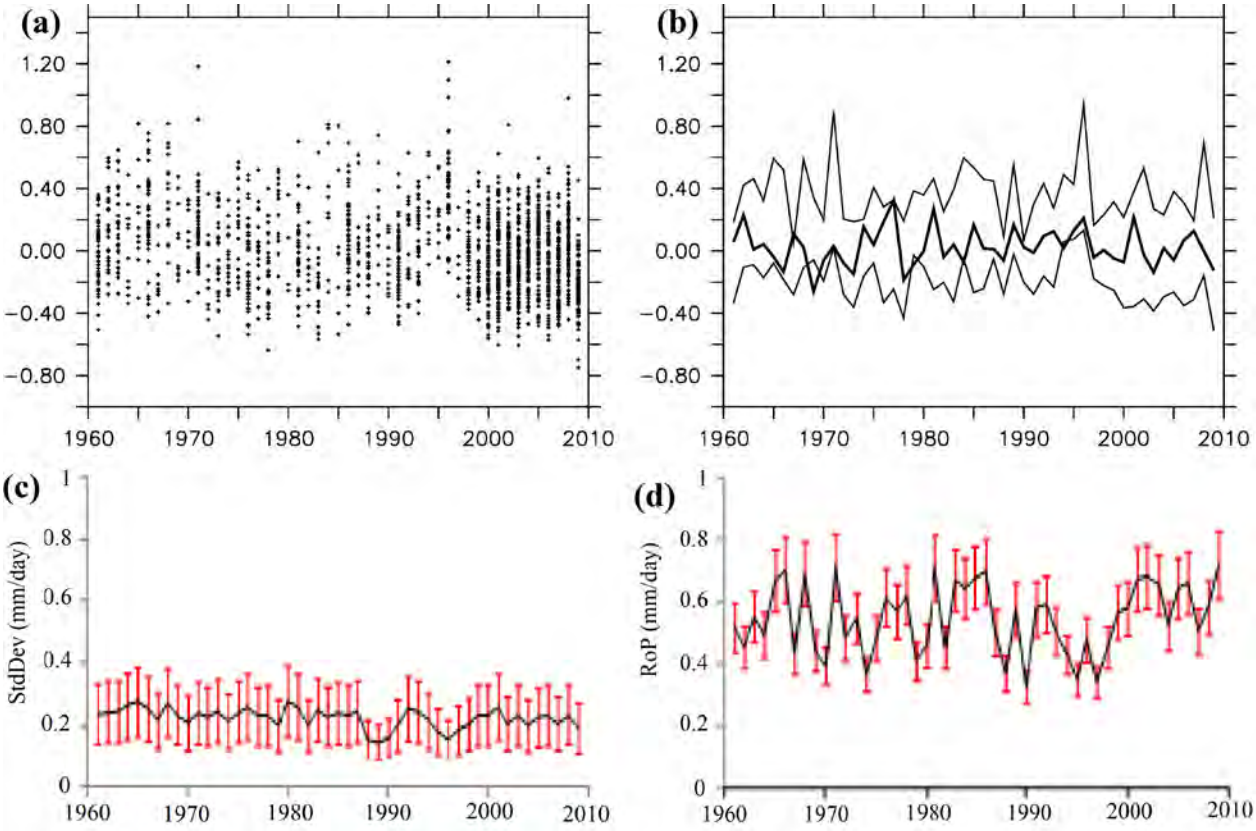

Figure 3.1 Annual variations in precipitation rates (mm day^{-1}) as anomaly of the climatological average over Limpopo Province (LMP) from a sample of the simulations for the month of July. **a:** mean anomalies of individual ensemble members (the black dots). **b:** the time series of the annual 90th and 10th percentiles of the values shown in panel a. **c:** time series of ensemble spreads of the data in panel a as measured by StdDev (standard deviation). **d:** time series of ensemble spreads as measured by RoP (range of possibility, the 10-80th percentile range). Red bars on plots of panel c and d represent 80% confidence intervals estimated through a Monte-Carlo bootstrap procedure.

Ensemble spreads as measured by RoP and StdDev vary with time (see Figure 3.1 panels c and d). It also varies with space and austral seasons (Figures 3.2 and 3.3), for precipitation and surface air temperature respectively. Ensemble spreads show that larger spreads are concentrated where the seasonal average values are higher. Higher ensemble spreads for precipitation are found over the central and north-eastern areas of the country during spring (SON), summer (DJF) and autumn (MAM). The regions of higher precipitation spread migrate towards the south-west, southern and eastern coasts during winter (JJA) following the patterns of seasonal rainfall distributions (Figure3.2).

Ensemble spreads for temperature are lower than those for precipitation and more uniform along the coasts than inland (Figure 3.3). This may be as a result of prescribed sea surface temperature used in the weather@home/SAF setup; hence, coastal areas in the HadRM3P-50km model may be constrained to follow the prescribed ocean temperature. Higher spreads are found inland where temperature variability is higher.

Seasonally, correlation coefficients between the RoP and StdDev measures of precipitation spread are generally around 0.7 and relatively uniform across the country and seasons (Figure 3.2). Correlation coefficients for temperature spreads are lower than those for precipitation and somewhat less homogenous (Figure 3.3).

There also exist large degrees of linear associations in measures of ensemble spreads provincial scales. The provinces are listed in Table 3.1 along with their abbreviations used throughout this report. The temporal correlations for the two measures at provincial scales are depicted by Figure 3.4 which shows correlation coefficients of inter-annual variations between RoP and StdDev for each month and province. These correlation coefficients are displayed for both parameters on provincial and monthly basis. For precipitation, there are strong direct relationship between the two measures, with correlations ranging between 0.4 and 0.96 in all the provinces. Similarly, average correlation between the inter-annual variations between measures of ensemble spread for temperature is strong, $0.38 < r < 0.93$ for all provinces, although slightly lesser when compared to those for precipitation.

Table 3.1 List of the nine South African provinces along with the abbreviations used to label them throughout this report

Abbreviation	**Province name**
ECP	Eastern Cape Province
FSP	Free State Province
GGP	Gauteng Province
KZP	KwaZulu-Natal Province
LMP	Limpopo Province
MLP	Mpumalanga Province
NCP	Northern Cape Province
NWP	North West Province
WCP	Western Cape Province

Seeing as the StdDev and RoP measure the ensemble spread in rather different ways, high correlations coefficients indicate that, for the most part, the two measures are each recording the same variations in spread. In that case, it appears conclusions based on either of these two measures (or on both) are rather insensitive to the choice of measure. However, there are some locations and months with correlations between the two measures that are lower, due to changes in the shape of the frequency distributions. In these cases, results can be sensitive to

the choice of measure. Seeing as that the method of measuring variations in the limits of predictability must match the method of describing forecasts, the implication is that the degree to which variations in the limits of predictability might be usable in an operational setting may depend strongly on the method used to communicate the forecast.

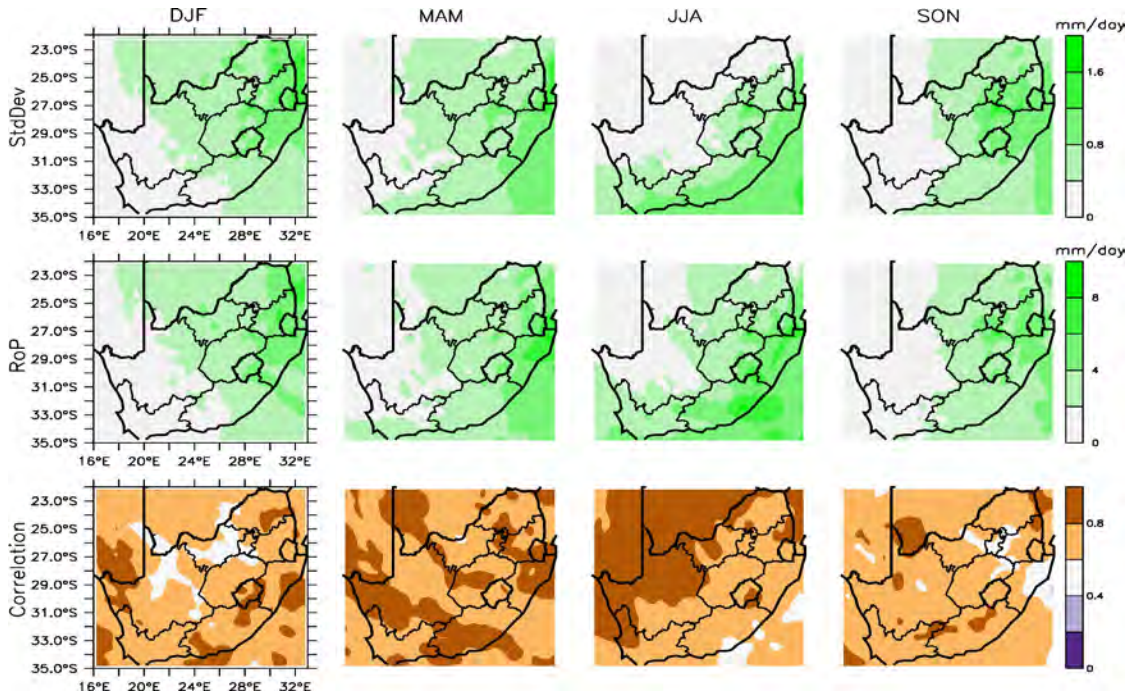

Figure 3.2 Seasonal spatial ensemble spreads for precipitation as evaluated by StdDev (first row) and RoP (second row). Third row: correlation coefficient (r) between StdDev and RoP. In columns are austral seasons: DJF – summer; MAM – autumn; JJA – winter; SON – spring.

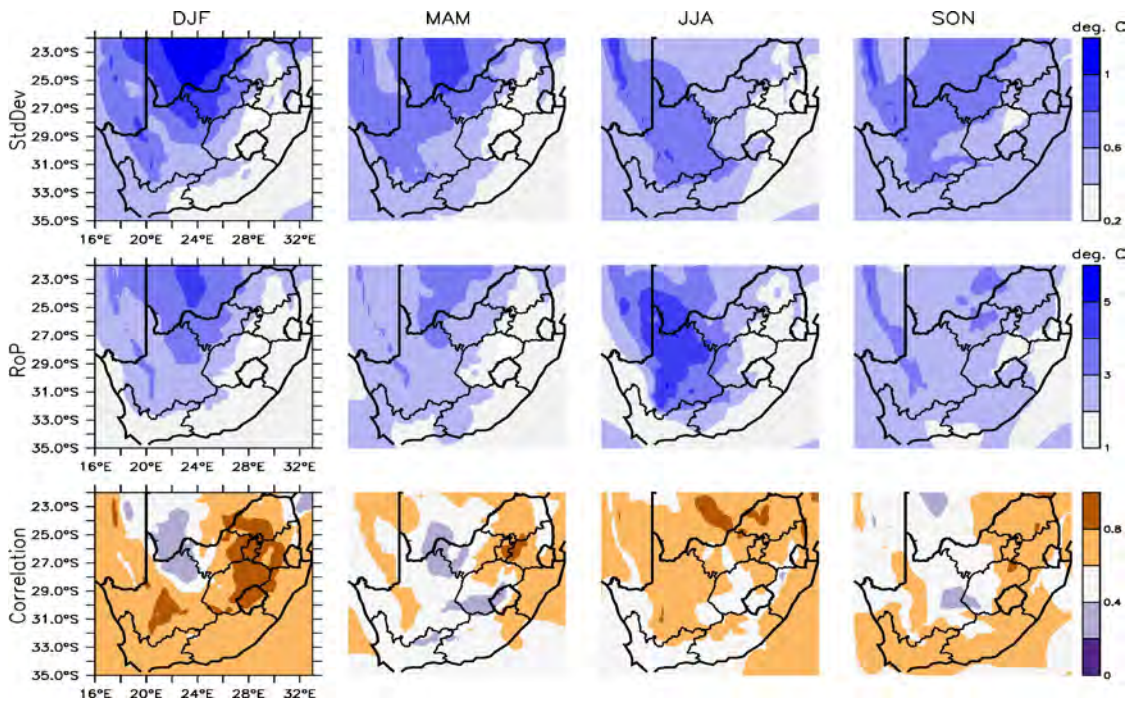

Figure 3.3 Seasonal spatial ensemble spreads for temperature as evaluated by StdDev (first row) and RoP (second row). Third row: correlation coefficient (r) between StdDev and RoP. In columns are austral seasons: DJF – summer; MAM – autumn; JJA – winter; SON – spring.

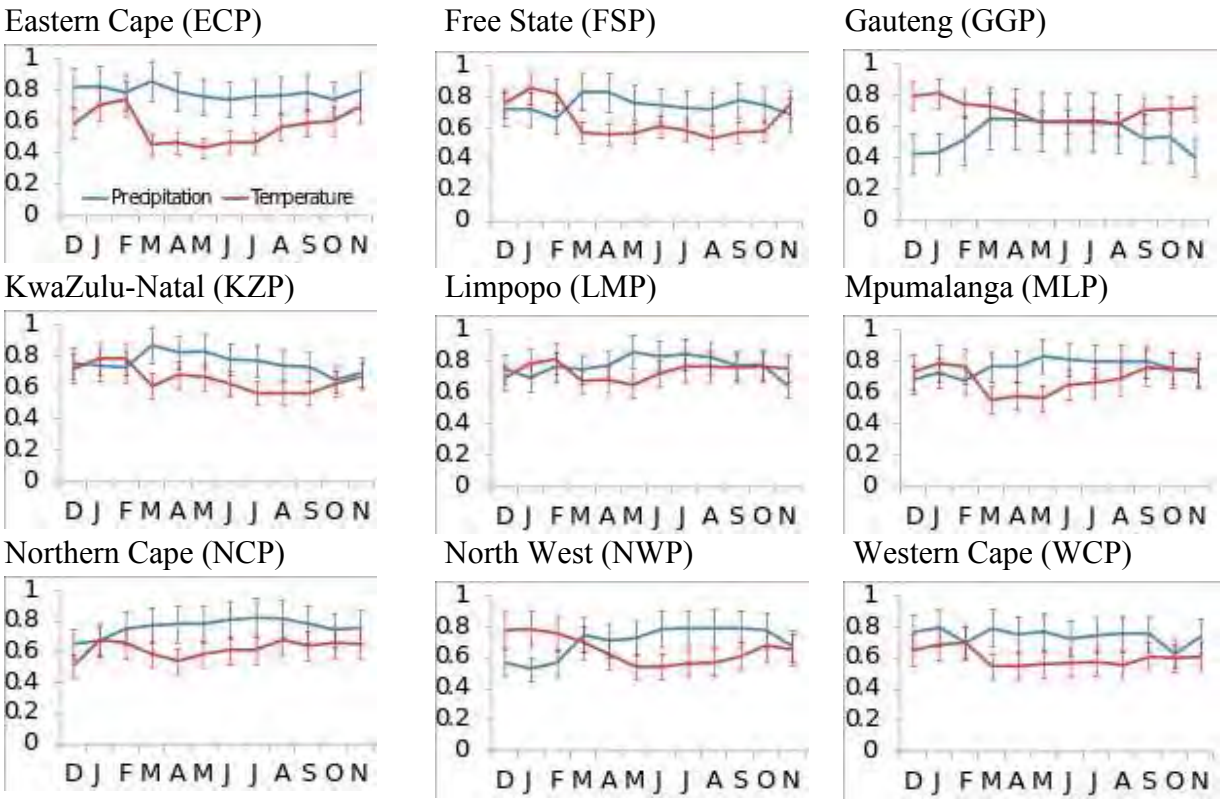

Figure 3.4 Correlation coefficients (r) of inter-annual variations between RoP and StdDev for precipitation (blue lines) and temperature (red lines) for each province and month, calculated over the full period of simulations. Error bars indicate 80% confidence intervals estimated through a Monte-Carlo bootstrap procedure.

4 Variations in the potential spread of seasonal forecasts over South Africa

4.1 Spatial details of long-term trends

This section reports on the existence of interannual variability and long-term trends in the limits of predictability, using the simulations discussed in Section 2.2 and the methods outlined in Section 3. It describes work reported in Lawal et al. (2014b).

Inter-annual linear trends have been calculated from the time series of the two measures of spread, StdDev and RoP, introduced in Section 3.3 and Figure 3.1, using the output from the regional model from the weather@home/SAF simulations (Section 2.2). If "cases with large (small) ensemble spread should be associated with large (small) forecast uncertainty" (Grimit and Mass, 2007) is assumed; then, negative trends of ensemble spread will indicate a narrowing of the range of possible monthly values from the forecasts, and vice-versa for positive trends.

Figures 4.1 and 4.2 contain respectively precipitation (mm/day/year) and surface air temperature (^{o}C year^{-1}) spatial seasonal trends of ensemble spreads as evaluated by the two measures of spread. In Figure 4.1, precipitation RoP trends show tendency for widening, which is not so strongly reflected by StdDev, suggesting that there exist inter-annual variations in the shape of the distribution. Relatively speaking, coastal areas are dominated by widening of ensemble width (positive trends) in DJF. Extreme north and western coast areas are dominated by narrowing of ensemble spreads (negative trends) in MAM. The central parts of the country and the northern parts of Northern Cape Province (NCP) are under the influence of narrowing trends in JJA.

For temperature, Figure 4.2, both measures show similar spatial structure, although RoP has a general tendency toward a widening spread in DJF and MAM relative to StdDev. While coastal areas experience a narrowing of ensemble width in SON, narrowing trends are confined to inland positions in JJA. In DJF and MAM, on the other hand, inland areas experience a widening trend.
Figures 4.1 and 4.2 focus on spatial details at the expense of sub-seasonal details and uncertainty characterization; therefore, the next section discusses evaluation of these trends on provincial levels and on a monthly basis. Inter-annual linear trends, based on sample of size 30 to 1000 sub-sampled at size 30 to 100, was evaluated from the time series of these two measures shown in Figure 3.1. A Monte-Carlo bootstrap re-sampling method, in line with Buckland (1983), Johnson (2001), and Buhlmann (2002), was used to characterize sample uncertainty in the results. The values from available simulations for each year were selected at random with replacements and the calculations performed again on these re-sampled data, with these processes repeated one-thousand (1000) times in order to generate an empirical frequency distribution function of results consistent with the simulation data.

4.2 Sub-seasonal details and uncertainty characterization in long-term trends

Some provinces have experienced a widening (positive trends, reflecting looser constraints on the forecast atmospheric state) or narrowing (negative trends, reflecting tighter constraints on the forecast atmospheric state) of the ensemble spreads as indicated in Figures 4.3 and 4.4. The thick bars in Figures 4.3 and 4.4 indicate the sample means, while the error bars represent the 80% confidence intervals estimated through Monte-Carlo bootstrap procedures. As expected for Gaussian distributions, trends in the StdDev measure are generally less than half as large as those in the RoP measure.

The majority of the trends in Figure 4.3, monthly trends in ensemble spread for precipitation over the nine South African provinces, are positive from autumn to the middle of spring (October), except for a dip in winter. Trends in the precipitation spread range from narrowing of 7.5 mm to a widening of 75 mm over the half-century period according to the RoP measure, and a narrowing of 12 mm to a widening of 15 mm according to the StdDev measure. In general the central and eastern provinces experience a narrowing of ensemble width from November to January, with some provinces such as Limpopo (LMP) and Mpumalanga (MLP) also experiencing narrowing later into summer. The southern coastal provinces (Eastern Cape (ECP) and Western Cape (WCP)) experience a widening in most months, however, the NCP shows little change. Zero trends in ensemble spreads are sparsely distributed and do not follow specific pattern in either measure.

Figure 4.4 shows monthly trends of ensemble spread for surface air temperature over the nine South African provinces. There is distinct duality between the coastal and inland provinces. For the most part, inland provinces exhibit widening trends. Coastal provinces exhibit narrowing of the ensemble spreads from September to December. The trends in the temperature spread range from a narrowing of 0.3^{o}C to a widening of 1.125^{o}C over the full periods according to the RoP measure, and a narrowing of 0.03^{o}C to a widening of 0.5^{o}C according to the StdDev measure.

Of the 108 province-month realizations for each variable and measure, 45 of the RoP cases and 62 of the StdDev cases for precipitation have the zero trends outside their 80% confidence intervals; 62 of the RoP cases and 71 of the StdDev cases for temperature do so as well. At random, only 22 cases would be expected, indicating that these trends are generally reflecting real changes occurring within the climate model framework. By inference, the range of possible seasonal forecasts, as represented by RoP and StdDev, can vary from one year to another over South Africa. These ranges depict the limits to quantitative prediction of seasonal climates over South Africa. Recall that this experiment was carried out within the framework of the HadAM3P / HadRM3P model pair, which is not used in any contemporary seasonal forecast service, therefore, the possibility exists that the exact values of these trends in ensemble spread are specific to this model pair and may not reflect those in other forecast model setups. However, the presence of these trends in this

modeling setup is highly suggestive of possible similar trends in contemporary active multi-model prediction settings. Such trends may thus be useful in the characterization of skills of current forecasts in relation to the assessment of past skill. Therefore, relationship of these measures of spread with forecast skills shall be treated in the later stage of this paper.

In relations to operational applications, this experiment has not considered what may be the driving forces or the physical processes behind the variability in the long-term trends of the ensemble spreads. The variability of these trends may be remotely-forced or locally-based. Suggestive factors that may cause the variability in these trends are (1) the model and its simulation techniques; (2) trends in the mean state of the atmosphere which may lead to more possibility for spreads; (3) a shift in the frequency of weather patterns; (4) changes in cloud cover which could affect the variability of temperature by altering the radiative balance of the source of energy; (5) changes in sea surface temperature; (6) atmospheric composition which alters atmospheric transparency thereby affecting the climatology of which seasonal prediction is based; etc. Investigating the roles of these factors, either remotely-forced or locally-based, is the subject of the next chapter (Section 5).

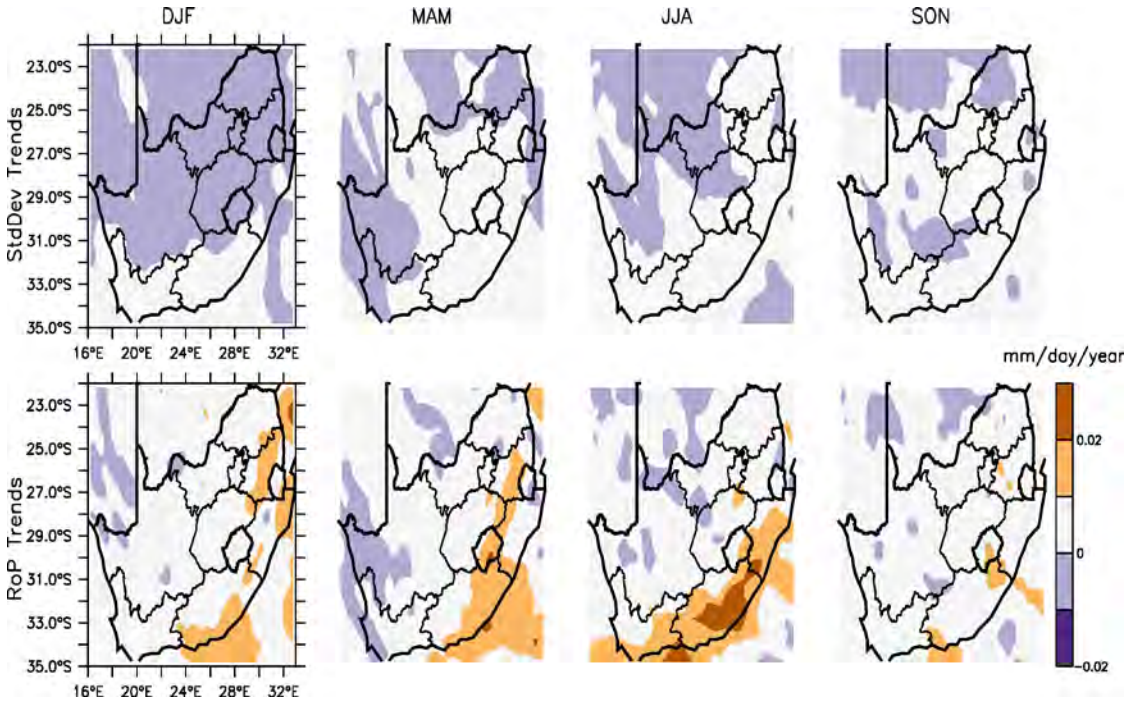

Figure 4.1 Seasonal spatial trends (mm day^{-1} year^{-1}) of ensemble spreads for precipitation as evaluated by StdDev (upper row) and RoP (lower row). In columns are austral seasons: DJF – summer; MAM – autumn; JJA – winter; SON – spring.

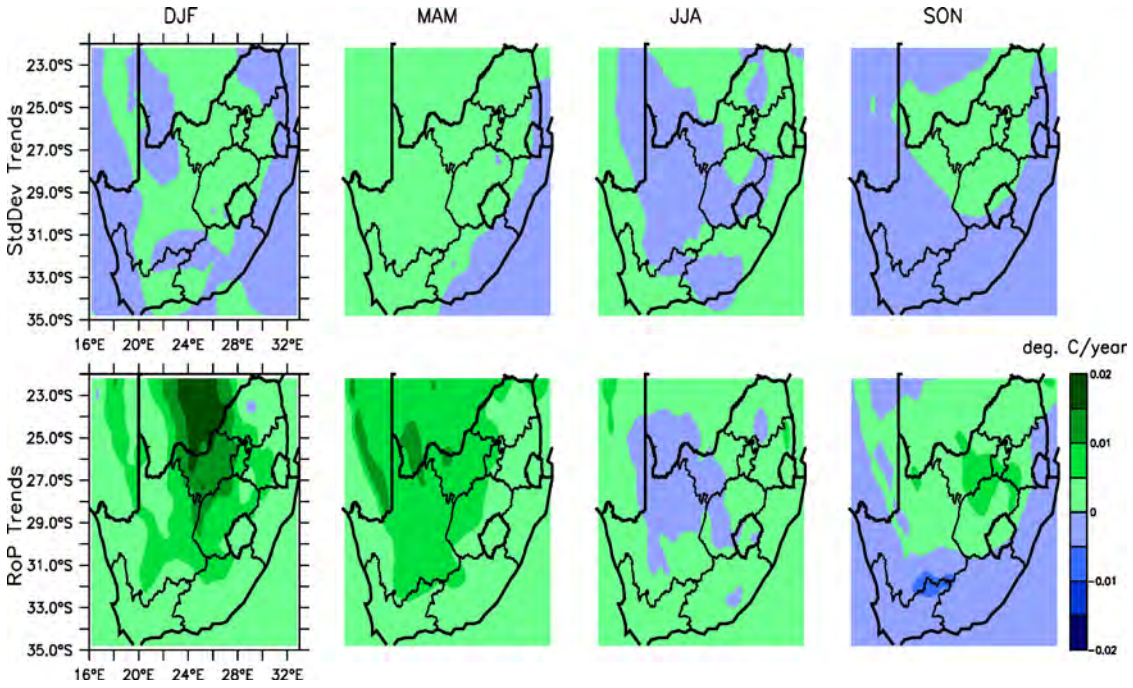

Figure 4.2 Seasonal spatial trends (^{o}C year^{-1}) of ensemble spreads for temperature as evaluated by StdDev (upper row) and RoP (lower row). In columns are austral seasons: DJF – summer; MAM – autumn; JJA – winter; SON – spring.

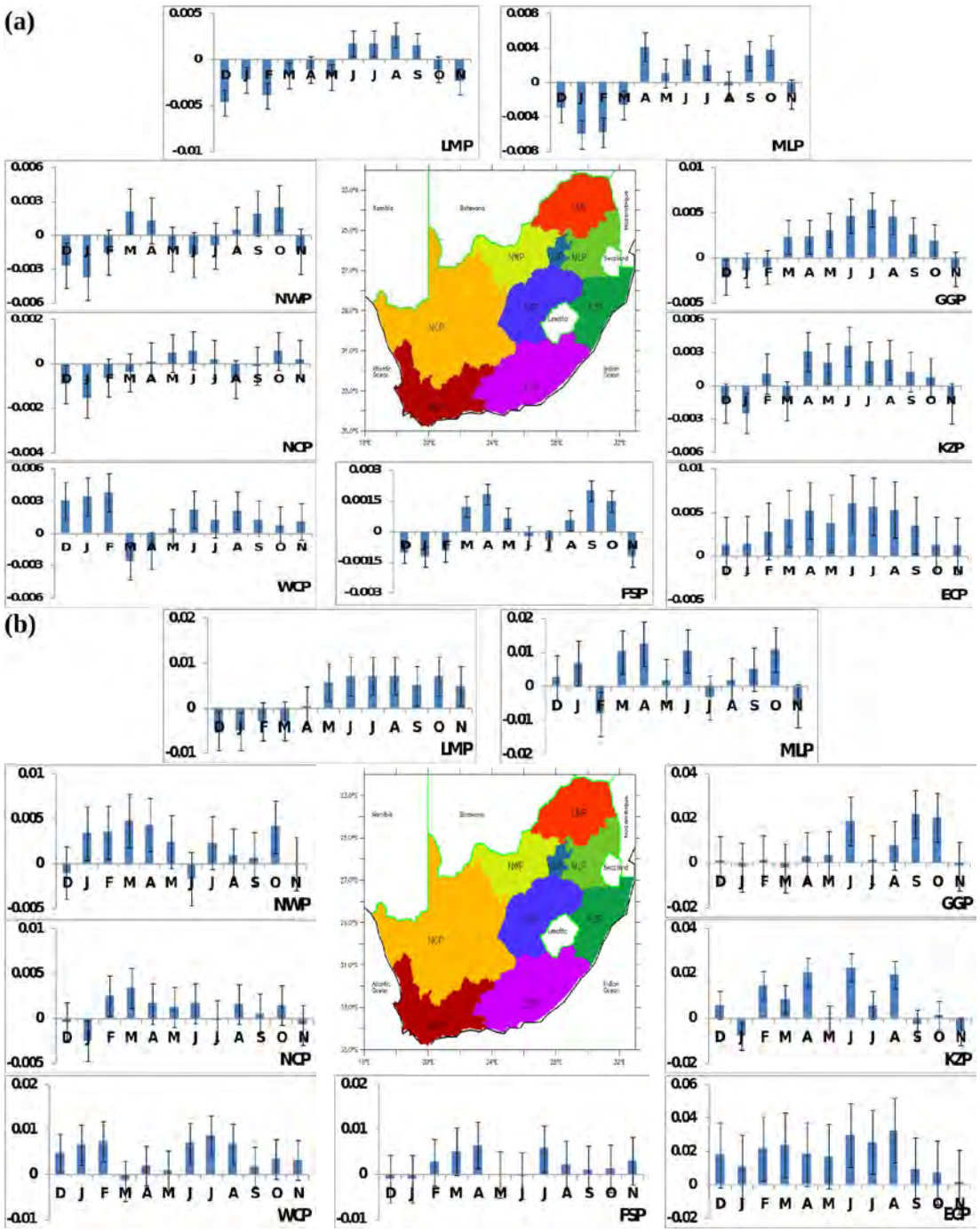

Figure 4.3 Monthly trends (mm day^{-1} year^{-1}) of ensemble spreads for precipitation over the nine South African provinces. **a:** StdDev, **b:** RoP. Black error bars indicate 80% confidence intervals estimated through a Monte-Carlo bootstrap procedure. Provincial abbreviations are as stipulated in Table 3.1.

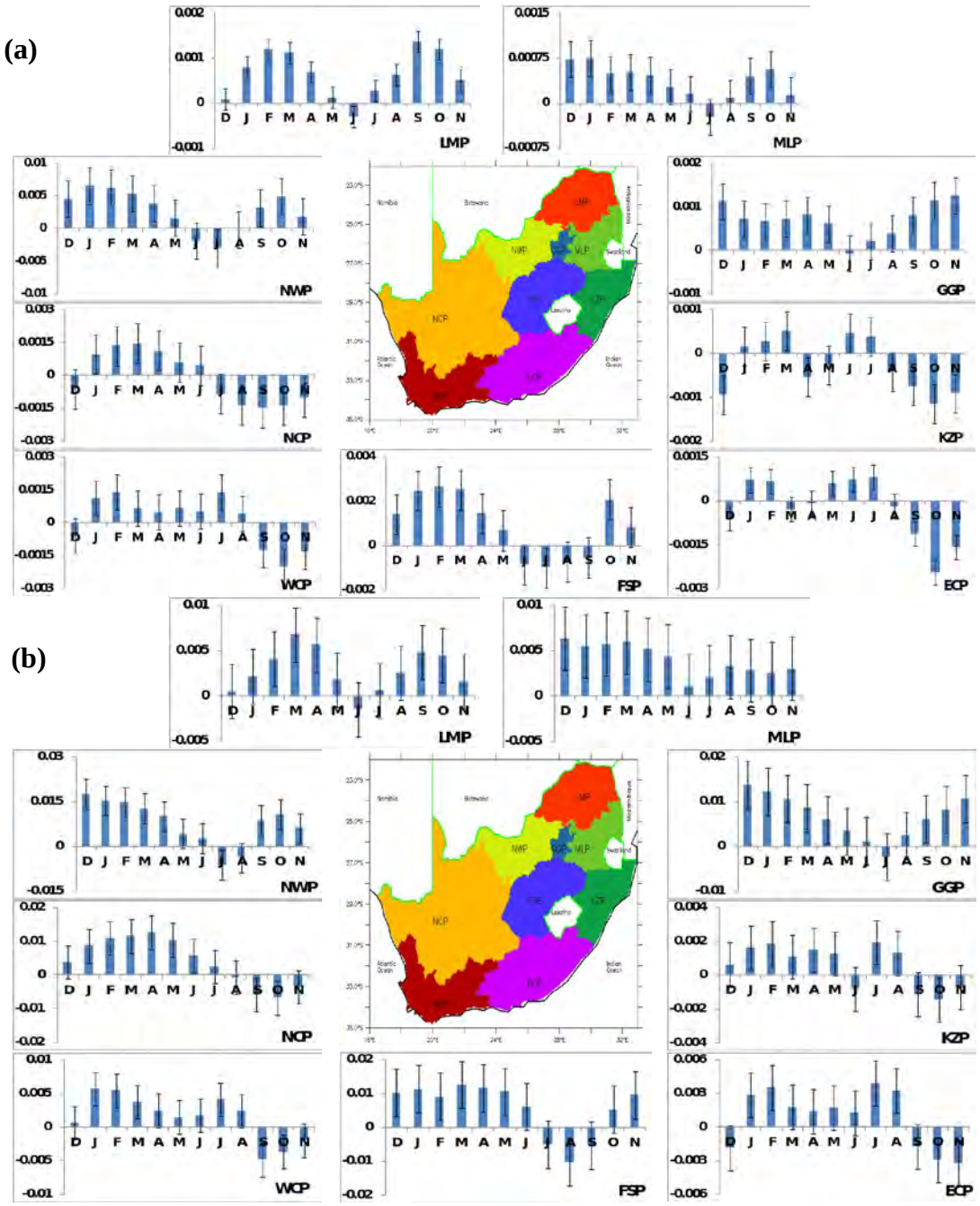

Figure 4.4 Monthly trends (^{o}C year^{-1}) of ensemble spreads for temperature over the nine South African provinces. **a:** StdDev, **b:** RoP. Black error bars indicate 80% confidence intervals estimated through a Monte-Carlo bootstrap procedure. Provincial abbreviations are as stipulated in Table 3.1.

5 The relationship between South African seasonal climate predictability and climate indices

5.1 Preamble and justification

This section reports on whether interannual variations in the limits of predictability are themselves potentially predictable, using the simulations discussed in Section 2.2 and the methods outlined in Section 3. It also examines whether variations in the limits of predictability relate to forecast skill in the real-world setting. Broadly speaking, year-to-year variations are found in some months to be related to the state of the El Niño/Southern Oscillation phenomenon, and an expected relationship between the limits of predictability and of forecast skill exists for the climate model configuration used in this project. This section is based on work reported in Lawal et al. (2014a, b).

A question on whether the nature of seasonal forecast predictability, for a particular location and time of year, varies from year to year in a way that is itself predictable has been answered in the last chapter. It was found that the inter-annual variability and long-term trends in the ensemble spreads of monthly temperature and precipitation over the South African provinces was larger than expected based on error sampling alone. This suggests that there may be potential to characterize predictability in the corresponding forecasts, in other words adding a quantitative estimate of the skill of a forecast that can vary from year to year. However, one requirement to realize that potential will be the existence of predictors of the variations in the ensemble spreads which are in turn predictable to some degree. This constitutes an unanswered question from the last chapter. In view of this, we hereby aim to advance the understanding of predictability of South African seasonal climate by examining the relationship of variations in sea surface temperature (SST) and indices of large-scale climate variability with variations in the ensemble spread of atmospheric model simulations.

Studies such as Landman and Goddard (2005), Landman et al. (2005), and Friederichs and Paeth (2006) carried out investigations on the relationship between the SSTs and the chaotic South African seasonal atmospheric states; they found strong relationships between the SSTs and the ensemble mean in an ensemble forecast system. Murphy (1988b) and Tang et al. (2008) acknowledged that in an ensemble forecast system ensemble mean is the most superior among all the other ensemble attributes such as ensemble spread and signal-to-noise ratio. The reason for this is because studies found little or no relationship between the ensemble spread and the forecast skills of the ensemble mean (Kumar et al., 2000; Tippett et al., 2004; Tang et al., 2008). They are rather of the opinion that predictability is more related to signals in the initial conditions and amplitudes of ensemble mean anomaly based on climate prediction models used. Nevertheless, studies have also found that ensemble spreads can be utilized to assess the reliability and skill of a forecast (Murphy, 1988b; Whitaker and Loughe, 1998; Tang et al., 2008; Nester et al., 2012). Therefore, the year to year variations in the ensemble spreads reflect variations in the predictability of seasonal forecasts. A yet to be answered question is – are there SST influences on seasonal climate predictability via ensemble spread? Answering this will assist forecasters and modelers alike on some aspects

of physical processes that climate models should be able to simulate well in order to improve on the seasonal climate predictability issues.

5.2 Domain, datasets and analysis procedures

Here, the domain of study remains the Republic of South Africa. Emphasis will also be on provincial averages while provincial abbreviations are the same as those used in the preceding chapters. Hottest and coldest seasons in terms of temperature will be discussed while that of wet seasons will be discussed in term of onset (spring), peak (summer) and cessation (autumn) of precipitation. Precipitation results over South Africa for the dry season (winter) are largely meaningless except over the Western Cape Province (WCP) which has its rainy season during this period.

The same measures of spread as used in Section 3.3 and 4 are utilized for both parameters. Global gridded monthly observed SST, Kaplan SST-V2 data, was acquired from the Physical Science Division (PSD) of National Oceanographic and Atmospheric Administration (NOAA/OAR/ESRL) based in Boulder, Colorado, USA (http://www.esrl.noaa.gov/psd; Parker et al., 1994; Reynolds and Smith, 1994; Kaplan et al., 1998). Correlation coefficients, r, between the global gridded SST and the provincial measures of ensemble spread were calculated and analyzed for the relevant seasons and both climate variables. This would indicate which areas of the ocean surfaces the South African predictability measures are sensitive to. De-trending operations were carried out on the measure of spreads and the observed SST used in this study. The reason for de-trending is because this study is interested in the year to year variability relevant to seasonal forecasting rather than the long-term trends. However, analyses without the de-trending showed negligible differences.

5.3 Correlations of provincial-seasonal ensemble spread with global SST

Figures 5.1 and 5.2 show an illustrative subset of maps indicating correlations between the observed SST and the provincial measures of ensemble spread. The maps in Figure 5.1 are of the correlations between the provincial precipitation RoP and the observed SST during the onset of the rain season, austral spring, in eight of the provinces and the cessation season for WCP. Figure 5.2 displays the maps of the correlations between the provincial temperature StdDev and the observed global SST during the winter season. Generally, r ranges from -0.82 to +0.86 for both parameters and measures of spreads. Both provincial precipitation and temperature ensemble spreads significantly co-vary with SSTs at various oceanic regions. This co-variability differs from season to season. Most province have significantly positive/negative spread-SST correlations over the mid latitude to Antarctic / southern zones of the Pacific, Atlantic and Indian Oceans. Many provinces also exhibit some significantly positive/negative correlations over the tropical axis of these Oceans.

Since these measures of spread co-vary with SST globally, the oceans may provide useful predictors of variations in seasonal predictability. Some aspects of oceanic variability are so generally useful for describing seasonal forecasts that they are summarized in convenient indices. Some of these indices represent variations in ocean temperature signals in the

tropical, mid latitudinal and southern parts of Pacific, Atlantic and Indian Oceans where we have noted significant correlations. Thus, there is the possibility that along with being useful predictors of seasonal climate over South Africa, these indices may also be useful predictors of the potential skill of that forecast.

The climate indices to be considered are (1) Antarctic Oscillation (AAO), (2) Indian Ocean Dipole (IOD), (3) Multivariate ENSO Index (MEI) and (4) Tropical Southern Atlantic (TSA). See Table 5.1 for the summary of each of these indices. The AAO is a measure of atmospheric circulation rather than SSTs, but we include it here because it is such a dominant descriptor of southern mid-latitude circulation. AAO measures the pressure gradient between the Southern Hemisphere pole and mid latitudes (Kalnay et al., 1996; Rayner et al., 2003), and thus equator-ward / pole-ward shifts of the southern mid latitude storm track (Thompson and Wallace, 2000). The El Niño/Southern Oscillation (ENSO) has influence on South African precipitation anomalies (Fauchereau et al., 2009; Landman and Beraki, 2010) which may occur through modulation of the local Walker circulation and SSTs in the neighboring Indian and Atlantic Oceans (Reason et al., 2000; Reason and Jagadheesha, 2005). IOD phases are more active during autumn-cessation period; the IOD describes the center of the Walker circulation ascending branches over the eastern Indian Ocean and the south eastern corner of the South Atlantic Ocean (Izumo et al., 2010). Williams et al. (2008) showed that TSA, through several idealized climate model experiments, exhibited a self-evident boost in daily rainfall and rainfall extremes over southern Africa, via locally-based effects such as increased convection and remotely-based effects such as an adjustment of the Walker-type circulation. All of these indices are thus relevant to the large-scale seasonal circulation over the South African region.

Data for these climatic indices were also acquired from the website of the Physical Science Division (PSD) of National Oceanographic and Atmospheric Administration (NOAA/OAR/ESRL) based in Boulder, Colorado, USA (http://www.esrl.noaa.gov/psd). All temporal and spatial information are from 1961 to 2009. Provincial-seasonal measures of spread were correlated with the climatic indices on seasonal time scales. The data used in this study have different sample sizes for each year, hence a Monte-Carlo bootstrap re-sampling procedure (Stephenson and Doblas-Reyes, 2000; Johnson, 2001; Buhlmann, 2002) was used to sample uncertainty in the results, with the re-sampling conducted 1000 times.

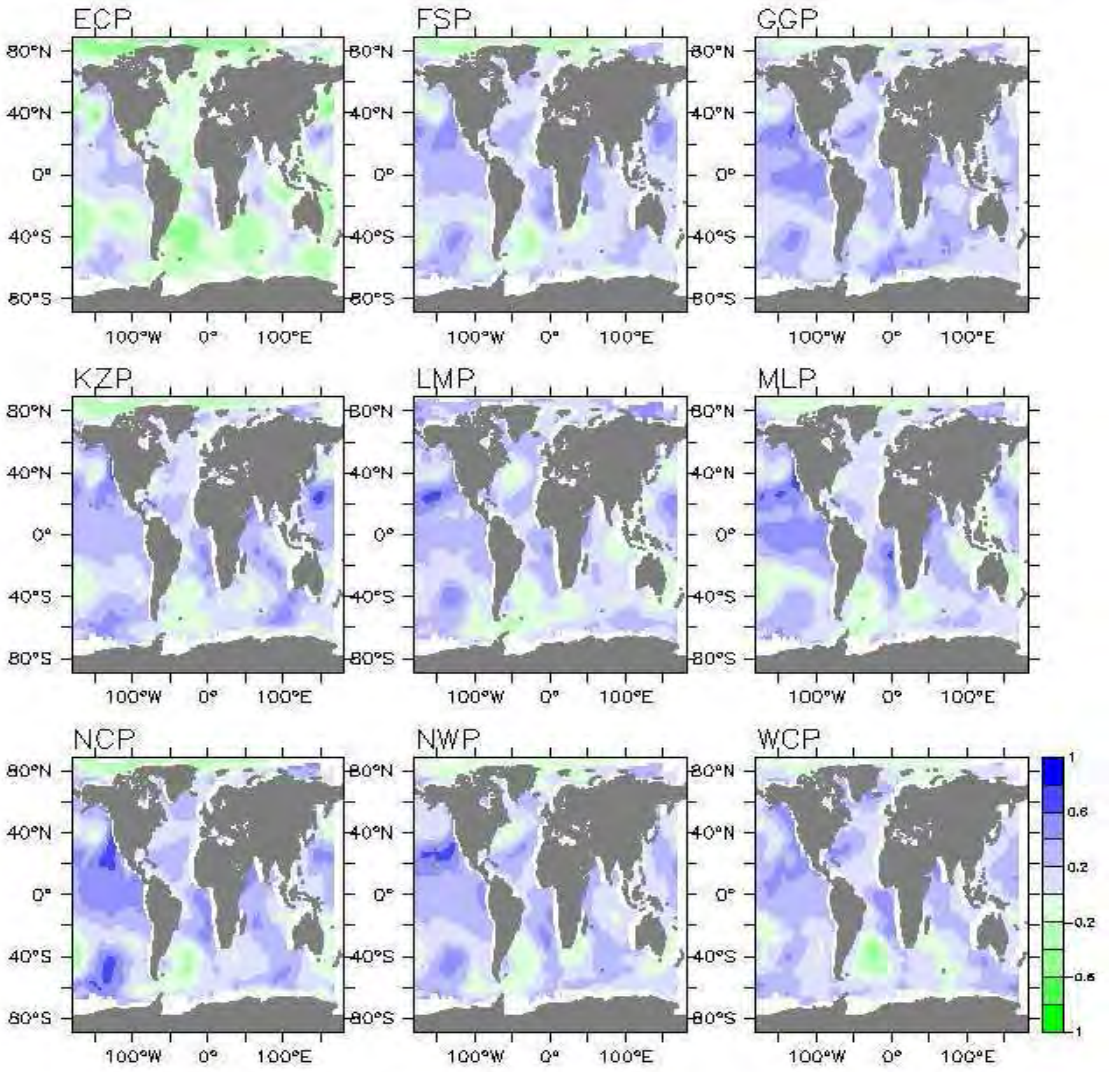

Figure 5.1 Maps of the correlations between time series of the RoP measure of the ensemble spread for provincial precipitation and the observed global SST during spring onset of the rain season for all provinces except WCP, for which it is the cessation period. The trend was removed from all data before calculations. The provinces and their abbreviations are listed in Table 3.1.

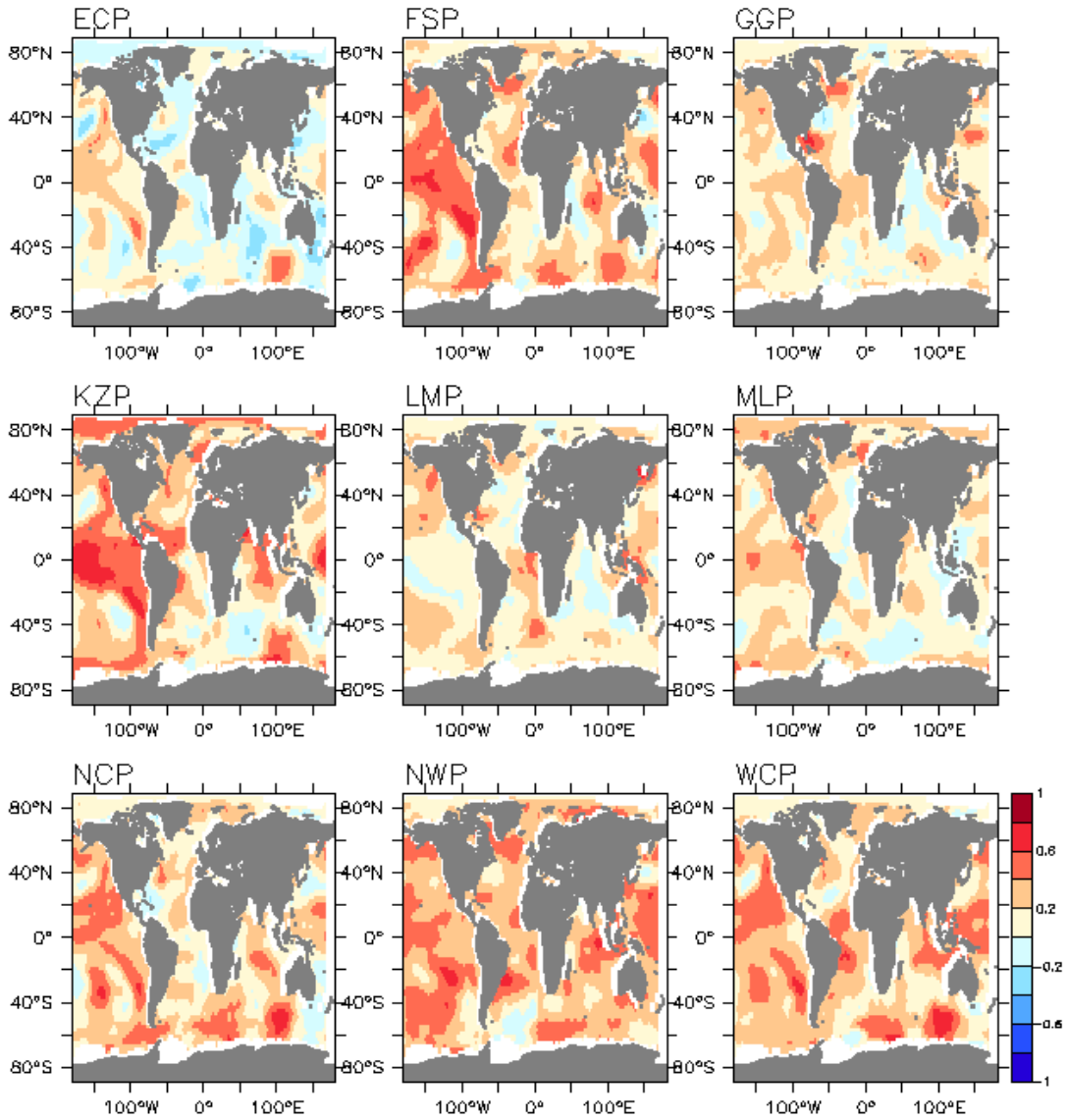

Figure 5.2 Maps of the correlations between time series of the StdDev measure of the ensemble spread for provincial temperature and the observed global SST during the cold winter season. The trend was removed from all data before calculations. The provinces and their abbreviations are listed in Table 3.1.

Table 5.1 List of climate indices used in this study. All indices except the IOD were obtained from http://www.esrl.noaa.gov/psd/data/climateindices/list/.

Climate index	Abbreviation	Description	Reference
Antarctic Oscillation	AAO	Normalized difference in the zonal mean sea-level pressure pattern between 60°S and 40°S. It is a measure of equator-ward / pole-ward shifts in the southern mid latitude storm track. Source: http://www.esrl.noaa.gov/psd/data/correlation/aao.data	Kalnay et al. (1996), Rayner et al. (2003)
Indian Ocean Dipole	IOD	A shift of SST between positive, neutral and negative phases over the western and eastern Indian Ocean. It interacts with El Nino – Southern Oscillation (ENSO). Constructed from SST variability over the Indian Ocean for 35°E-115°E and 25°S-20°N domain.	Annamalai et al. (2005), Izumo et al. (2010)
Multivariate ENSO Index	MEI	Measure of combined atmosphere – ocean El Nino – Southern Oscillation (ENSO) phenomenon, representing shifts of warm surface waters and associated atmospheric convection back and forth across the tropical Pacific Ocean. Source: http://www.esrl.noaa.gov/psd/data/correlation/mei.data	Rasmusson and Carpenter (1982), Wolter and Timlin (2011)
Tropical Southern Atlantic	TSA	A measure of SST gradient in the Gulf of Guinea. Source: http://www.esrl.noaa.gov/psd/data/correlation/tsa.data	Enfield (1999)

5.4 Correlations of provincial-seasonal precipitation spread with climate indices

Panels on Figure 5.3 depict the seasonal correlations between the precipitation spread for the nine South African provinces and climate indices. Average r spans between +/-0.47; but when the error bars are considered, r spread across +/-0.8 which are more notice-able during peak (summer) and dry (winter) seasons. The correlations range from significantly weak to strong relationships in both directions of direct and inverse proportions. There is a high degree of agreement between the correlations using the RoP and StdDev measures. Clear cases of non-zero r agreements can be found in dry (winter) season MEI for Northern Cape Province (NCP) and WCP. Eastern Cape Province (ECP) measures of spread correlated significantly with AAO while Gauteng Province (GGP) correlated with TSA. However, provincial rainfall totals in this season are so small as to have any impacts, except over ECP and WCP. During the spring (onset) season measures of spread over many provinces correlated significantly with more than one climate index. For instance, Free State Province (FSP) and GGP correlated significantly with IOD. FSP, GGP, NCP, North West Province (NWP) and WCP also correlated significantly with MEI while FSP and GGP also responded to TSA. During the summer rain peak, both measures of spread agreeably correlated significantly with MEI over WCP. In autumn (cessation) period, only FSP measures of spread correlated significantly with TSA. Few instances of major differences are in AAO over Limpopo Province (LMP) and (ECP) during peak and onset seasons respectively. In general, the degrees of correlations differ from index-to-index, season-to-season and province-to-province. There is no gross spatial pattern to the correlations at the national scale.

Figure 5.3 is summarized in Table 5.2, which shows the frequency of province-season combinations with correlations inconsistent with zero at the 10% significant level. For each season in the table, if the indices and the measures of spread are independent, then approximately 1 out of 9 provinces per index would be expected to be significant by random chance; counts above 1 are thus suggestive that we are finding evidence of physically-based co-variation. The 1-in-9-expected-by-chance rule of thumb should be considered a bare minimum, rather than sufficient; because the provinces are hardly independent of each other climatologically. Therefore, on seasonal time-scale, MEI is the most influential regarding precipitation predictability over South Africa. MEI is the only index that has more than the required statistical provincial-seasonal realizations during rainfall onset and peak periods. However, its influence is zero during cessation period when TSA dominates. Furthermore, IOD and TSA processes may also determine precipitation predictability during the onset period.

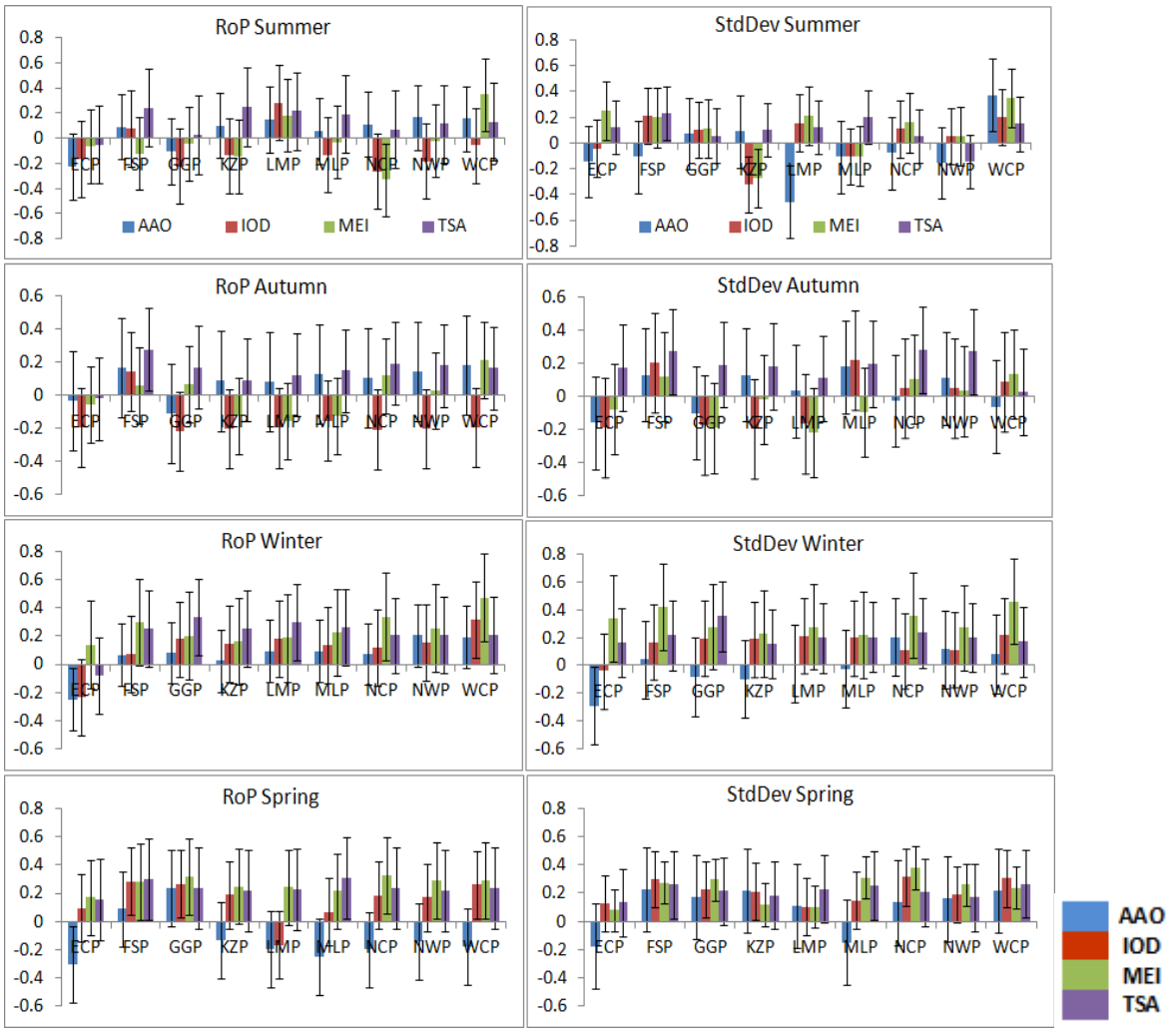

Figure 5.3 Correlations between measures of seasonal precipitation spread for the nine South African provinces and the indices of large-scale climate variability listed in Table 5.1 (AAO, IOD, MEI, and TSA). Black error bars indicate 90% confidence intervals estimated through a Monte-Carlo bootstrap procedure.

Table 5.2 Frequency of significant correlations between provincial-seasonal predictability measures and the large-scale climate indices listed in Table 5.1. At random, only 1 out of 9 provinces per index are expected to have correlations significantly different from zero at the two-sided 10% significant level. On precipitation side, note that the peak and dry seasons are respectively dry and wet seasons for WCP.

Climate index	Precipitation			Temperature		
	Season	RoP	StdDev	Season	RoP	StdDev
AAO	Peak (Summer)	0	2	Hot (Summer)	0	0
IOD		0	1		1	2
MEI		2	3		3	7
TSA		0	1		4	4
AAO	Cessation (Autumn)	0	0			
IOD		0	0			
MEI		0	0			
TSA		1	3			
AAO	Dry (Winter)	1	1	Cold (Winter)	0	0
IOD		1	0		1	3
MEI		2	4		2	6
TSA		2	1		0	1
AAO	Onset (Spring)	1	0			
IOD		3	5			
MEI		4	6			
TSA		2	3			

5.5 Correlations of provincial-seasonal temperature spread with climate indices

The seasonal correlations between the measures of spread for the nine South African provinces and climate indices for temperature are illustrated on the panels of Figure 5.4 for summer and winter. In similarity to precipitation analysis, no province, no season and no climate index demonstrates any particular pattern in the seasonal-provincial distributions of r during these two seasons. Potential correlations span from -0.6 to +0.8. There exist some degrees of structural similarities between the RoP and StdDev graphical representations on Figure 5.4. Both measures of spread agreeably in summer correlated significantly with MEI over ECP, KwaZulu-Natal Province (KZP) and WCP; with IOD over ECP and with TSA over FSP, MLP and NWP. In winter, measures of spread over KZP and WCP correlated significantly with MEI.

Summaries of the frequency of significant correlations are given in Table 5.2. The table shows the frequency of province-season combinations with correlations inconsistent with zero at the 10% significant level; where the condition is the same as that of precipitation on seasonal time-scale. That is, only 1 out of 9 provinces per index is expected to have a significant correlation in a given season by random chance. Therefore, this implies that IOD and MEI processes have significant influences on the South African near air surface temperature predictability measures in both summer and winter. However, MEI has more of

the required statistical provincial-seasonal realizations than IOD in both seasons. TSA's influences on the measures of temperature predictability is restricted only to summer season.

Precipitation over WCP and ECP in winter and year-round respectively results from frontal activities which are modulated by southern mid-latitude circulation (Tyson and Preston-Whyte, 2000). The AAO reflects the equator-ward / pole-ward variations in the position of the southern mid latitude storm track (Thompson and Wallace, 2000). Thus, the general lack of significant co-variability between the measures of spread and AAO over WCP and ECP suggests that the predictability of variations in the frequency and intensity of mid-latitude flows structures, such as cut-off-lows, are not related to the variations in the frequency and intensity themselves, at least in a linear way.

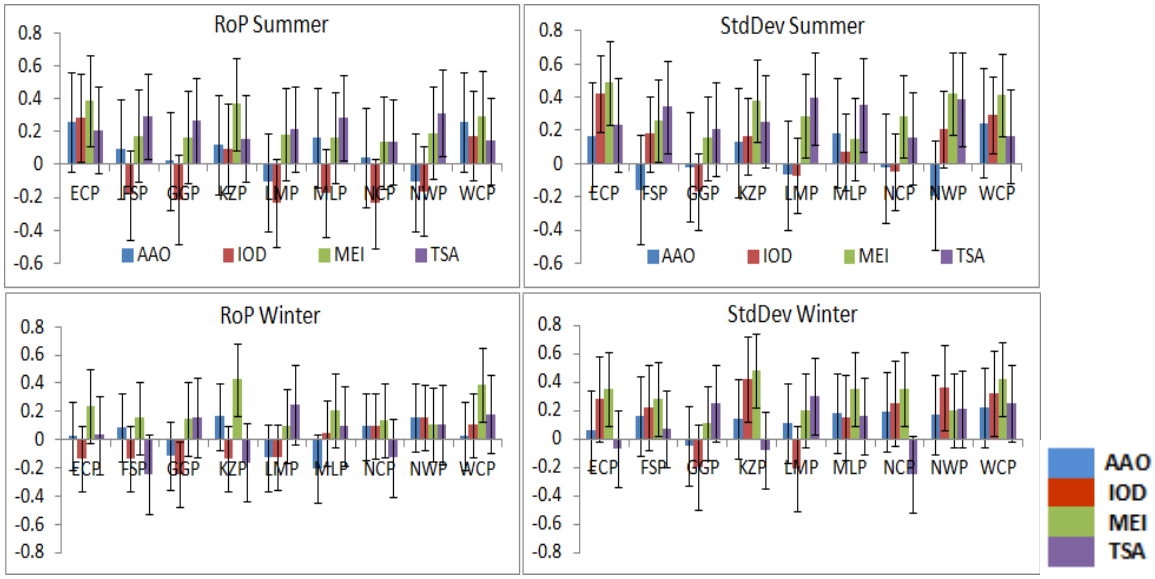

Figure 5.4 Correlations between measures of winter and summer temperature spread for the nine South African provinces and the indices of large-scale climate variability listed in Table 5.1 (AAO, IOD, MEI, and TSA). Black error bars indicate 90% confidence intervals estimated through a Monte-Carlo bootstrap procedure.

This study has been able to establish the facts that the South African provincial measures of predictability significantly co-vary with the observed global SST far and near on seasonal time scale, suggesting that the climatic driving factors / forces may be locally or remotely based. It further answered the probing question of whether there are any SST influences on seasonal climate predictability via ensemble spreads. Results from this study revealed that the degrees of co-variability differ from index-to-index, season-to-season and province-to-province. There are no clear large-scale patterns in the seasonal-provincial correlations, whether in space or across seasons. This study affirms that ENSO, as described by MEI, is the most influential in the predictability of seasonal precipitation over South Africa. It is the only climate index that has more than the required statistical provincial-seasonal realizations

during rainfall peak period in summer. This is in line with the earlier findings of Fauchereau et al. (2009) and Landman and Beraki (2010) that ENSO has the largest influence on South African precipitation anomalies. The IOD and also appear to have some role in influencing predictability in other seasons. This study is also indicating that there may be limits to the extent to which year-to-year variations in the predictability of seasonal climate forecasts might be understood, either because: (1) all significant climate predictors are of tropical origin; (2) the responses of predictability measures to predictors are, on the average, weak; (3) predictors are more complex in nature than can be represented by the traditionally simple climate index, or (4) because the responses in predictability measures are nonlinear in nature.

5.6 Statements of cautions

The results presented here come from analysis of a single climate modeling system; therefore, the robustness of the results to model selection is unknown. Moreover, this modeling system is not particularly modern and certainly does not represent a state-of-the-art model. But this study could not be conducted with a computationally expensive state-of-the-art model, because no computational resources exist, at the moment, for running the large ensembles of simulations required to precisely characterize variations in ensemble spread; therefore, these data sets are currently unique. Whether another model would reveal the same relationship is unknown, consequently the specific values should not be taken too literally.

Another concern is that this study only looked for linear relationships between predictors and the variations in predictability. Although significant correlations were found, there was no indication of the mechanism for causation. It may be that climate indices are influencing the atmosphere in a way that affects predictability, or that climate indices are responding to some other driver which is also affecting the seasonal climate predictability over South Africa; such a driver could be elsewhere within the climate system or could be external in nature, for instance through anthropogenic emissions.

Despite the removal of linear trends from the time series of the analysis, nonlinear responses to external drivers may still be present in the data, as suggested by the mostly positive correlations for temperature predictability against SSTs globally. Beyond all these, the mechanisms through which various predictors could affect the spread of simulations over South Africa remain undefined.

5.7 Implications of spread variations on forecast skill

Are these variations in simulation spreads in anyway supported by the observations? We investigated by a briefly evaluating seasonal forecast skills using ranked probability skill score (RPSS; Murphy, 1988a; Wilks, 1995). RPSS is more a measure of forecast relative accuracy. It compares the performance of an ensemble forecasting system against a simple climatological forecast through

$$\mathrm{RPSS} = 1 - \frac{\mathrm{RPSfcst}}{\mathrm{RPSclim}}$$

where RPSfcst is the ranked probability score for the forecast, which assesses how well the ensemble forecast predicted the category, in a discrete set of categories, into which the observations fell, and RPSclim is score if we a adopted a simple forecast of the probabilities observed over some climatological period. Murphy (1988a) and Wilks (1995) have shown that positive skills are normally desirable and that they represent a minimal level of acceptable performance by forecasts. The University of East Anglia Climate Research Unit (CRU; Mitchell and Jones, 2005) monthly dataset for precipitation and near surface air temperature were used as observations in our calculations of the RPSS.

On provincial basis we sorted seasonal values of measures of spread, StdDev and RoP, from each year into four equi-probable bins. Bin 1 contains the smallest values of the measures of spread while largest values are accommodated in bin 4. Corresponding hindcast and observed precipitation and temperature information in each bin were used to calculate RPSS on a seasonal-provincial basis. The results are graphically depicted in Figures 5.5 and 5.6 for precipitation and temperature respectively. For precipitation, all provinces and seasons exhibit patterns of lines tilting down towards the right, effectively showing that the narrower the ensemble spread the higher the skill of the hindcast. Both measures of spread also exhibited seasonal movements of skills. Figure 5.5 shows that almost all provinces are of positive RPSS in summer; the positive RPSS tends to negative in autumn and spring as bin 2 and beyond are approached while all provinces are of negative RPSS in winter. Figure 5.6 show that while tilting also exists for some seasons and provinces for temperature RPSS-spread comparisons, slopes for other seasons and provinces are not easily noticeable, in contrast to precipitation. Seasonal movements of skill in temperature are almost similar to those of precipitation, except for less obvious crossing of zero axes of RPSS as bins containing wider spreads are being approached.

Distributions of RPSS on Figures 5.5 and 5.6 show that there is observational evidence that the ensemble spread emanating from HadRM3P, the regional model used in this study, reflect some fundamental issues about the real climate system. To further support this, it is pertinent to note that most of the El Niño and La Niña years as displayed on http://ggweather.com/enso/oni.htm and as used by Landman and Beraki (2010) and Browne (2011) fall within bins 1 and 2.

The skill scores shown in Figures 5.5 and 5.6 are often not that high, sometimes not achieving the positive values normally considered desirable. Despite this, there is a clear linear relationship between the spreads of the ensemble of simulations and the skill scores, particularly for precipitation. Such a relationship could only arise if the ensemble spreads are reflecting true variations in the predictability from year to year. Given the low skill scores but strong relationship between the scores and the ensemble spreads, it may be that, at least for this model, the limits of predictability are in fact more predictable than the central forecast estimate itself.

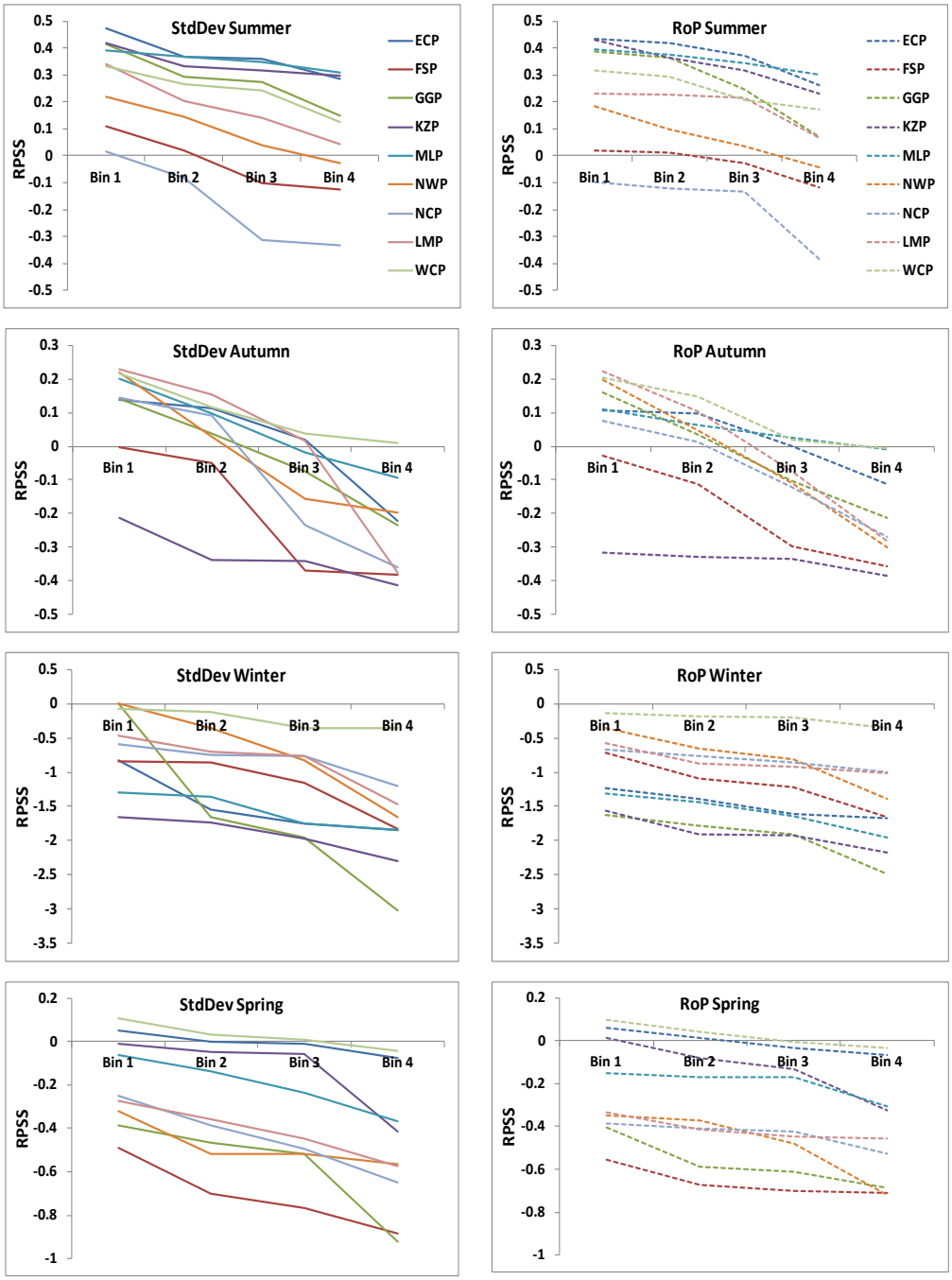

Figure 5.5 Average seasonal-provincial ranked probability skill score, RPSS, for precipitation as a function of ensemble spread. Measures of spread, StdDev (left panels) and RoP (right panels) were sorted into one of four equi-probable bins (horizontal axis). Corresponding hindcast and observed precipitation and temperature information in each bin were used to calculate RPSS on a seasonal-provincial basis. Bin 1 contains smallest values of the measures of spread while largest values are accommodated in bin 4.

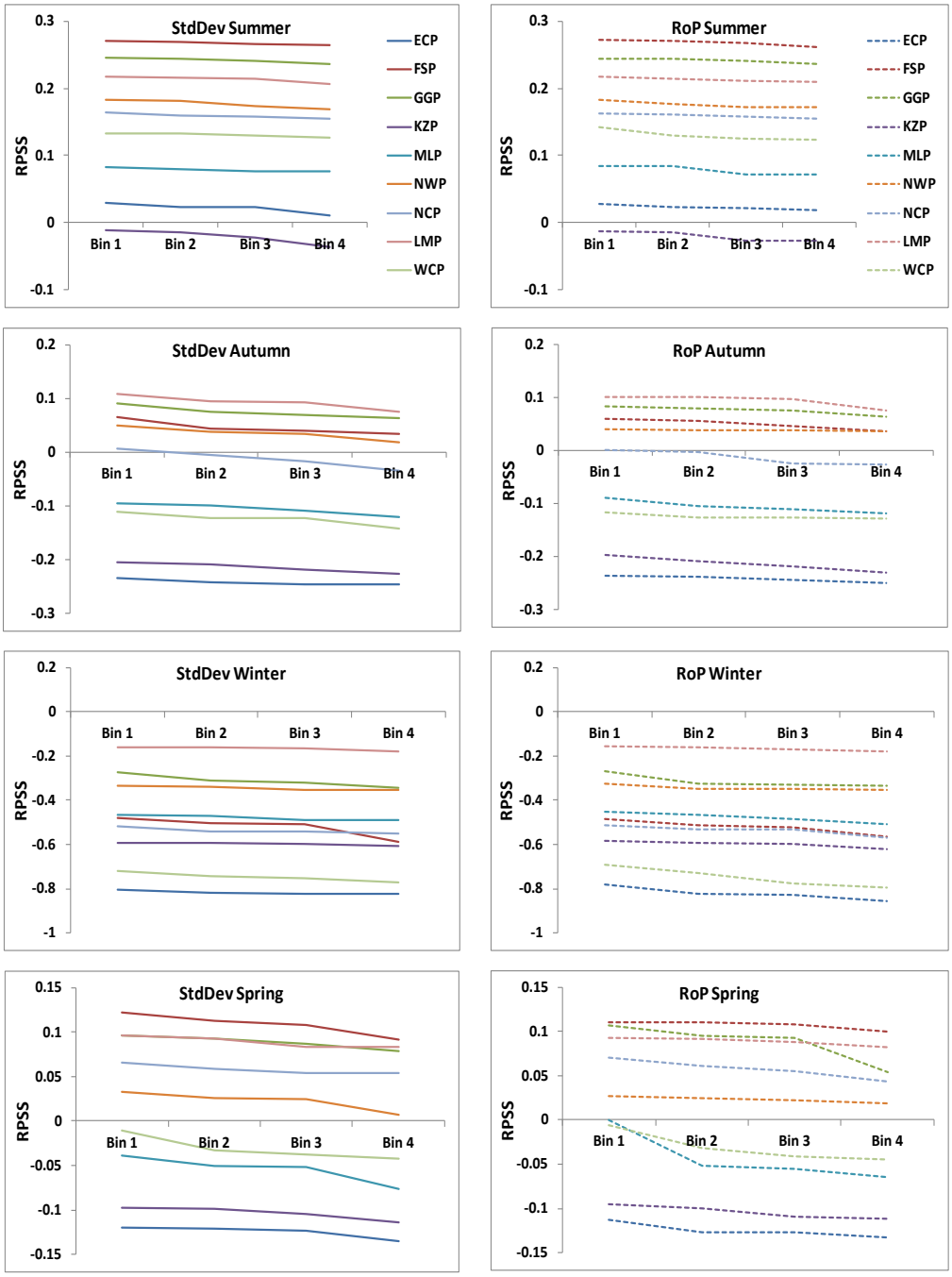

Figure 5.6 Average seasonal-provincial ranked probability skill score, RPSS, for temperature as a function of ensemble spread. Measures of spread, StdDev (left panels) and RoP (right panels) were sorted into one of four equi-probable bins (horizontal axis). Corresponding hindcast and observed precipitation and temperature information in each bin were used to calculate RPSS on a seasonal-provincial basis. Bin 1 contains smallest values of the measures of spread while largest values are accommodated in bin 4.

6 Simulations used in the attribution analyses

6.1 Purpose of simulations

This section begins the second part of the report, which examines the degree to which anthropogenic emissions may have altered the chance of monthly extreme events occurring. This section reports on the generation and characterization of simulations specifically designed for the task, and the application of these simulations to the problem of evaluating the attribution of the chance of extreme weather events to anthropogenic emissions will be discussed in Sections 7 and 8. In essence, those analyses involve the comparison of output from simulations driven under real world conditions against the output from simulations driven under conditions that might have been had anthropogenic greenhouse gas conditions never occurred. This section elaborates on descriptions in Stone et al. ("Designing a real-time weather risk attribution forecast system", in preparation).

The attribution studies reported in later sections are based on two sources of climate model simulations which are described in this section. The first source, generated at the University of Cape Town (UCT), comes in two forms: a forecast mode, and a hindcast mode. The second source of simulations from Lawrence Berkeley National Laboratory, U.S.A. (LBNL), follows a nearly identical experimental setup; but have only been generated in hindcast mode. The models used are HadAM3P-N96 (at about 1.5^{o} spatial resolution), HadAM3-N48 (about 3^{o}), and CAM5.1-2degree (about 2^{o}). All three are models of the atmosphere and land surface processes, thus they have been run under changing atmospheric composition, sea surface temperatures, and sea ice coverage. Specific details of the simulations are listed in Table 6.1 and in the following two sections.

6.2 UCT/HadAM3P-N96 and UCT/HadAM3-N48 simulations

6.2.1 Reference real-world forecasts

The Climate Systems Analysis Group (CSAG) at the University of Cape Town has been issuing seasonal weather forecasts since 2002 (issued at http://www.gfcsa.net/csag.html, Browne et al., 2011). Until June 2010, these forecasts were generated with a version of the U.K. Met Office's HadAM3 model (Pope et al., 2000). This version of HadAM3, run at N48 resolution (3.75^{o} longitude by 2.5^{o}) with 19 vertical levels, includes the mixed phase precipitation scheme as this has been found to improve the model precipitation over southern Africa (Wilson, 2000). Starting in June 2010, the publicly posted forecasts have been generated using the HadAM3P version of the U.K. Met Office model which is used as the standard driving global model in the PRECIS regional modeling project (Jones et al., 2004). HadAM3P shares the same underlying dynamical core as HadAM3, but uses more recently developed physical parameterization schemes and runs at N96 resolution (1.875^{o} longitude by 1.25^{o}) with 19 vertical levels. Neither model is of the resolution generally used in current state-of-the-art seasonal forecasting activities, but are rather more comparable to the coupled atmosphere-ocean models used both in the international CMIP5 project which formed the benchmark for the most recent Assessment Report of the Intergovernmental Panel on Climate

Change and also in the current international CMIP5 project serving the upcoming Assessment Report. However, HadAM3P at N96 is considered capable of resolving synoptic systems, while HadAM3 at N48 indicates some comparison for the potential importance of resolving these features.

Table 6.1 Simulations performed at UCT (HadAM3P-N96 and HadAM3-N48) in contribution to this project, and simulations obtained from LBNL (CAM5.1-2degree) following the same experiment setup. The right-most column lists the number of simulations generated following the specifications in the other columns with each simulation differing only in the exact weather state set at the start of the simulation.

Label	Description	Model	Period	N
All-Hist/est1	Driven with observed increases in greenhouse gas concentrations and monthly variations of sea surface properties (Produced toward Deliverable 1)	HadAM 3P-N96	1960-01-01 to 2013-07-31	10
			2008-09-01 to 2011-10-31	50
		HadAM 3-N48	1960-01-01 to 2008-12-31	10
			2009-01-01 to 2013-07-31	50
		CAM5.1 -2degree	1959-01-01 to 2012-12-31	56
NonGHG-Hist/ HadCM3-p50-est1	Like the All-Hist simulations but with greenhouse gas concentrations at pre-industrial levels and the ocean cooled accordingly (Produced toward Deliverable 5)	HadAM 3P-N96	2008-11-01 to 2013-07-31	10
			2008-09-01 to 2011-10-31	50
		HadAM 3-N48	2009-01-01 to 2013-07-31	50
		CAM5.1 -2degree	2008-01-01 to 2012-12-31	56

The generation of the forecasts follows a standard two-tiered approach, as outlined in Figure 6.1. For a forecast generated and issued in March, a 10-member initial condition ensemble of simulations is started from the beginning of January and run through the end of June,

providing a three-month forecast coverage (i.e. April-June in this example) (Figure 6.2). Monthly mean sea surface temperatures (SSTs) for mid-January and mid-February are taken from the National Oceanic and Atmospheric Administration (NOAA) Optimum Interpolation version 2 (OI.v2) observational products (Reynolds et al., 2002). SSTs for later months are estimated by adding the observed February SST anomaly from the 1960-2000 climatological mean to the climatological means of these later months. Daily SSTs are estimated through linear interpolation between the middles of the months; thus, in the March forecast January is the only month to have entirely observationally-based SSTs. A seasonally varying climatology of sea ice coverage is used, with obvious issues for forecasts in high latitudes. The atmospheric and land-surface initial conditions are taken from the end of the first month in the previous month's forecast simulation (e.g. for the March forecast they come from the end of December in the February forecast). No assimilation of data from observational measurements or analyses is performed, which is crucial for the attribution forecast because otherwise results would be strongly conditioned on the atmospheric state experienced under anthropogenic greenhouse gas forcing. This approach also means that concatenation of the first months of subsequent forecast simulations results in continuous hindcast series, which are also contiguous with the ten climatological hindcast simulations started in 1960. Of course, strictly speaking these hindcasts are "AMIP-style" simulations because the initial conditions are not derived from actual observed states, but the distinction disappears in the structural framework of this forecasting system.

In this report, we discuss forecasts generated from December 2008 through to February 2014 using both HadAM3-N48 and HadAM3P-N96 (Table 6.1). Some of the earlier forecasts were actually generated after the fact, but as if it was in real-time. The HadAM3-N48 forecasts described here are not the same as those issued publicly prior to June 2010, and differ in some specifics and in use of computing platform from those earlier publicly issued forecasts. These new HadAM3-N48 forecasts continue to be generated for research purposes and for the attribution forecast product described in this report but are not currently included as part of the publicly issued seasonal forecast.

6.2.2 Counterfactual "non-greenhouse-gas" forecasts

For each of these two forecast models, a second 10-member ensemble of simulations is generated to estimate what the forecast might have been had human activities never emitted greenhouse gases. For these non-greenhouse-gas, or "non-GHG", forecasts the prescribed greenhouse gas concentrations in the model are reduced to pre-industrial values and the prescribed SSTs are altered according to an estimate of the warming attributable to our historical greenhouse gas emissions (Figure 6.1). These non-GHG forecasts are identical to the real forecasts in all other respects, including in sea ice coverage. The non-GHG simulations were initially started from the October 2008 initial conditions of the real forecasts' hindcasts (i.e. for the December 2008 issue), and have been run separately from the real forecasts since then.

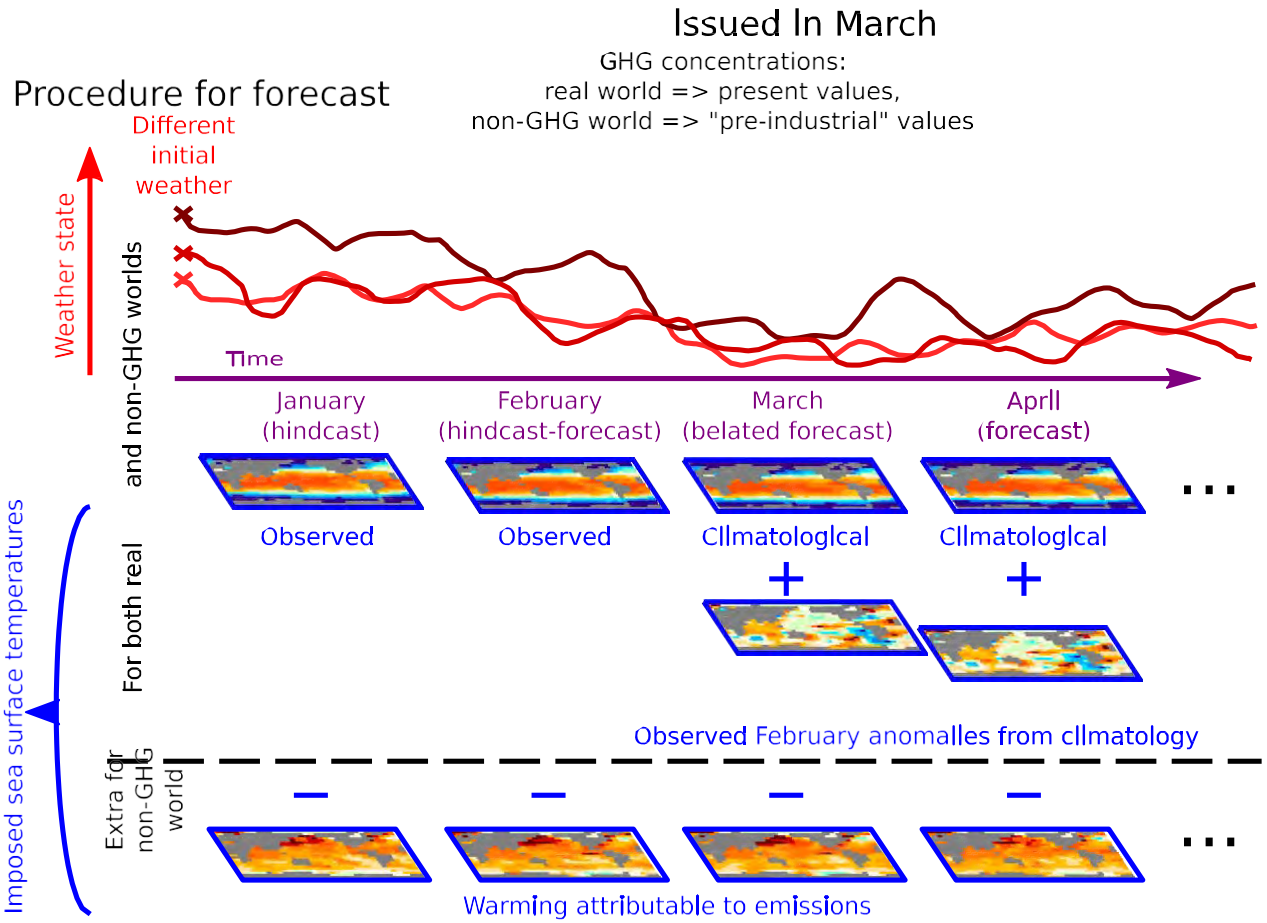

Figure 6.1 Schematic of the procedure for producing the seasonal forecasts used in the UCT attribution forecast system. Observed greenhouse gas concentrations are imposed for the real forecasts, while pre-industrial concentrations are imposed for the non-greenhouse-gas (non-GHG) forecasts. Sea surface temperatures for the non-GHG forecasts are modified by subtracting an estimate of the geographical warming attributable to historical greenhouse gas emissions.

The warming attributable to greenhouse gas emissions is estimated using an optimal total least squares regression analysis (Allen and Stott, 2003; Stott et al., 2003) on data from the HadSST2 dataset of gridded observational measurements (Rayner et al., 2006) and output from simulations of the HadCM3 coupled ocean-atmosphere climate model (Stott et al., 2006). This analysis estimates objective scaling factors by which the amplitudes of the modeled response patterns to various external forcings should be adjusted to match the observations. The analysis here indicates that the response of the HadCM3 coupled ocean-atmosphere model to anthropogenic greenhouse gas forcing should be adjusted by a factor of 1.3. In order for these forecasts to be generated in real-time, we are currently unable to follow Pall et al. (2011) in generating large ensembles sampling the uncertainty in the attributable pattern and scaling factor; thus we use only this single pattern-scaling estimate for now. This attributable SST warming estimate is subtracted from the SSTs used in the seasonal forecast as indicated schematically in Figure 6.1.

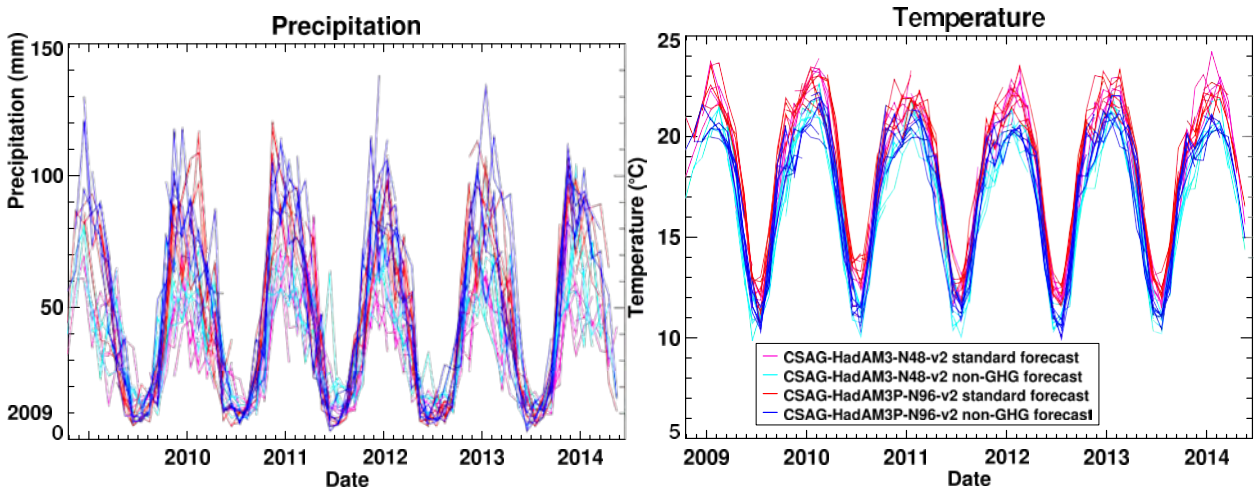

Figure 6.2 Time series of monthly temperature and precipitation over South Africa output from one of the forecast simulations each of HadAM3P-N96 and HadAM3-N48 and for each of the real-world and non-greenhouse-gas-world (non-GHG) scenarios. Each line shows the time series starting from the hindcast month, through the then-current month, and on through the three forecast months.

6.2.3 Additional hindcast simulations

In addition to the above sets of 10 simulations generated with both models, additional sets of 50 simulations were generated with both models and for both scenarios (real-world and nonGHG-world) in hindcast mode (Table 6.1). These simulations cover the September 2009 (after spin-up) to October 2011 period. These are fully consistent with the hindcast output from the HadAM3P-N96 forecast, but because of slight configuration differences, the 50-member HadAM3-N48 simulations must be considered separately from the 10-member forecast simulations.

6.2.4 Simulations with an updated model configuration

An additional set of simulations generated at UCT are nearing completion. These simulations are with the HadAM3P-N96 model, run specifically under the protocols of the C20C+ Detection and Attribution Project (Section 6.5.1). These simulations are currently in the "hindcast" mode and have been augmented in the following ways from the HadAM3P-N96 simulations described above:

- Inclusion of time-varying aerosol burdens, stratospheric ozone, stratospheric (volcanic) aerosol burden, and solar luminosity in the "real-world" simulations, whereas these were not varied through time in the above simulations.
- Inclusion of time-varying land covers in both the "real-world" and "natural-world" simulations, whereas land cover was not varied in the above simulations.
- Inclusion of time-varying sea ice coverage, whereas only the climatological mean annual cycle was used in the above simulations.

- As with the above simulations, a 10-member ensemble of "real-world" simulations has been run from 1960 to present. However, an additional 40 simulations have been run starting in 1996.
- The counterfactual world is for a "natural world" in which all anthropogenic emissions had never occurred.
- 50 "natural world" simulations are being run for the 1996 to present period.
- Ocean surface temperatures for the "natural world" simulations have been cooled according to the "CMIP5/est1" estimate forming the common benchmark estimate for the C20C+ Detection and Attribution Project (Stone, 2014).
- Sea ice coverage has been altered in the "natural world" simulations for consistency with the cooler ocean according to the method of Pall et al., 2011 (Stone 2014).

Two additional sets of simulations for the "natural world" scenario, but each set using a different attributable ocean warming estimate than the "CMIP5/est1" estimate, are also planned. Together, these simulations will comprise a full contribution to the core experiment of the C20C+ Detection and Attribution Project. Additionally, these new simulations will form the basis for an updated UCT seasonal forecasting system. While generated as part of this project, these simulations have not yet been analyzed in the studies reported in the following sections.

6.3 LBNL/CAM5.1-2degree simulations

Lawrence Berkeley National Laboratory has produced a similar set of simulations (corresponding to the hindcast mode) with the CAM5.1-2degree model. This model as a completely different origin from the HadAM3 models and thus can be considered useful for ascertaining the sensitivity of results to structural and parameter uncertainty in model formulation. These simulations number 56 for both real-world and nonGHG-world scenarios and cover the January 1959 through December 2012 period for the real-world simulations and the January 2008 through December 2012 period for the nonGHG-world simulations. These simulations included some interannual variations in atmospheric composition not included in the HadAM3 runs. They used the same NOAA OI.v2 sea surface temperatures and greenhouse gas attributable warming estimate. However, they also included observed variations in sea ice coverage as well as an adjustment of sea ice coverage in the nonGHG-world scenario for consistency with the cooler ocean temperatures (Pall et al., 2011; Stone, 2014).

6.4 Characteristics of the output of these simulations

Estimates of the degree to which anthropogenic emissions have altered the chance of extreme events based on these simulations, as discussed in the following sections, depend on the simulations spanning the range of possible weather realizations during the time period and at the location under investigation. However, the simulations introduced above have been produced with atmospheric models. The anomalous ocean state, for instance whether an El Niño event has occurred, is purely prescribed based on observations. Thus conclusions in the following sections are conditional on the observed ocean state. How much does this matter?

Figure 6.3 shows monthly output at two different locations. The average temperature over the Niño 3.4 region of the tropical Pacific is a standard measure of the El Niño/Southern Oscillation (ENSO) phenomenon. As expected, 1.5m surface air temperatures over this region from the HadAM3P-N96 model are tightly constrained by the prescribed ocean surface temperatures 1.5m below the measurement height. Thus within each scenario, interannual variations in the sea surface temperatures overwhelm inter-simulation spread. For the model grid box situated over Kimberley, Northern Cape, however, the situation is very different. Kimberley is used here to represent a continental location far from local interaction with ocean. In this case model spread dominates over the interannual variability, but there do remain instances of interannual differences, for instance in the earlier cessation of the wet season simulated in 2009 than in subsequent years. Thus, it appears that while the conditionality on observed sea surface temperatures may not be a major issue in many cases, it remains important that attribution studies examine sensitivity to it. The simulations discussed in this section, are the first to comprise multiple years for the nonGHG-world scenario and thus are the first to permit examination of this sensitivity.

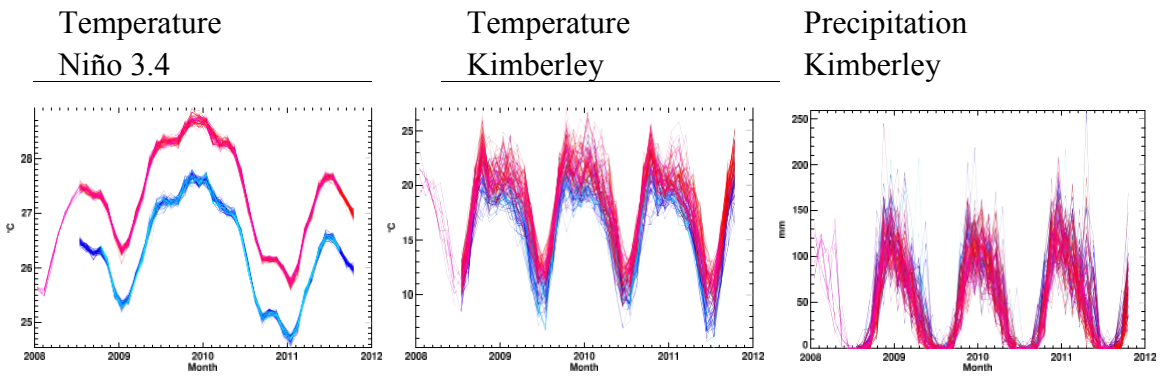

Figure 6.3 Monthly surface air temperature and precipitation from the HadAM3P-N96 attribution simulations. Red and pink denote All-Hist/est1 simulations while light and dark blue denote NonGHG-Hist/HadCM3-p50-est1 simulations. See Table 6.1 for a description of these simulations. a) temperature over the Niño 3.4 region of the tropical Pacific, b) temperature at the model grid box located over Kimberley, c) precipitation at the model grid box located over Kimberley.

6.5 Application of simulations beyond this project

6.5.1 International CLIVAR C20C+ D&A Subproject

The International CLIVAR Climate of the 20th Century Plus Project (C20C+) is an international collaboration of approximately two dozen climate modeling groups around the world. At the C20C+'s 5th Workshop in Beijing, China, in 2010, it was agreed that C20C+ would adopt a new core project, name the "Detection and Attribution Subproject" (D&A Subproject) (Kinter and Folland, 2011). Following trial experiments and other preparatory work, the importance of the D&A Subproject as a core element of C20C+ was reaffirmed at

the 6th Workshop in Melbourne, Australia, in 2013.

The C20C+ D&A Subproject will generate a large number of atmospheric climate model simulations of the past 50 years representing plausible alternative realisations of weather given the climatic boundary conditions that have been observed (http://portal.nersc.gov/c20c). These boundary conditions include anthropogenic radiative forcings (such as greenhouse gas concentrations, sulphate aerosol burden, etc.), natural radiative forcings (changes in the solar luminosity, explosive volcanic eruptions), and ocean surface conditions (temperature, sea ice coverage). These models will also generate large numbers of simulations driven under conditions representing plausible estimates of what the climate might have been in the absence of past anthropogenic emissions. Together, these simulations will be used for analysis of past trends in extreme weather events, attribution of changing probability of extreme events, and for other analyses of climate variability.

The UCT/HadAM3P-N96 All-Hist/est1/v1-0 ("real-world") and NonGHG-Hist/HadCM3-p50-est1/v1-0 ("nonGHG-world") simulations under taken in the project reported here, along with the LBNL/CAM5.1-2degree simulations, have served as a trial experiment for the C20C+ D&A Subproject. These simulations are thus serving as the template for the core experiment of the C20C+ D&A Subproject now underway since late 2013. In addition, the UCT/HadAM3P-N96 All-Hist/est1/v2-0 and NonGHG-Hist/CMIP5-est1/v2-0 simulations run under this project constitute UCT's contribution to the core C20C+ D&A Subproject; given the early starting date relative to other institutions, UCT's simulations will be amongst the first completed.

6.5.2 Analysis by other researchers

The role of the All-Hist/est1/v1-0 and NonGHG-Hist/HadCM3-p50-est1/v1-0 simulations of UCT/HadAM3P-N96 as a trial experiment for C20C+ includes being published on the C20C+ D&A Subproject's data portal at http://esg.nersc.gov (under project "c20c"). Researchers at the following institutions have specifically reporting downloading and analyzing the UCT and LBNL simulations:

- ETH Zurich, Switzerland
  - Angélil, O., D. A. Stone, M. Tadross, F. Tummon, M. Wehner, and R. Knutti. 2014. Attribution of extreme weather to anthropogenic greenhouse gas emissions: sensitivity to spatial and temporal scales. Geophysical Research Letters, submitted.
- Lawrence Berkeley National Laboratory, U.S.A.
  - See talks, posters, and papers in preparation by D. Stone and M. Wehner listed in Section 10.1.
- Stanford University, U.S.A.
- University of Melbourne, Australia
  - Lewis, S., and D. Karoly. Can we attribute Australia's record 2010-2012 rainfall to a particular cause? Poster at 6th Workshop of the International CLIVAR C20C Project, Melbourne, Australia, November 2013.

Output from these simulations was also distributed by USB memory stick to 22 African (including South African) researchers at the Africa Climate Conference in Arusha, Tanzania, in October 2013.

Taken together, the HadAM3P-N96 and CAM5.1-2degree simulations described above constitute a unique data set. While "event attribution" ensembles representing the real world and a natural world that might have been have been generated at a handful of stations worldwide, the simulations described above are the only ones to span multiple years. They are also the only case where two climate models have been run under the same experimental setup, thus allowing a crude form of inter-model comparison for the first time.

7 Attribution of extreme events to anthropogenic greenhouse gas emissions

7.1 Experimental approach

This section describes analyses of the monthly climate output from the attribution simulations described in Section 6. In particular, these analyses were designed to estimate the degree to which anthropogenic emissions have altered the chance of unusual monthly weather events. This comprises one experimental approach to characterizing the degree to which anthropogenic emissions have altered the occurrence of extreme weather events, frequently termed "event attribution" (Stott et al., 2013). This section elaborates on results presented in Stone et al. ("Designing a real-time weather risk attribution forecast system", in preparation) and Stone et al. ("Human contribution to extreme monthly weather over South Africa", in preparation).

The approach used here follows the risk-based methodology described in Stone and Allen (2005). While Stone and Allen (2005) used the "Fraction Attributable Risk" (FAR) measure, in this section we adopt the "Risk Ratio" (RR) measure (Figure 7.1). If the chance of the event under current real-world climate conditions is Preal and the chance under the conditions of a counterfactual contemporary world in which human had never emitted greenhouse gases is PnonGHG, then the Risk Ratio is:

$$RR = \frac{Preal}{PnonGHG}$$

Note that the FAR is related to the RR through $AR = 1 - \frac{1}{RR}$ (1)

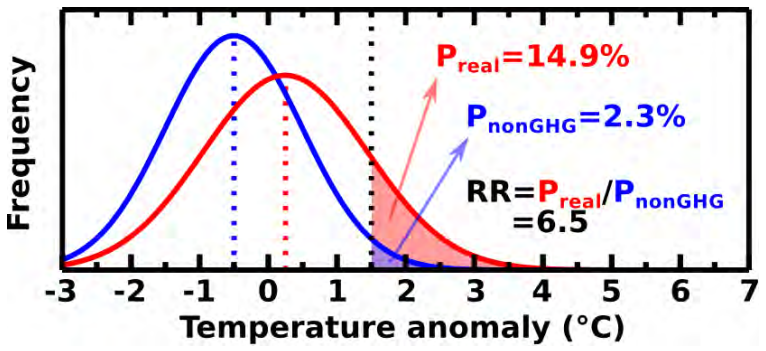

Figure 7.1 Schematic of the estimation of the Risk Ratio. If we have estimates for the probability distribution of some weather metric in both "real-world" and "nonGHG-world" conditions, then the RR is the ratio of the area of those distribution beyond a certain threshold.

In the analyses reported in this section, we have estimated the Preal and PnonGHG values from the climate model simulations discussed in Section 6. This estimation is either from

direct sampling of the empirical distribution, in cases where the threshold falls well within the main area of the distribution, or from a Gaussian fit to the model output (or the logarithm of in the case of precipitation) in cases where the threshold falls within the tails of the distribution. More advanced statistical estimation techniques exist, but within the current experimental nature of the project these estimation methods have proven sufficient robust.

7.2 Monthly attribution forecast

The Weather Risk Attribution Forecast (http://www.csag.uct.ac.za/daithi/forecast/), started prior to this project but further developed as part of this project, produces monthly estimates of the degree to which our emissions have altered the chance of unusual events. This is a systematic system, meaning that events are defined prior to occurrence. Advantages of this approach are:

- Selection of events is not biased by events that occurred or for which we expect a certain attribution result;
- Estimates can be made as part of a seasonal forecast system as described in Section 6, i.e. estimates are available at the time of occurrence of the events, rather than one year later.

One outcome of this setup is that many attribution estimates end up being for events that do not end up occurring.

Events are defined for each month along the following criteria:

- 58 regions, each approximately 2 Mm^2 in size, are used shown in Figure 7.2. These regions are based on political and economic bodies, on the basis that responses to extreme events tend to be coordinated along these regional definitions.
- The thresholds used are the 1-in-10 year threshold experienced during the previous years starting in 1960. Thresholds are estimated from the same calendar month in those previous years.
- Thresholds are applied for unusually hot months, cold months, wet months, and dry months.

An example of the forecast result for October 2013, issued in September, is shown in Figure 7.2 for the HadAM3P-N96 model. Based on input from others on how various potential users might interpret results, these maps simplify the numerical results through classification into six categories. These categories are based on the primary RR thresholds of “there is a change” and “the change is at least a factor of two”. They do not reflect the best estimate of the actual change, but, based on a Monte Carlo uncertainty analysis, what we can say with confidence:

- If we are confident that the chance has at least doubled (red)
- If we are confident that the chance has at least increased, but we cannot confidently say it has at least doubled (yellow)
- If we are confident that the chance has at least halved (dark blue)
- If we are confident that the chance has at least decreased, but we cannot confidently say it has at least halved (light blue)

- If we cannot say anything confidently about an increase or decrease in the chance (grey)
- If we are confident that the chance has no more than doubled or halved (green)

The first five categories listed above are mutually exclusive and comprehensive. However, the green "not much change" category overlaps the yellow and light blue "at least some change" and grey "cannot detect change" categories.

The attribution forecast service's website posts results for the one-month lead forecast, as shown in Figure 7.2, and then posts updated results three months later when the "hindcasts", using observed rather than forecast sea surface temperatures, are available. Analyses have indicated that there are no systematic differences between the forecast and hindcast attribution estimates (not shown).

The example shown in Figure 7.2 is typical of most months. According to the calculations, we are confident that the chance of an unusually hot October 2013 was at least doubled because of anthropogenic greenhouse gas emissions over most regions, while the chance of the month being unusually cool was at least halved. The tendency for northern high-latitude regions to have less confidence in there being as large an increase in the chance of a hot month becomes stronger in the northern winter months. This contrast between high latitudes and lower latitudes is the combined consequence of the higher atmospheric variability in higher latitudes and the neglect of atmospheric variability of oceanic origin in the tropics in the lower latitudes. Together, these mean that generally globally uniform (to first order) warming shift occurs against very different backgrounds of climate variability. Current monthly attribution maps for precipitation, based on 10 simulations, tend to reflect sampling noise rather than underlying signals. Analyses on the larger hindcast ensembles covering 2009-2011 described in Section 6.2 do indicate systematic patterns, however, as will be described in the following subsections.

7.3 Collective analysis

Two questions emerge from the maps shown in Figure 7.2.

- Are the spatial patterns seen in Figure 7.2 stable from month to month?
- If a different climate model had been used, would the map have looked similar?

Fortunately, the simulations described in Section 6 are able to address both these questions.

Figure 7.3 shows the frequency of occurrence of each of the categories for unusually hot months in each region for all 36 months in the January 2009 through December 2011 period. The colours used in the pie charts are identical across to those used in Figure 7.2. These results come from analysis of 60 simulations of HadAM3P-N96 for both the real-world and nonGHG-world scenarios, 50 simulations for HadAM3-N48, and 56 simulations for CAM5.1-2degree. Figure 7.4, 7.5, and 7.6 shows the results for unusually cold, wet, and dry months respectively.

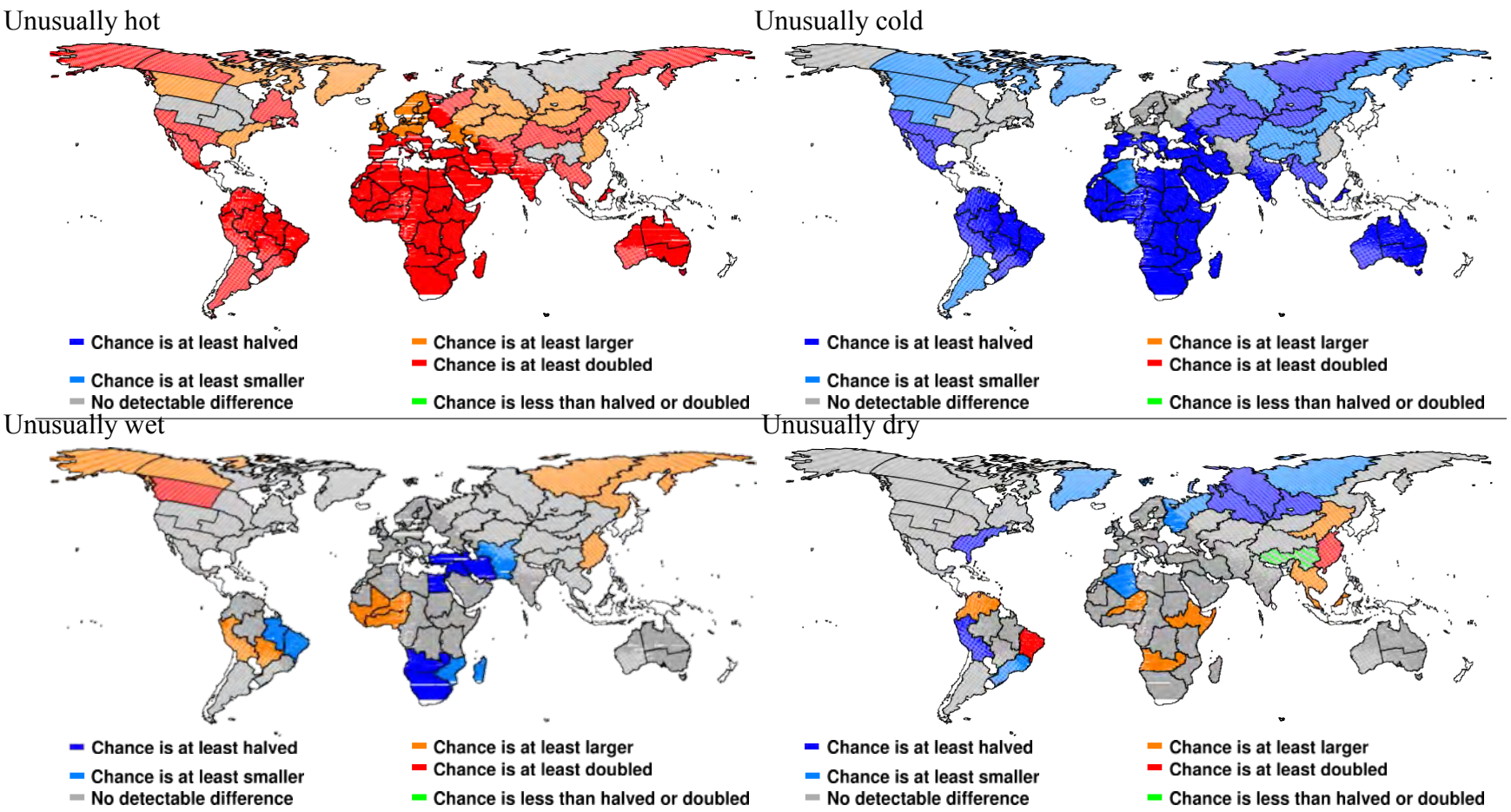

Figure 7.2 An example attribution forecast from the HadAM3P-N96 model. This shows the attribution results forecast in September 2013 for October 2013. Each of the regions are assigned one of six classifications based on an analysis of the "attribution forecast" simulations described in Sections 6.2.1 and 6.2.2 and in Figure 6.1.

For many lower latitude regions, particularly the African regions, the “confident in at a doubling” of the chance of unusually hot events category occurred in all 36 months. Results are less consistently confident of a large change in northern high latitudes. There are two reasons for this. First, because sea ice coverage was not expanded for the HadAM3P-N96 and HadAM3-N48 nonGHG-world simulations, these models are seeing -1.8◦C water when they should be seeing much colder ice. This factor is visible in the difference between the results of these two models and of CAM5.1-2degree, which did include a sea ice expansion in the nonGHG-world simulations. Second, to first order these maps are comparing the magnitude of the mean warming signal to the magnitude of the interannual variability. Because interannual variability in temperature is greater in the northern high latitudes than elsewhere in the world, particularly than in the tropics, the more or less uniform warming does not so clearly exceed the interannual variability. Similarly, the magnitude of the interannual variability in the tropics may be underestimated in these simulations, which do not include possible realisations of the ocean other than what was observed. Broadly, this results in unusually cold months (Figure 7.4), except of course that the dominant categories are for “at least a decrease” and “at least a halving” of the chance.

Not surprisingly, the results for unusually wet and dry months (Figures 7.5 and 7.6) are not as monochromatic as for the temperature extremes. All three models show a frequent “at least an increase” in the chance of an unusually wet month conclusion for northern high and mid latitudes, with a shift toward the “at least a decrease” and “no major change” categories in the low latitudes, including South Africa. The results for unusually dry months are largely the opposite. The models generally share a similar structure in results within the African continent as well, with East Africa behaving more like higher latitudes for dry events (“at least a decrease” in the chance), and more equatorial regions having more of a tendency for the “at least an increase” category.

Broadly, then, these analyses address our two questions. First, the spatial patterns visible in the maps for temperature events in the Figure 7.2 example are representative of general large scale characteristics of attributable signals, at least as within the experimental setup of these climate models. The spatial patterns for precipitation extremes are less strong, but nevertheless are indicative of tendencies over the continental areas. Second, the results are quite robust against the selection of climate model, even on the sub-continental scale.

7.4 Results for South Africa, Namibia, and Botswana

In this section we focus on the region including South Africa, which also includes Namibia and Botswana. For temperature, each country has contributed to the results according to its surface area. For precipitation, though, the contribution reflects the total precipitation occurring within in each country, thus because South Africa is generally wetter than the other two countries, the precipitation results are strongly biased toward wetter regions of South Africa.

The attribution category assigned to this region, for each month of the January 2009 through

October 2011 period, are shown in Figure 7.7. For hot and cold events, the results are remarkably strong and consistent. Analyses of both the HadAM3-N48 and CAM5.1-2degree indicate that we are confident that the chance of a hot event was at least doubled because of our emissions in every single month during that period; results from HadAM3P-N96 are nearly as strong. For cold events, analyses of all three models indicate that we are confident that the chance was at least halved for all of the months.

For unusually wet dry months, all three models agree that whenever a confidence change in the chance is notable, it is for an increased chance of dry months and a decreased chance of wet months (Figure 7.7). Generally, however, there is no notable change in the chance during the December-February wet season months, with the most notable and consistent changes being in the transition months. While the models are usually consistent with one another in terms of assigned class, there may be some differences between years. This latter result raises the intriguing, and challenging, prospect that attribution results for wet and dry events over this region are actually somewhat sensitive to the prescribed ocean temperatures in this atmospheric modeling experimental setup.

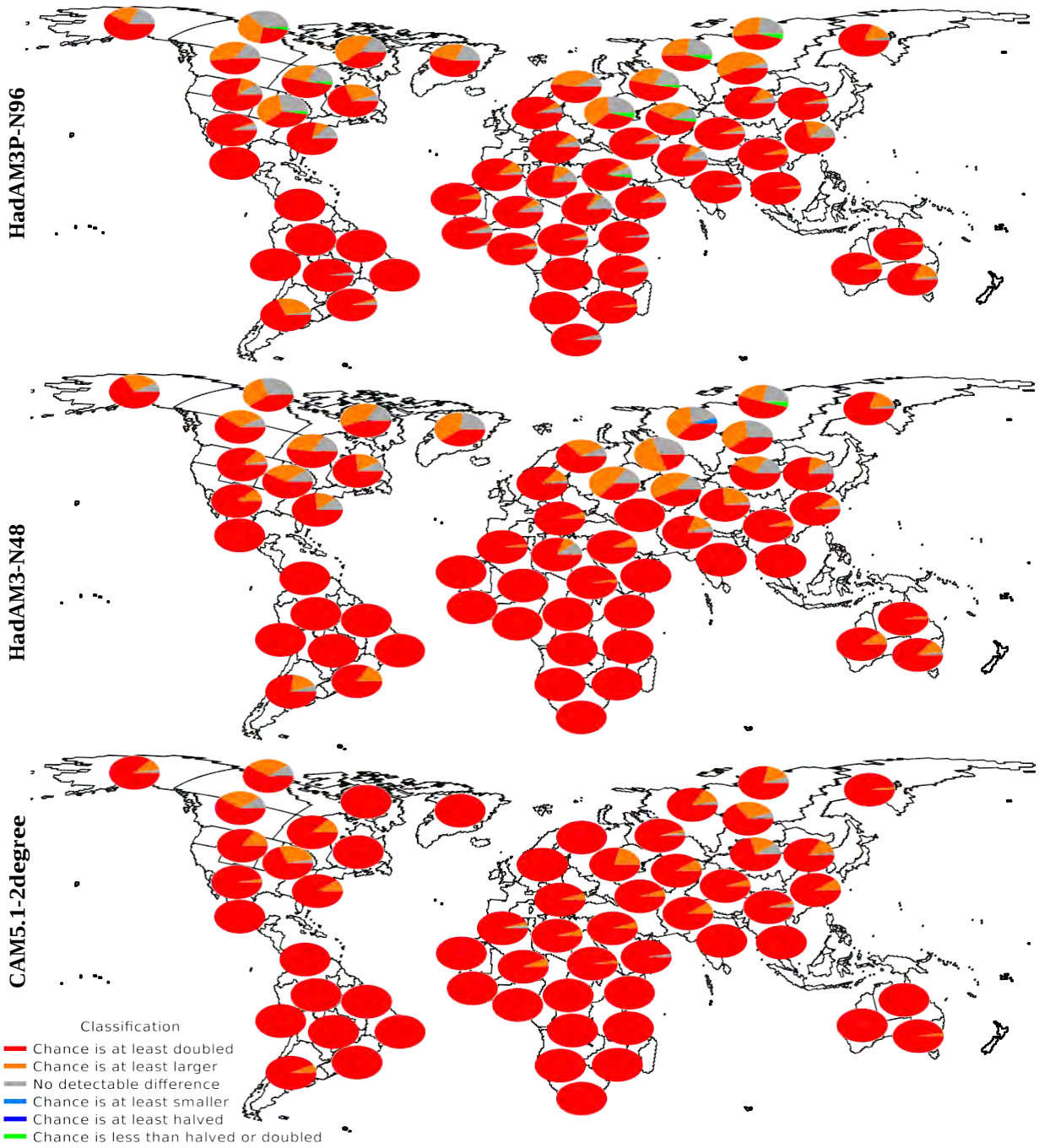

Figure 7.3 Pie charts showing the frequency of occurrence of each of the categories listed in the Figure 7.2 legend for unusually hot months over each region during all months in the 2008-2011 periods.

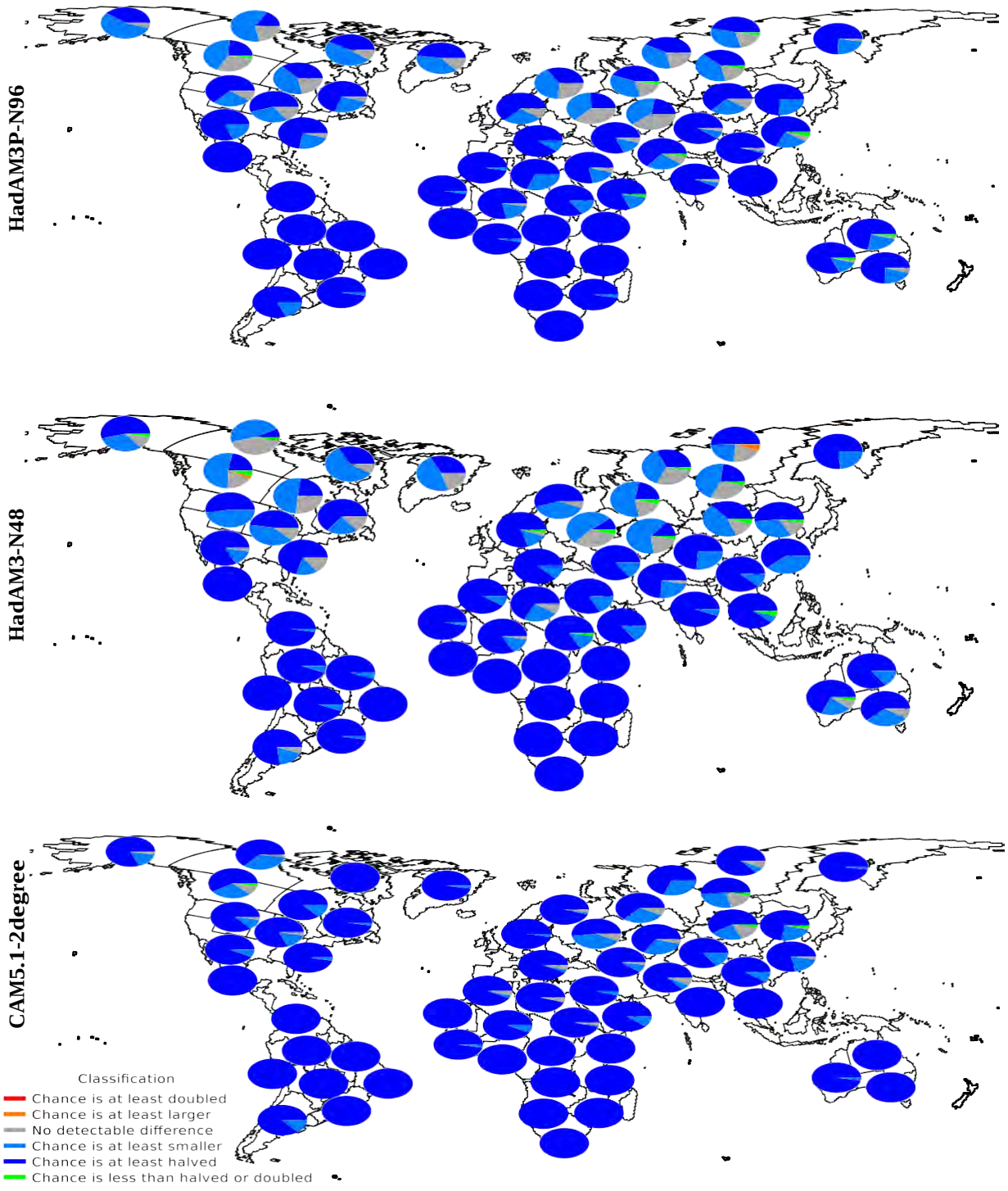

Figure 7.4 Pie charts showing the frequency of occurrence of each of the categories listed in the Figure 7.2 legend for unusually cold months over each region during all months in the 2008-2011 periods.

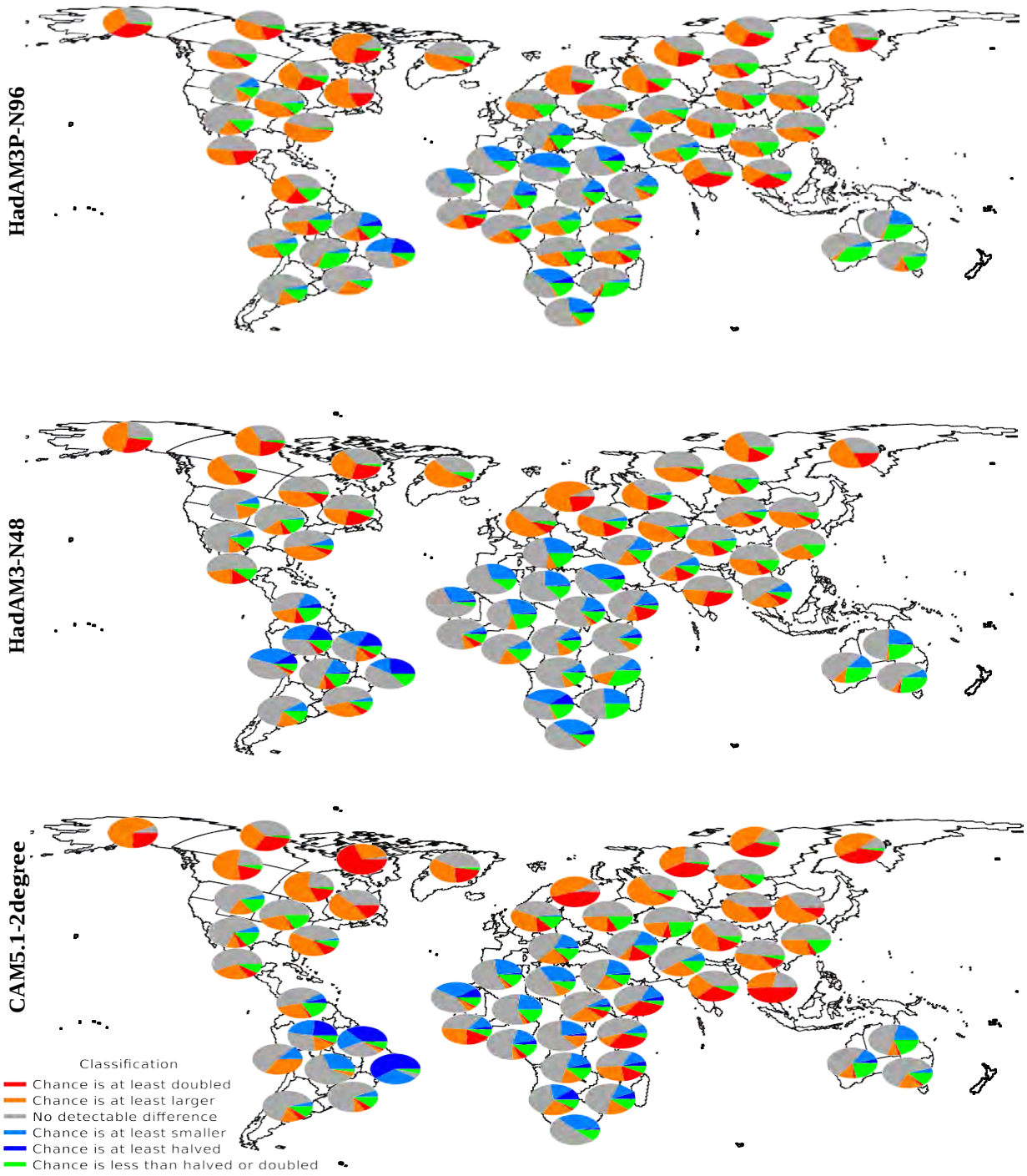

Figure 7.5 Pie charts showing the frequency of occurrence of each of the categories listed in the Figure 7.2 legend for unusually wet months over each region during all months in the 2008-2011 periods.

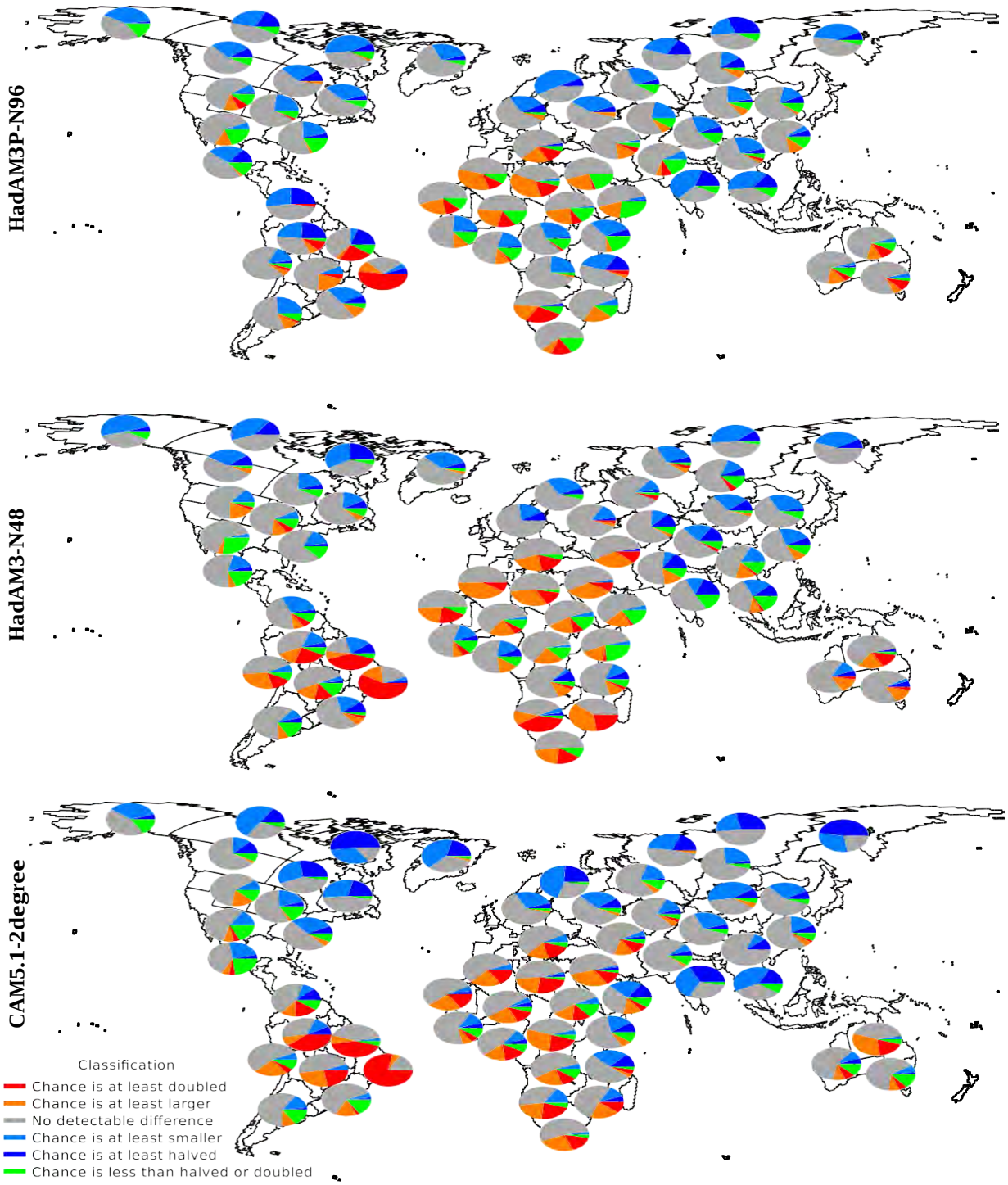

Figure 7.6 Pie charts showing the frequency of occurrence of each of the categories listed in the Figure 7.2 legend for unusually dry months over each region during all months in the 2008-2011 periods.

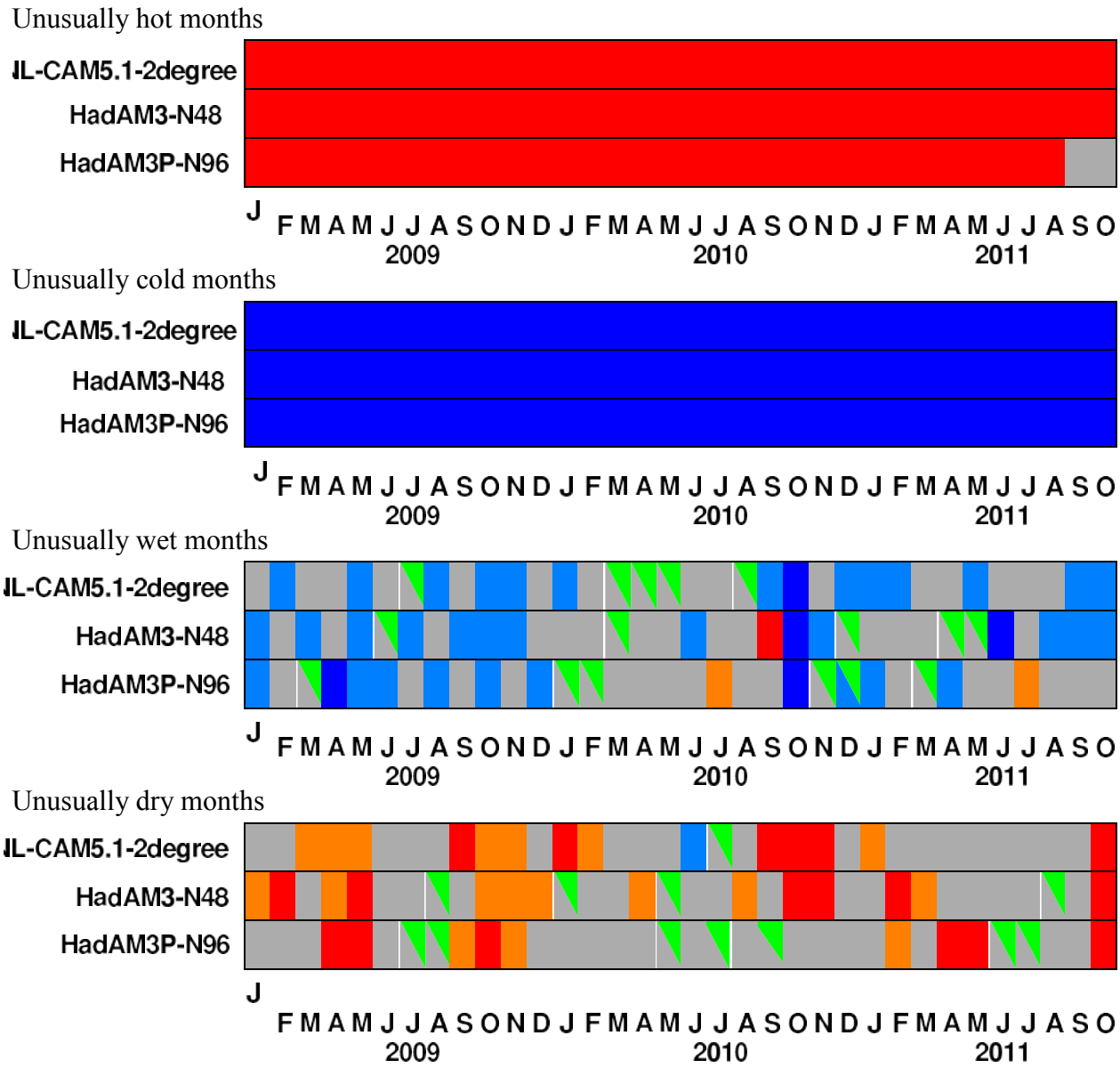

Figure 7.7 The attribution categories assigned to the South Africa/Namibia/Botswana region during the January 2009 through October 2011 period. This is the period when the three climate models have large ensembles of simulations: 60 for HadAM3P-N96, 50 for HadAM3-N48, and 56 for CAM5.1-2degree. Some months have been assigned by the "no major change" (green) class and another class, in which they are both included as triangles. The colors correspond to the same classification as in Figure 7.2.

8 Attribution of floods in the Okavango Basin

8.1 Background

This section comprises a case study of the predictability and attribution techniques developed in earlier sections to a hydrological system, specifically streamflow discharge into the Okavango Delta, Botswana. It uses simulations discussed in Section 6 and methods introduced in Sections 3 and 7. This section summarizes research on the attribution of the chance of high floods reported in (Wolski et al., 2014), with the addition of some analysis of the limits of predictability not yet published.

The Okavango Basin in southern central Africa (Figure 8.1) has experienced high floods in 2009-2011 (Figure 8.2, with considerable economic and societal impacts: villages and houses were flooded, bridges closed or washed away, water and electricity supply interrupted. The hydrology and climate conditions in that system cause that flooding occurs as a result of accumulation of individual rainfall events during entire rainy season occurring over a relatively large area, rather than as a result of intense short events of limited spatial extent. This offers an opportunity to apply the risk-based event attribution methodology in a context of spatial and temporal scales different from these used in typical attribution studies, such as that of Pall et al. (2011) and Kay et al. (2011).

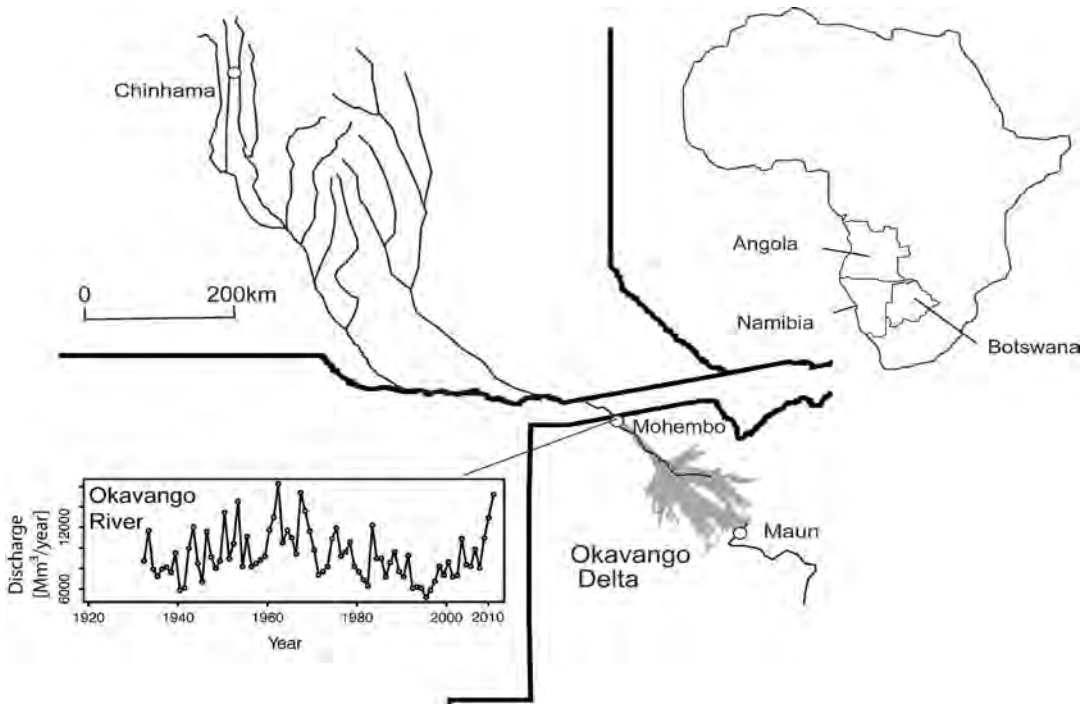

Figure 8.1 Location of the Okavango River Basin. The inset shows annual river discharges at Mohembo since 1934. Note the strong multidecadal variability, marked by high flows during the 1960s and in the recent few years.

8.2 Study site

The Okavango basin is located in central Southern Africa (Figure 8.1) and extends across a relatively smooth climatic gradient from a high rainfall zone in the highlands of Angola, towards the semi-arid north of Botswana. The climate of the basin is affected by the interaction of three air masses: cold dry air from the southern Atlantic, warm moist air from the southern Indian Ocean and warm moist air from the equatorial Atlantic, and influenced by the movement of the Inter-tropical Convergence Zone (ITCZ) and the Zaire Air Boundary (ZAB). The rainy season occurs during the austral summer (October-April) and accounts for 95% of total annual rainfall.

The hydrological system is broadly divided into two parts: the upper, having a character of a typical river catchment, runoff from which contributes 2/3 of water balance inputs to the lower part; and the lower part consisting of the Okavango Delta wetlands and terminal rivers, where the water's ultimate sink is evaporation to the atmosphere. The annual flood takes the form of a mono-modal (only in higher rainfall years bimodal) event, with flood peak progressively delayed in the downstream direction, such that at the inflow to the Okavango Delta it occurs 3 months and in terminal parts of the system 6-7 months after the middle of the rainy season (Figure 8.2).

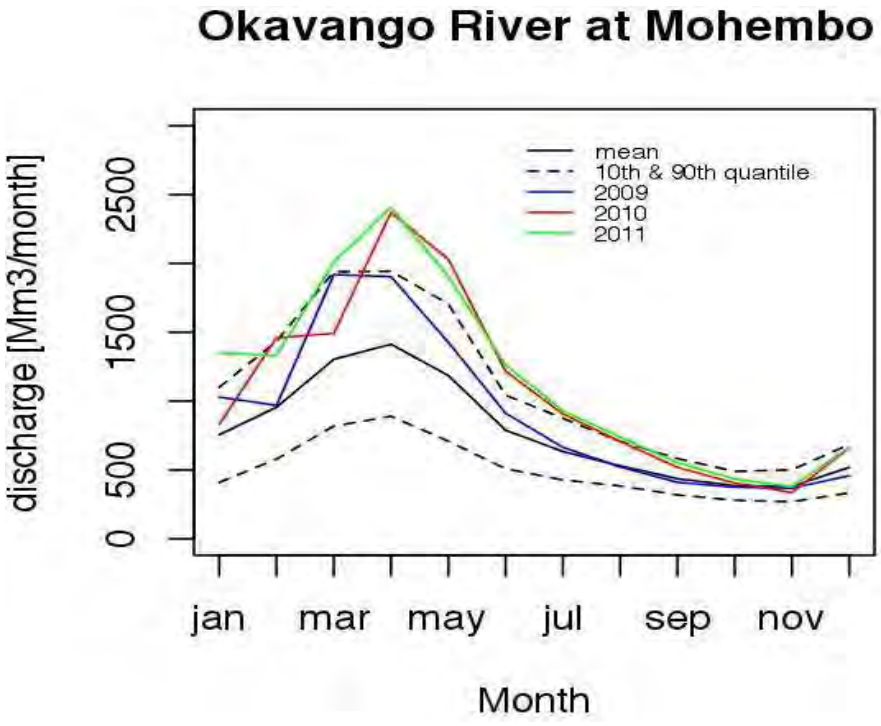

Figure 8.2 Measured monthly flood hydrographs of the Okavango River at Mohembo for the three analyzed years, and discharge statistics for 1934-2012.

8.3 Methods

This study follows the attribution method developed by Stone and Allen (2005) and Stott et al. (2004), and applied in the context of attribution of hydrological extreme events by

Pall et al. (2011) and Kay et al. (2011).

The main aspects in which the current study differs from these earlier studies is in that Pall et al. (2011) and Kay et al. (2011) analyzed events at time scales in the order of hours to weeks with recurrence interval of approximately 300 years, while our focus is on accumulation of events during the entire rainy season occurring on average once in 4-25 years. As a consequence, while the other studies used an ensemble of 1000 simulations to adequately sample rare conditions, our study could be limited to 50 ensemble members. Additional differences are in that the other studies used several estimates of the attributable ocean surface warming, whereas we use a single estimate. In contrast, we focus on resolving other aspects of the modeling setup, specifically studying across multiple years and climate models. Like those other studies, we examine the greenhouse gas contribution specifically, rather than the full anthropogenic contribution (i.e. we do not consider the contribution of anthropogenic aerosols).

In this study we use two atmospheric climate models: HadAM3P-N96 (Section 6.2) and CAM5.1-2degree (Section 6.3. For simulating hydrological conditions in the Okavango catchment we use a semi-conceptual hydrological model of the catchment, developed earlier and used in numerous earlier studies (e.g. Wilk et al., 2006; Hughes et al., 2011; Wolski et al., 2012b), known as the Pitman model. The model runs on a monthly time step, and discretizes the Okavango catchment upstream of Mohembo (Figure 8.1) into 22 sub-catchments. The model accounts for processes of evaporation, transpiration, infiltration, surface runoff, interflow, groundwater recharge, groundwater transport and channel flow. The model uses monthly rainfall and monthly air temperature as inputs, and outputs monthly river discharge at the outlet of each sub-catchment.

Considering that the region is characterized by a relatively low topographic relief and NE-SW rainfall gradient which is well reflected in the climate model rainfall fields and that the catchment hydrological model uses data at a coarse spatial sub-basin and monthly time scale, we decided to perform main part of the analyses using the climate model output directly from both climate models. We have, additionally, downscaled rainfall based on the TRMM 3B42 dataset and HadAM3P-N96, for which a set of variables used in the process was readily available. This data set was meant to provide information on influence of GHG emissions on the daily rainfall intensities, which could have had impact on runoff unnoticed in monthly data. Importantly, the downscaled data set is not meant to form the basis for comprehensive sampling of errors and uncertainties arising during various ways of linking climate models and hydrological models – for that, we would need a number of downscaling and bias-correction procedures. Rather, it provides information about the order of magnitude of possible systematic errors and uncertainties involved in such linking.

For the direct use of climate model output to drive the hydrological model, the monthly climate model variables of rainfall and temperature were firstly re-gridded to a higher resolution (0.1 degree) using a binomial interpolation. Subsequently, aerial averages for each

sub-catchment were calculated. Since raw climate model rainfall and temperature data are known to contain biases, time series of rainfall and temperature were bias corrected. Two correction procedures were used: scaling of mean and variance, and histogram equalization. But since differences between results of the two procedures were not qualitatively different, only the first one is presented here. In that procedure a multiplier and an offset are derived on a calendar month-to-month basis, such that mean and variance of the "real world" ensemble for the 1960-2002 periods match these of the reference dataset in the same period (in this case Pitman model dataset developed by Wilk et al. (2006)). The multipliers and offsets are then applied to individual climate model datasets for the 2008-2011 period for both "real world" and the "non-GHG world" (non-greenhouse-gas world) ensembles (Sections 6.2 and 6.3). The advantage of this simple solution is that the Pitman model can be used with climate model data without the need for its re-calibration.

For downscaling we have used a procedure based on self-organizing maps (SOM downscaling or SOM-D, Hewitson and Crane, 2006). Since temperature data could not be downscaled due to lack of daily observations, the hydrological model was run with downscaled rainfall and bias-corrected climate model temperatures. The downscaling was performed only for HadAM3P-N96 data.

In order to ascertain a relative contribution of differences in rainfall and temperature between the "real world" and "non-GHG world" on flood attribution results, a simple sensitivity analysis was performed. Specifically, a set of simulations was designed to describe a world that might have been had rainfall been affected by greenhouse gas emissions but temperature had not. Thus the hydrological model was run with rainfall data from the "real world" climate model simulations but temperature data from the "non-GHG world" simulations.

The risk-based approach compares the chance of exceedance of a threshold in the "real world" mode (Preal) against the chance of exceedance of that same threshold in the "non-GHG world" (PnonGHG). Recent event attribution assessments have used the fraction attributable risk (FAR) measure to quantify the degree to which the forcing from CO2 emissions has increased the chance of a specific event (Stone and Allen, 2005):

$$FAR = 1 - \frac{PnonGHG}{Preal}$$

For a situation when risk increases due to anthropogenic forcing, the FAR falls into the range of 0-1, with 1 expressing a situation when the given event never occurs in the reference "non-GHG world" conditions and thus is entirely attributable to the forcing, and 0 indicating no influence of the forcing onto the probability of that event.

In the case of our study, simulations with both climate models indicate reduced probability of occurrence of high floods in the "real world" conditions, with the consequence that Preal < PnonGHG and FAR < 0. FAR, perhaps more appropriately named FAIR, is useful for

characterising the fraction of attributable increased risk. Therefore we have reversed the index definition to express the fraction of decrease in risk that is attributable to GHG-induced climate change, i.e.:

$$FADR = 1 - \frac{Preal}{PnonGHG}$$

Thus, fraction of attributable decrease in risk (FADR) falls in the range of 0-1 when emissions have resulted in a decrease in the chance of the event. Calculations of FADR and uncertainty associated with it were performed for two flood indices: total annual discharge and maximum monthly discharge. For that, Preal and PnonGHG were drawn, using a bootstrapping procedure, from log-normal probability distributions approximating the distributions of the considered indices for each of the analysed years, obtained from ensemble simulations with the bias-corrected and the downscaled climate model data.

8.4 Aspects of predictability of the Okavango hydro-climate

Here we report on an analysis of how much the limits of predictability of Okavango discharge, as measured by the spread of simulations, varies from year to year, following from the analysis in Section 4. The observed and simulated annual mean stream flow discharge at Mohembo is shown in Figure 8.3 for all years since 1965. Stream flow discharge of the Okavango River at Mohembo integrates the hydroclimatic conditions in the entire upper catchment, and is the main determinant of conditions in the Okavango Delta and thus is a good expression of the overall system's state. The simulated hydro-climates were derived for a 10-member initial condition ensemble of HadAM3P-N96 and a 50-member ensemble of CAM5.1-2degree (Section 6.2 and 6.3). Both climate models were forced with 1960-2011 observed sea surface temperatures and radiative forcing. Climate model data (rainfall and temperatures over the Okavango River catchment) were bias-corrected (for bias in mean and in variance, but with preservation of ensemble spread) and used to force the hydrological model of the Okavango River catchment. Total annual discharges were calculated for the November-October hydrological year.

Both ensembles maintain relatively good probabilistic skill, although this can be partly attributed to the bias correction of the input data. Importantly, there are systematic differences between observations and ensemble means that are to a certain degree contemporaneous between the two climate models. Neither of the climate model ensembles is able to adequately envelope the dry period of occurring in 1993-1999 and the wet period occurring in 2010-2011 period. In order to assess the possible influence of large scale climate variability modes on these differences, indices expressing two of such variability modes – NAO and ENSO – are plotted in the figures. There appears not to be any clean-cut relationships between these indices and ensemble-observations differences, neither between these indices and observed discharges.

HadAM3P-N96

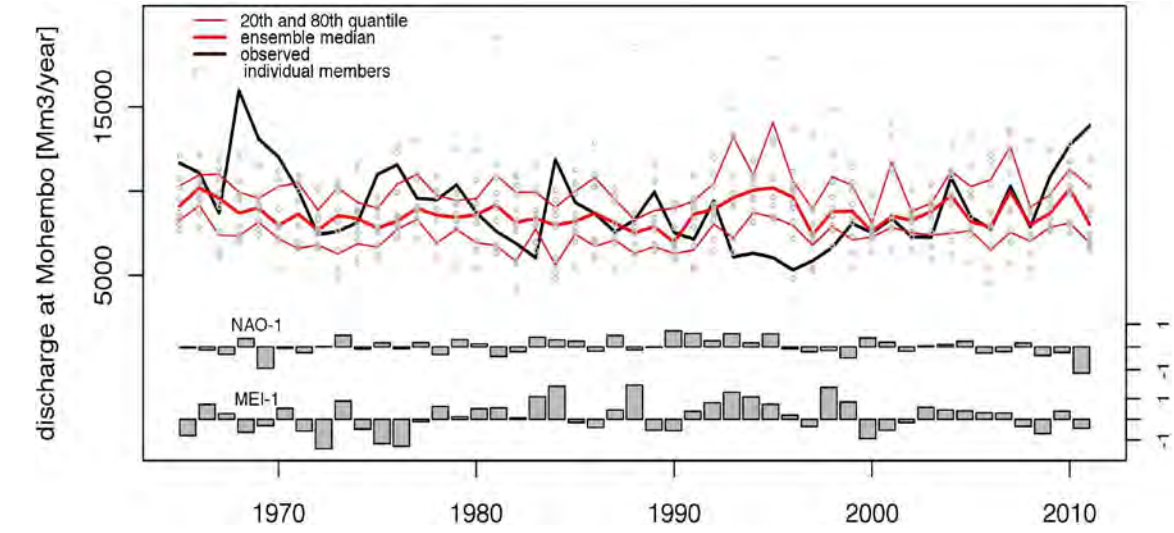

CAM5.1-2degree

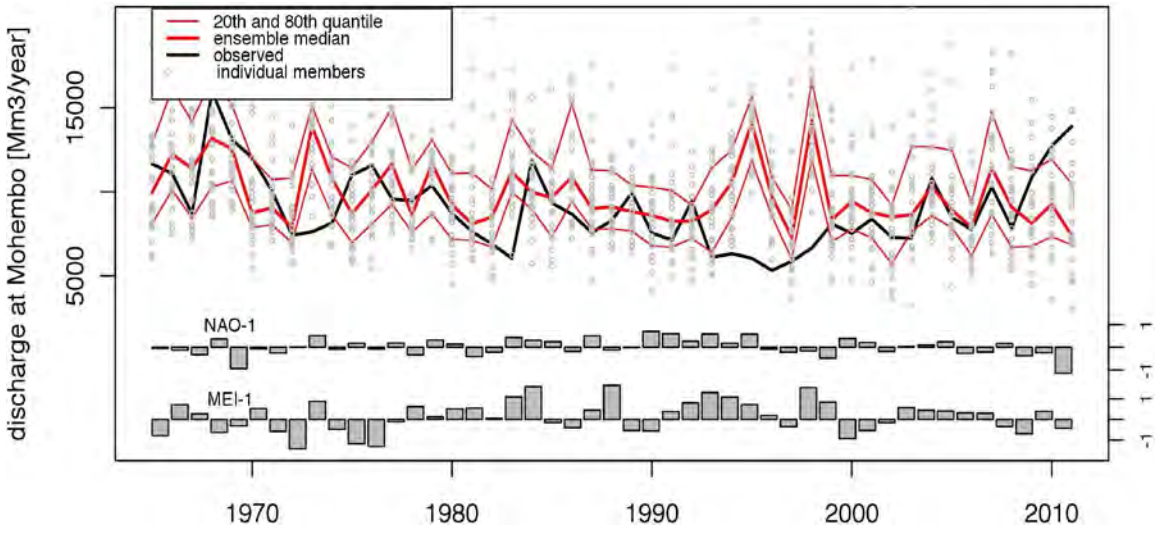

Figure 8.3 Results of 50-member ensemble simulations of Okavango River discharges with Pitman model driven by climate simulated by HadAM3P-N96 (top) and CAM5.1-2degree (bottom). North Atlantic Oscillation (NAO) and Multivariate ENSO Index are included to illustrate their influence on deterministic skill of the simulations.

The spread of discharge in the simulations in Figure 8.3, as measured by the 20-80th percentile range, varies noticeably from year to year. Are such variations related to hindcast skill, as was found in Section 5.7 for rainfall over South Africa? The relationship between the spread of simulations and the skill is plotted in Figure 8.4. Here the model skill is measured as the absolute error of the median of the model simulations relative to the observed value. At either extreme of the predictability measure there are some indications of a relation with model skill. In particular, the two years with the narrowest range have relatively good skill, while the two years with the widest range have relatively bad skill. However, as a whole, a clear relationship encompassing all years is not visible. An important caveat here is that the

simulations have had difficulty in reproducing some of the decadal variability visible in the observed time series in Figure 8.3 and that may be contaminating the visibility of any relationship that might exist. For instance, the years with the worst skill, during the mid-to-late 1990s are clearly doing so because the models have failed to accurately represent the distribution of possible stream flow for those years, irrespective of whether the models predicted a large uncertainty for those years.

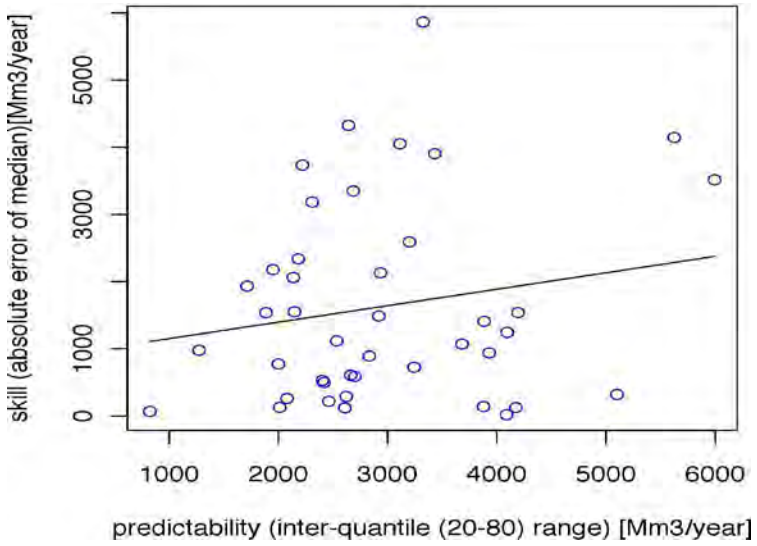

Figure 8.4 Relationship between deterministic skill and predictability for 50-member ensemble simulations of Okavango River discharges with Pitman model driven by climate simulated by HadAM3P-N96 for 1965-2012 period. Predictability is measured as the 20-80th percentile range of the simulations, while skill is measured as the absolute error of the median of the simulations against the observed value.

8.5 Attribution results

In this section we move on toward examining the degree to which emissions have contributed to the chance of high floods in the Okavango Basin, following from the techniques implemented in Section 7. Comparison of the "real world" and "non-GHG world" simulations of Okavango River discharges at Mohembo indicate overall lower discharges in the "real world" conditions (Figure 8.5). The difference is observed consistently during the three analyzed years, during low and high flow stages and across the post-processing methods and climate models. The differences are relatively large compared to uncertainty in each of the ensembles (visualized through the 10th and 90th percentiles), and the differences are statistically significant at 0.05 significance level (assessed with a Mann-Whitney test on a month-to-month basis). The effects on the distribution of monthly river discharges during the three analyzed years are manifested through generally less frequent discharges of magnitude exceeding 1000 Mm^3 $month^{-1}$ in the "real" versus "non-GHG" worlds, and more frequent discharges in the range of 500-700 Mm^3 $month^{-1}$ (Figure 8.6).

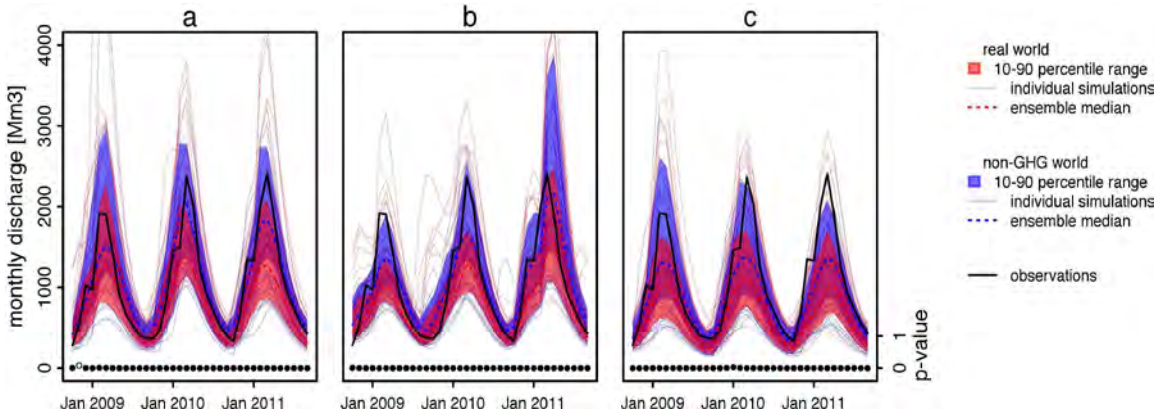

Figure 8.5 Attribution results for 2009-2011 floods, measured by discharge at Mohembo, based on **a)** bias-corrected HadAM3P-N96 simulations, **b)** downscaled HadAM3P-N96 simulations, **c)** bias-corrected CAM5.1-2degree simulations. Circles display p-value of Mann-Whitney test for differences between "real world" and "non-GHG world" ensemble distributions, with solid ones indicating significance at 0.05 level. In almost all cases (with the lone exceptional month in panel a possibly occurring during the spin-up phase of the simulations), the distributions of "real world" and "non-GHG world" are significantly different.

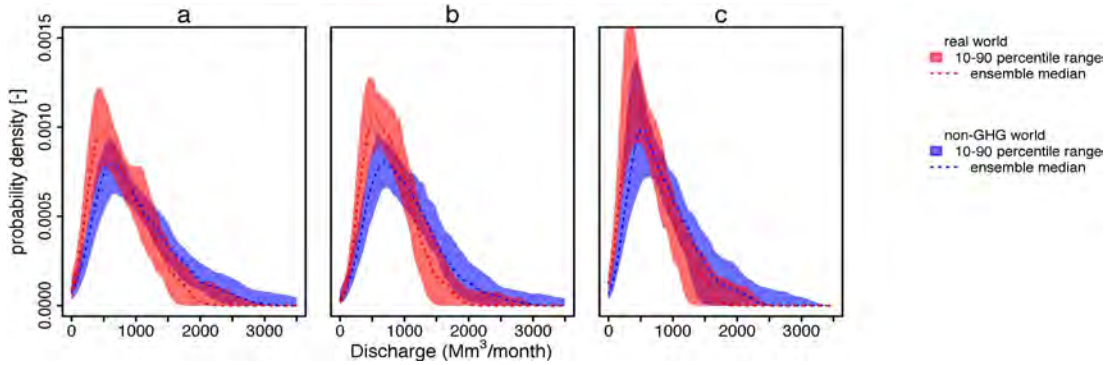

Figure 8.6 Empirical probability distributions of monthly discharges at Mohembo from **a)** the bias-corrected HadAM3P-N96 simulations, **b)** the downscaled HadAM3P-N96 simulations, **c)** the bias-corrected CAM5.1-2degree simulations. According to all three estimates there is a substantial shift away from high discharges toward low discharges from the "real world" to the "non-GHG world" scenarios.

The differences in river discharges and runoff components between "real world" and "non-GHG world" result, obviously, from a combination of the differences in rainfall and differences in air temperature. We have visualized the differences in air temperature through distributions of monthly air temperature-derived potential evapotranspiration (PET, calculated within the hydrological model using the Hargreaves formula, Hargreaves and Samani, 1985) for a selected location in the upper part of the basin (Figure 8.7). There is a clear shift in the distribution of monthly PET by approximately 14-20 mm month^{-1}, reflecting the "real world" simulations being approximately 1.5^{o}C warmer than the "non-

GHG world" ones.

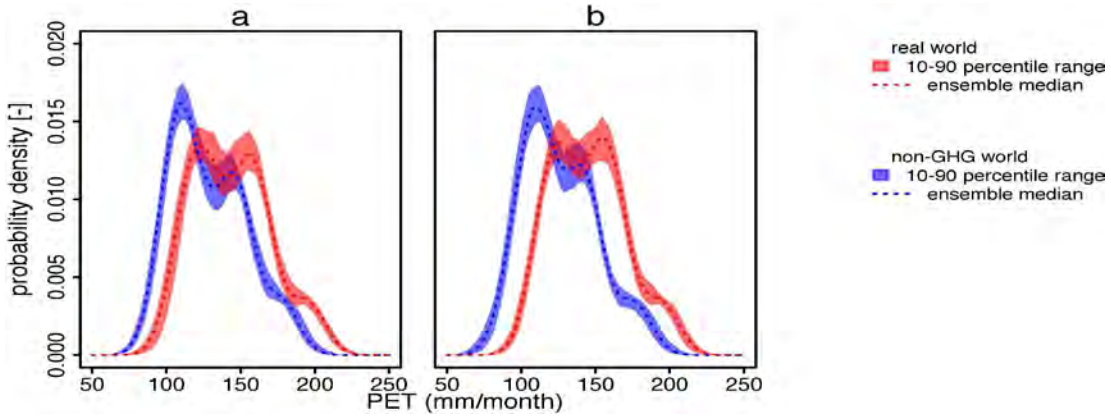

Figure 8.7 Empirical probability distributions of monthly temperature-derived potential evapotranspiration (PET) for a selected upstream location (Chinhama): **a)** bias-corrected HadAM3P-N96 and **b)** bias-corrected CAM5.1-2degree simulations. With both models there is a substantial shift toward lower PET in the "non-GHG world" simulations.

Differences in monthly rainfall are less pronounced to the extent that in bias-corrected HadAM3P-N96 simulations no differences are noticeable (Figure 8.8). In the two other sets of simulations there are fewer months with rainfall around 150 mm month^{-1} (x-axis value of $^{o}5$ log(mm month^{-1}) in Figure 8.8) in the "real world" compared to "non-GHG world", an effect stronger in the upstream (northern) sub-catchments.

Downscaled HadAM3P-N96 results allow for assessment of differences between the "real world" and "non-GHG world" in terms of the structure of daily rainfall that underlie the monthly signal. Analysis (not shown) indicates that there is a decrease in number of rain days in the upper (northern), and a no change or minimal increase in the lower (southern) part of the Okavango catchment. There is, however, no clear signal in changes of rainfall intensities, in median or in higher percentiles. The overall effect is that of lower monthly and seasonal totals in the northern, upstream part of the catchment, and not changed or minimally higher totals in the southern, lower part of the catchment in the "real world" simulations compared to the "non-GHG world" simulations. The higher rainfall only occasionally leads to higher surface runoff as the latter is conditioned on the status of soil moisture, which is depleted due to higher evapotranspiration. Since surface runoff from the southern sub-catchments is a minor component of stream flow (which is generated mainly in the higher rainfall zone in the northern sub-catchments), the effect is insignificant at the scale of the basin.

The "non-GHG world-temperature" simulations (i.e. simulations with "non-GHG world" temperatures and "real world" rainfall) allow a diagnosis of the relative role of rainfall and temperature in the river discharge signal. Results from the two climate models differ in the role and contribution of air temperature/PET and rainfall (Figures 8.9 and 8.10). Had AM3P-N96-based "non-GHG world-temperature" simulations have fewer higher discharges (>1000 Mm^3 month^{-1}) in the "real world" mode, as well as more frequent lower discharges

(<1000 Mm^3 $month^{-1}$), both in the bias-corrected climate model and the downscaled datasets (Figure 8.10). These effects are similar in character, although smaller in magnitude, to the cumulative effects of both rainfall and temperature (Figure 8.6). In HadAM3P-N96 simulations, therefore, rainfall and air temperature seem to "act" in the same direction, and their effects cumulate.

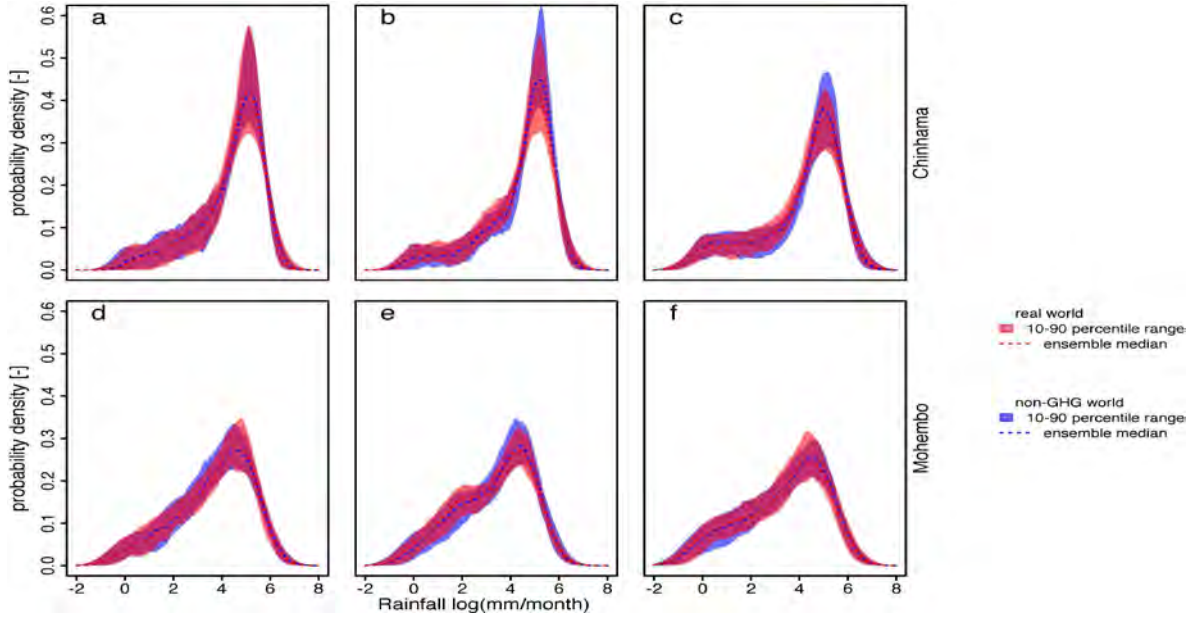

Figure 8.8 Empirical probability distributions of monthly rainfall for an upstream (Chinhama, upper row) and downstream (Mohembo, lower row) location, in the bias-corrected HadAM3P-N96 simulations (a, d), the downscaled HadAM3P-N96 simulations (b, e) and the bias-corrected CAM5.1-2degree simulations (c, f). There is little difference in rainfall between the two scenarios at either location.

CAM5.1-2degree-based "non-GHG world-temperature" simulations produce a different effect. The rainfall differences between "real world" and "non-GHG world" are minimal and do not induce noticeable changes in river discharges (Figure 8.10). Therefore, the overall effect i.e. fewer high discharges and more frequent low discharges (as visible in Figure 8.6) must be driven by increases in evaporation caused by the warmer air temperature, and not by changes in rainfall.

Given that GHG emissions have affected the discharge distributions in the simulations, we can ask how this is reflected in the chance of large discharge events. We consider the chance of total annual discharges corresponding to these that occurred in 2009, 2010 and 2011, i.e. 10860, 12730 and 13890 Mm^3 $year^{-1}$ respectively. These levels correspond to 78th, 92nd and 96th percentile of observed range of discharges (obtained from log-normal probability density function fitted to the 1934-2011 observations). For peak monthly discharges, the analogous values are: 1920, 2370, 2400 Mm^3 $month^{-1}$, and 80th, 94th and 95th percentile. Distributions of FADR values for each of the 2009-2011 years estimated using each of the three model

combinations are shown in Figure 8.11. There are specific similarities and differences between the three years and three model setups. On the one hand, results for 2010 and 2011 are generally consistent across the model combinations, indicating that the chance of the observed events is at least a factor of three lower than it would have been without emissions, with most likely values between 6 and 8. However, while the three model setups agree on the existence of an influence for 2009, the downscaled HadAM3P-N96 results indicate very strong reduction of the chance (at least a factor of 10) of high discharge risk attributed to emissions while for the bias-corrected CAM5.1-2degree and HadAM3P-N96 the reduction is lower, by a factor of 4 and 2 respectively.

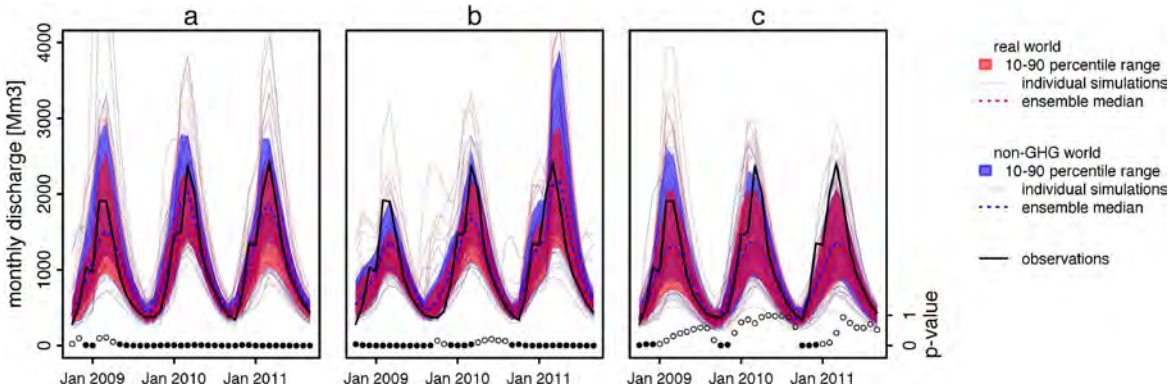

Figure 8.9 Monthly discharges at Mohembo, using "real world" rainfall and "non-GHG world" air temperatures for **a)** bias-corrected HadAM3P-N96 simulations **b)** downscaled HadAM3P-N96 simulations and **c)** bias-corrected CAM5.1-2degree simulations. Circles display p-value of Mann-Whitney test for differences between "real world" and "non-GHG temperature-world" ensemble distributions, with solid ones indicating significance at 0.05 level. The results closely match those in Figure 8.5, indicating that the difference in potential evapotranspiration between the two scenarios overwhelms any rainfall differences.

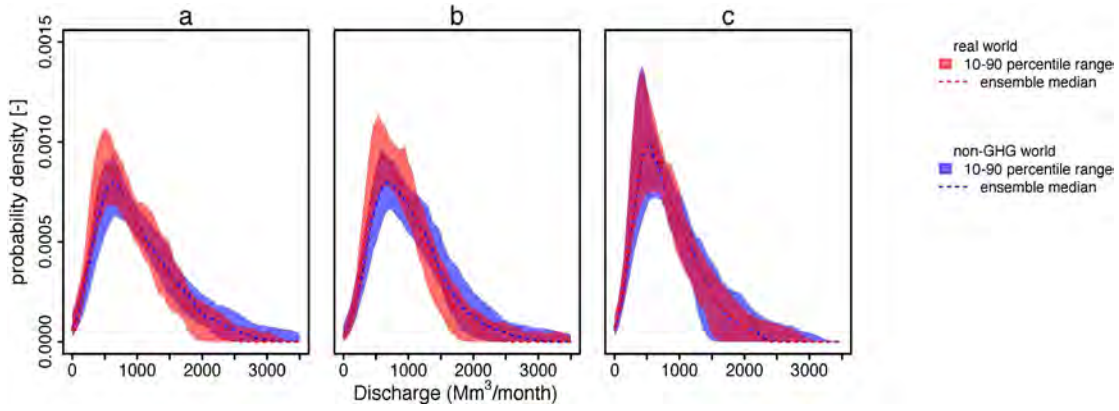

Figure 8.10 Empirical probability distributions of monthly discharges simulated with "real world" rainfall and "non-GHG world" air temperatures from **a)** bias-corrected HadAM3P-N96 simulations, **b)** downscaled HadAM3P-N96 simulations, **c)** bias-corrected CAM5.1-2degree simulations.

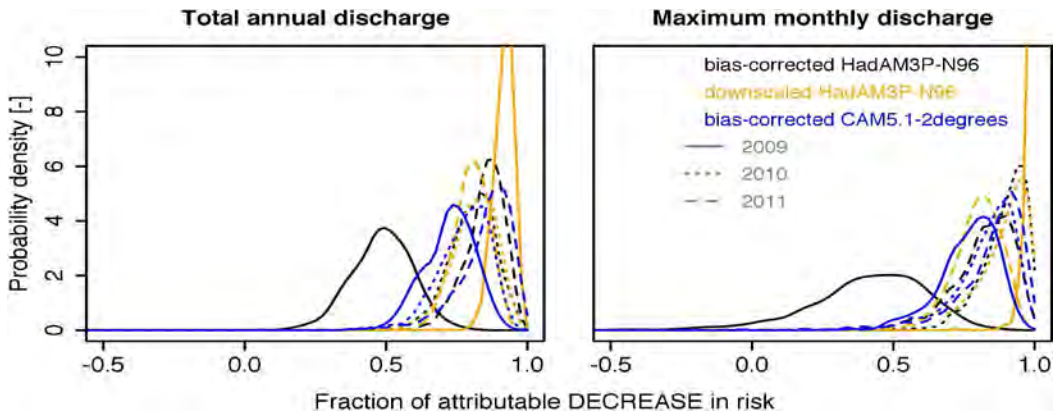

Figure 8.11 Fraction of attributable decrease in risk (FADR) for **left)** total annual discharge, and **right)** maximum monthly discharge

Even considering uncertainty in FADR estimates, it is clear that the three sets of simulations agree in that there is reduction in risk of floods of magnitudes corresponding to those observed in 2009-2011. This decrease in risk is significant at the 0.01 level (i.e. given our results there is less than 1% chance that the risk actually increased), in all but HadAM3P-N96 simulations for 2010, where the p-value is 0.05 for peak monthly discharge.

8.6 Discussion and conclusions

This study demonstrates the application of the "time-slice" method of estimating attributable risk of Pall et al. (2011) in the context of a large, relatively poorly gauged catchment subject to annual flood events. In terms of strengths, this evaluation has been possible using a relatively moderate modeling resource (compared, for example, to ensembles of atmosphere-ocean climate models). The method, as used here, also demonstrates the ability to derive results which are robust to different ways in which the analysis may be approached, such as the selection of particular years and choice of an atmospheric model. We have clearly demonstrated that consistent conclusions may be reached i.e. that greenhouse gas emissions have decreased the chance of large discharge events in the Okavango basin.

However, this study also highlights some important aspects with the approach that bear consideration. Most particularly, previous studies with the time slice approach (Pall et al. 2011; Kay et al. 2011) only examined a single year and noted that the sensitivity of results to the choice of year was unknown. Under this approach, the estimated effect of emissions is conditional on the pattern of ocean surface temperatures realized in the given year. For instance, during the period covered by this study an El Niño event occurred in the tropical Pacific in 2009-2010, while a La Niña event occurred there in 2010-2011 and 2008-2009 was a neutral year. It could be that the effect of emissions is different depending whether the prescribed ocean is in a neutral, El Niño, or La Niña state. In our study we found differences in the estimated magnitude of the attributable risk of Okavango flooding across the three years. An analysis of what aspects of the ocean are important in determining these differences would require a larger number of years to be analyzed, but it is noteworthy that the results

presented here indicate that the "time-slice" approach should not be applied just to one year but rather to a collection of years (with different SST conditions) during the era of interest. Resources for such analyses are promised by the C20C+ Detection and Attribution Project (Kinter and Folland, 2011, http://portal.nersc.gov/c20c).

In terms of the Okavango, like Kay et al. (2011), we have found an important role of the thermal aspect of climate change on the risk of extreme flood events. In the case of the Okavango, though, unlike in England, anthropogenic emissions cause reduction or minimal change in rainfall, which combines with increase in temperature leading to an overall reduction in flood likelihood. At least some of the temperature impacts likely results from the nature of hydrological processes generating Okavango floods: the flat topography and permeable soils favor infiltration and cause runoff to be dependent on antecedent soil moisture and groundwater levels, which in turn are moderated by evaporation. This combines with the large size of the catchment and causes the annual event to integrate over a large number of variable rainfall episodes spread out over space and time, whilst evaporation continues apace.

Ultimately, this analysis has revealed an attribution paradox. Recent years have experienced a trend toward high floods in the Okavango (Jury, 2012). This effect arises during an era of climate change driven by emissions of greenhouse gases; and is seemingly consistent with the general expectation of intensification of weather and increase in extreme floods, under a warmer climate. As a consequence the observed increases in flood magnitudes are often registered as caused by anthropogenic climate change by the affected public and authorities. Our modeling analysis indicates, however, that those emissions can in fact substantially decrease the risk of flooding, driven by the well-understood mechanism of increased evaporation in a warmer world, combined with relatively minor simulated changes in precipitation. In this context, the occurrence of the 2009-2011 high floods can be taken as evidence that the interannual variability in anomalous ocean temperatures may be more important in determining flood risk than the overall ocean warming.

Our results are broadly consistent with the results of several modeling studies on hydrological conditions under climate change projections carried out previously for the basin (Andersson et al., 2006; Hughes et al., 2011; Wolski et al., 2012a, b). These, similarly to our work, indicate a lack of agreement between climate models in direction and magnitude of projected rainfall, and a consistent increase in air temperatures, and thus PET. The resulting overall tendency of the multi-climate-model ensemble is towards drier conditions and lower flooding in the future. The confidence in our results is subject to limitations of models and methods, and there are several aspects that have to be considered in that context. These do no relate just to our study, but are faced by any study dealing with hydrological effect of changing climate, so we expand on them below.

First is the quasi-periodic multi-decadal climate variability. Quasi-periodic oscillations in the Okavango discharges have been detected by McCarthy et al. (2000), and related to region-

wide signal in rainfall revealed in paleoclimatic records (Tyson et al. 2002). The years analyzed in our study fall within the peak of the 60-80 year quasi-periodic cycle. Jury (2012) indicated a relation between tropical multi-decadal oscillations and signals in the Atlantic, and rainfall in the Okavango region, suggesting that the former are partly responsible for the increase in rainfall and river discharges observed since the mid-1990s, leading to that peak. In this context, our results show that in the world without anthropogenic emissions, the magnitude of discharges during that peak would likely have been higher. This conclusion is, however, reliant on the assumption that the underlying SST/climate system dynamics leading to that peak would have occurred in the "non-GHG world". At this stage, this assumption cannot easily be verified. The influence of anthropogenic global warming on global modes of climate variability and their manifestations at local scales is the subject of intense research and coherent results are only beginning to emerge. For example, Power et al. (2013) show intensification of El-Niño-driven drying in the western Pacific Ocean and rainfall increases in the central and eastern equatorial Pacific under projected future climate. The influence of ENSO on the Okavango is, however, limited, and the anthropogenic climate change-driven transformation of the processes underlying Okavango multi-decadal quasi-periodicity has not, to our knowledge, been studied. Understanding of these will be needed to obtain a greater confidence not only in our results, but also in results of any climate change projections in the Okavango region.

Second is the revealed sensitivity of results to increases in air temperatures. This effect is reliant on the assumption that an increase in air temperature leads to an increase in PET – implicit in our use of a temperature-based method of estimation of PET applied in the hydrological model. Although that assumption is physically feasible and justifiable, several recently published studies indicate that in real systems, increases in air temperature may not be associated with increases in evaporation (e.g. Hoffman et al., 2011). The decoupling of temperature and evaporation results from the influence of weather variables such as cloudiness and humidity, or secondary effects of land cover, changes in which may counteract the effect of increasing temperature. It is uncertain whether such weather dynamics occur in the Okavango region, as there are no long-term data enabling relevant analyses. However, Wolski (2009) has performed comparison of PET changes based on data from 7 climate models and using Hargreaves, Penman-Monteith and Penman methods, the two latter utilizing climate-model-derived humidity, wind speed and incoming solar radiation. There were no systematic differences between the methods, with PET sensitivity to temperature in the order of 2-3% $^{o}C^{-1}$. This gives us confidence that our assumption is correct, at least within the climate model domain.

Third is the issue of uncertainties involved in the hydrological model. To that extent, Hughes et al. (2011) have conducted sensitivity analysis of the Pitman hydrological model of the Okavango by perturbing a set of its parameters within plausible ranges, and contrasted these with uncertainty range resulting from spread of multi-climate-model climate projections. Their results indicate that while hydrological model uncertainty is not trivial and translates into a simulated range of 10% of peak flows, intra-climate-model uncertainty gives a wider

range of 70% of peak flows. In our simulations, range of the initial condition ensemble is even wider: in the order of 100-170% of mean value of peak monthly discharge, with a consequence that the model uncertainty plays a minor role in the interpretation of results of the attribution procedure.

Lastly, our results face the issue of uncertainties involved in the process of transforming output of coarse resolution climate models into hydrological model input. This issue is illustrated by the differences in results obtained from downscaled and bias-corrected climate model data. To quantify that uncertainty would demand a much larger ensemble of data processing procedures — there are numerous generic statistical downscaling procedures in use, a large number of possible combinations of a regional model and a global model for generating dynamically downscaled variables, and a plethora of bias correction procedures in use and development (Maraun et al., 2010). In view of this diverse landscape of procedures, the task of systematic assessment of uncertainties exceeds the scope of this project and necessitates the use of subjectively selected (in our case on the basis of experience of working with) methods. Forthcoming initiatives such as CORDEX (Giorgi et al., 2009) and the C20C Detection and Attribution Project (Kinter and Folland, 2011; http://portal.nersc.gov/c20c) promise resources and data enabling more systematic analyses, similar to these achieved through CMIP3 (Meehl et al., 2007) and CMIP5 (Taylor et al., 2012) in terms of climate model results.

In summary, even considering the context of numerous sources of uncertainty, our results are robust across the two climate models and the various data processing procedures in terms of general conclusion — that the probability of occurrence of high floods during 2009-2011 in the current climate is likely lower than it would have been in a climate without anthropogenic greenhouse gases, although the exact magnitude of this decrease remains unquantified. This result contributes to the body of knowledge informing the climate change adaptation planning in the Okavango basin.

9 Conclusions and recommendations

9.1 Summary of products from this project

In the proposal for this project, four main products were envisaged: atmospheric model hindcast simulations; scientific papers; a public paper; and an improved seasonal forecast product. Further specifics on these envisaged products are listed in Table 9.1. Most of these products have been delivered as envisaged, while some have taken a slightly different format following from developments within and outside the project.

Table 9.1 Four products envisaged from this project in the project's proposal

Product	Target Group	Application
Atmospheric model hind-cast simulations	Researchers in climate and climate-related fields	Public climate model data for the analysis of historical trends and variations in climate and the risk of extreme weather
Scientific papers	Seasonal forecasters, technical users of seasonal forecast	Scientific papers describing the results for use in evaluating the applicability of seasonal forecasting
Public paper	Users of seasonal forecast products	Paper describing the implications of the results for the usefulness of seasonal
Improved seasonal forecast product	Users of the CSAG seasonal forecast	A seasonal forecast product based on more informed understanding of capabilities

9.1.1 Atmospheric model hindcast simulations

A first set of these simulations were produced as described in Section 6.2. Output from these simulations has been posted on the data portal of the International CLIVAR C20C+ Detection and Attribution Project (http://esg.nersc.gov, project "c20c") and distributed by USB stick to 22 African researchers.

A second set of these simulations, reported in Section 6.2.4 using an updated model configuration and following the protocols of the International CLIVAR C20C+ Detection and Attribution Project (Section 6.5.1), are currently nearing completion and will also be published on the C20C+ D&A Project portal.

9.1.2 Scientific papers

Scientific manuscripts arising from this project are listed in Section 10.1. At the time of submission of this report, one M.Sc. thesis has been published, two papers were in press, two papers are under review, and three papers and a Ph.D. thesis remain in progress. In addition,

work from this project has been presented in 15 talks and 10 posters at conferences and workshops. Other researchers are also currently analyzing climate model output generated under this project and preparing papers (Section 6.5.2).

9.1.3 Public paper

A public paper has not been written at this stage, but rather public communication of the project has taken other forms:

- Three media interviews concerning the Weather Risk Attribution Forecast service (Section 10.1.6).
- An upgrade to version 3 of the Weather Risk Attribution Forecast web site and continued monthly attribution assessments on the web site.

9.1.4 Improved seasonal forecast product

The results of the investigations into the degree to which uncertainty in seasonal forecasts may vary as a function of time have revealed the possible existence of such variations, particularly in terms of long-term trends. The possibility of integrating that knowledge in terms of an operational seasonal forecast, however, requires some further work, as detailed below.

The new simulations described in Section 6.2.4 will form the basis of an updated UCT seasonal forecast system running under a more realistic configuration producing a larger number of simulations. While some separation of products should be maintained, insights into the characterization of extreme events will be incorporated into the seasonal forecast product, providing forecasts of the chance of unusually extreme seasons.

9.2 Conclusions from the investigations forming this project

The studies reported in Sections 4, 5, and 8 revealed that, within a forecast model setting, there are variations in seasonal predictability through time, as represented by the spread of the model simulations. In particular:

- These variations in predictability were found to be related to the skill of the forecasts when evaluated by observations, this indicating that the variations visible in the ensemble of model simulations are indeed reflected in real-world predictability.
- There exist long-term trends in these variations in predictability, some of which amount to a substantial fraction of the average predictability. These long-term trends vary according to season and location across South Africa.
- Just like it affects the mean forecast, the El Niño/Southern Oscillation may affect the uncertainty in seasonal forecasts. However, overall the relation to other indices of ocean states otherwise useful for seasonal prediction did not show substantial links to the uncertainty. Overall the links were not as strong as might have been expected, but this may have related to the linear nature of the analysis conducted in this study.
- In the setting of one particular hydrological system case study (Section 8), variations in predictability appeared weak. Given the ensemble size of simulations used, the analysis was not particularly powerful, however.

The studies reported in Sections 7 and 8 reveal some robustness in estimates of the degree to which anthropogenic emissions have affected the occurrence of extreme events. In particular:

- Estimates appear to be largely insensitive to selection of climate model.
- Estimates do appear to have some sensitivity to the conditionality imposed by the prescribed sea surface temperatures, revealed through differences in results from year to year under near-identical anthropogenic forcing states.
- Analysis of model simulations indicates that temperature extremes over South Africa have been strongly affected by anthropogenic greenhouse gas emissions, while precipitation extremes have only been moderately affected during the transition seasons.
- Effects of emissions on hydrological extremes may be mostly arising through the warming signal, rather than through changes in precipitation.
- A rather simple systematic service for event attribution can result in consistent and stable conclusions.

9.3 Implications of results from this project

9.3.1 Predictability of seasonal forecasts

The analyses of the limits of predictability indicate some potential for adding some measure of confidence to seasonal forecasts. But how well this can be implemented depends largely on how seasonal forecasts are presented. In this project, seasonal forecasts were interpreted as being a "best estimate" with an uncertainty range. But many meteorological services adopt different ways of presenting forecasts. A popular method is to use three classes: "below average", "near average", and "above average". These can also be described as "low", "medium", and "high", or with cold/hot or dry/wet adjectives. In practice these classes are determined as the terciles of the distribution of realized weather from past years during some climatological reference. While a confidence measure could be added to these forecasts, it is unlikely that this confidence would be determined from the sources of variations in predictability examined in this project. Instead, in a changing climate, the difference of the current climate for the reference climatological climate dictates both the prediction and, probably, the confidence (Liniger et al., 2007). For instance, seasonal forecasters at the U.K. Met Office have found that their current tendency to never forecast much of a chance of a cold season and to do so with high confidence, has two consequences. First, it means there is little information content in their forecasts. Second, it means that the public often think the Met Office has made a bad forecast when the summer is not unusually hot: people tend to only remember the past few years, and thus they are basing their evaluation on a much more recent — and warmer – reference period. Thus possible implementation and usefulness of forecast uncertainty characterization as evaluated in this project may depend strongly on the framework used for communicating the forecast.

9.3.2 Climate change drivers of hydrological extremes

The analysis of the Okavango floods described in Section 8 reveal that the sensitivity of hydrological systems to climate change may differ markedly in nature from their sensitivity

to interannual variability. While South Africa does experience a stronger variation in temperature during the annual cycle than other parts of Africa, it is still fair to say that hydrological systems in South Africa are moisture-controlled: that is, they are controlled by when, where, and how much precipitation falls, not by temperature variations. However, in the climate change context temperature is changing markedly while rainfall, if changing at all, is changing by a relatively small amount against a large background interannual variability. Already, it seems, the chance of extreme floods may have decreased from past decades due simply to the evaporation from the larger warming. This sensitivity of catchment flows to warming was also found in a much wetter and cooler environment, autumn flooding in England and Wales (Kay et al. 2011), suggesting that it may be a fairly robust characteristic of the climate change impact on hydrological systems. The recognition of an important role of temperature in hydrological systems, thus moving away from the historical seasonal forecasting paradigm, will thus not only be important for climate change impact studies but also for seasonal forecasting itself.

9.3.3 Operational event attribution services

This project continued development of an operational event attribution service. That development to Version 3 involved some modifications arising from experiences from the previous Version 2, most notably a shift from 10 Mm^2 regions to 2 Mm^2 regions, which both are more relevant to many potential users and also tend to more closely reflect the spatial scale of many more notable weather events. The method of using political/economic definitions, based on responses to events, also provides a framework for examining impact events. These regions are being adopted in other studies beyond those in this project.

The Weather Risk Attribution Forecast (WRAF) remains the world's only real-time systematic attribution service and thus has been closely watched by meteorological agencies (such as the U.K. Met Office leading the European Union FP7 EUCLEIA project, and U.S. NOAA) who are considering applying their considerable expertise and skill to implement their own operational services. The WRAF is thus serving as a feasibility study for many. Notably, results from the attribution forecast have proven robust and stable.

There are some aspects of the WRAF though that requires development, beyond standard improvement of climate modeling elements. Most particularly, while professing to consider "weather risk", the WRAF is currently only considering weather probability. Getting to risk and thus making results relevant for most potential users will require two steps. First, results will have to move beyond weather events, to consider "impact events". For instance, we are currently planning on feeding the output from the new HadAM3P-N96 simulations described in Section 6.2.4 through the VIC hydrological model over Africa, thus providing stream flow time series for the analysis of the chance of flooding and low flows. Switching from weather events to hydrological events will require a modified consideration of what constitutes an event: the monthly definitions currently used, which are already questionable for rainfall during the dry season over southern Africa, will not be appropriate for river systems with an annual flood. The second step will require a comparison against other drivers of change, for

instance the effect of land cover change on flooding. Once the various possible drivers in the chance of flooding are considered, it will be possible to characterize the relative importance of anthropogenic emissions (Huggel et al., 2013).

9.3.4 African capacity in the detection and attribution of climate change and climate change impacts

The WRAF is a service developed in Africa which has no equivalent elsewhere in the world, thus there is already some African capacity for event attribution analysis. However, given the potential importance of event attribution for African nations within a prospective "loss and damage" framework for allocation of climate change adaptation funding (Huggel et al., 2013), development of a continental capacity for event attribution analysis that does not depend on foreign generosity is crucial, a point recognized in the conclusions of the Africa Climate Conference in Arusha, Tanzania, in October 2013.

In this light, UCT and the African Center of Meteorological Application for Development (ACMAD) are leading activities to begin building capacity in event attribution analysis. UCT took the first steps with dissemination of its climate model output to 22 African scientists at the African Climate Conference. Current work is focusing on funding a workshop and subsequent fellowships, both with UCT and ACMAD and with several non-African institutions.

9.4 Where we stand after this project

This project explored the possibility for expanding seasonal forecast products in two directions: toward providing additional information about the confidence of the forecast; and toward a separate product assessing the degree to which anthropogenic emissions have affected extreme weather, but which runs in parallel with a seasonal forecast product.

In terms of the first new direction, this project was an exploratory study. While long-term trends in the spread of seasonal forecast simulations, considered a proxy for confidence in this context, were found to potentially be considerable, the development of understanding of the cause if interannual variations was, to some degree, not self-consistent. While the relationship between popular ocean surface predictors and the variations in confidence do not appear to be very strong, there was nevertheless a clear relationship between the pattern of variations in confidence and variations in forecast skill: considering that this modeling system often had low forecast skill, this leaves open the possibility that confidence in the forecast itself may be as or more predictable than the "best estimate" forecast itself. The main next step from this project will be in determining how this confidence information can be effectively included as part of existing seasonal forecast products, with a particular consideration of their communication approaches.

In terms of the second new direction, this project started with an existing "event attribution" product, developing it further and examining patterns in the results. As discussed above, there are two main next steps in this area. The first is to improve and promote communication of

the product within Africa (and beyond), as a cornerstone of capacity development in "event attribution" research. The second is to move the product away from being a purely meteorological product toward one that actually provides information on the attribution of weather risk, including how the anthropogenic contribution to change compares against other drivers of risk; as highlighted in Section 8, hydrological systems would seem to provide the ideal first target in this regard.

10 List of products

10.1 Publications, presentations, and interviews arising from this project

10.1.1 Published and accepted papers

- Angélil, O. 2013. Spatial and temporal influences on human attribution to extreme weather risk: a global study. M.Sc. thesis, ETH Zürich, Zurich, Switzerland, 73pp.
- Wolski, P., D. Stone, M. Tadross, M. Wehner, and B. Hewitson. 2014. Attribution of floods in the Okavango Basin, Southern Africa. Journal of Hydrology, doi:10.1016/j.jhydrol.2014.01.055, accepted.
- Angélil, O., D. A. Stone, M. Tadross, F. Tummon, M. Wehner, and R. Knutti. 2014. Attribution of extreme weather to anthropogenic greenhouse gas emissions: sensitivity to spatial and temporal scales. Geophysical Research Letters, accepted.

10.1.2 Submitted papers

- Lawal, K., D. Stone, T. Aina, C. Rye, and B. Abiodun. 2014. Trends in the potential spread of seasonal forecasts over South Africa. International Journal of Climatology, submitted.
- Lawal, K., D. Stone, B. Abiodun, C. Rye, and T. Aina. 2014. On the relationship between South African seasonal climate predictability and climate indices. Climate Dynamics, submitted.

10.1.3 Papers in preparation

- Cerezo Mota, R., A. Favre, D. Stone, R. Jones, and B. Hewitson. Impacts of land-scheme and integration domains on African precipitation.
- Lawal, K. A. Limits of predictability of the South African seasonal climate. Ph.D. Thesis.
- Stone, D. A., O. Angélil, C. Lennard, M. Tadross, M. F. Wehner, and P. Wolski. Human contribution to extreme monthly weather over South Africa.
- Stone, D. A., C. Lennard, M. Tadross, M. F. Wehner, O. Angélil, M. R. Allen, J. Imbers Quintana, P. A. Stott, and P. Pall. Designing a real-time weather risk attribution forecast system.

10.1.4 Talks

February 2012: Stone, D. A. "Playing through a real-time attribution service: questions and thoughts". International Detection and Attribution Group Meeting, National Center for Atmospheric Research, Boulder, Colorado, United States.

September 2012: Lawal, K. A. "Assessing the predictability of South African seasonal climate using HadRM3P". 5th Annual Science Symposium 2012, 7-8 September, University of Cape Town, Cape Town

September 2012: Lawal, K. A. "Assessing the predictability of South African seasonal climate using HadRM3P". The Annual Conference of the South African Society of Atmospheric Sciences, 26-27 September, Cape Town

November 2012: Lawal, K. A. "Assessing the predictability of South African seasonal climate using HadRM3P ensemble spreads". National Global Change Conference, 26-28 November, Boksburg

September 2012: Lawal, K. "Assessing the predictability of seasonal climates over South Africa using HadRM3P". University of Cape Town's Science Postgraduate Students Council 5th Annual Science Symposium 2012, University of Cape Town, Cape Town.

October 2012: Lawal, K. "Assessing the influences of extreme climatic events on the predictability of South African seasonal climates". SATREPS Symposium on Prediction of Climate Variations and its Application in the Southern African Region, CSIR International Conference Center, Pretoria.

March 2013: Stone, D. "First contributions to the C20C Detection and Attribution Project". Climate 2013, Lawrence Berkeley National Laboratory, Berkeley, California, United States.

May 2013: Lawal, K. "Investigating the variations in the predictability of South African seasonal climates through HadRM3P ensemble spreads". International Conference on Seasonal to Decadal Prediction, Toulouse, France.

June 2013: Stone, D. "First contributions to the C20C Detection and Attribution Project". 12th International Meeting on Statistical Climatology, Jeju, South Korea.

June 2013: Wolski, P. "Sensitivity of extreme rainfall events in Africa attributable to anthropogenic radiative and SST forcing". 12th International Meeting on Statistical Climatology, Jeju, South Korea.

October 2013: Lawal, K. "On the relationship between South African seasonal climate predictability and climate indices". Africa Climate Conference, Arusha, Tanzania.

October 2013: Stone, D. "The weather risk attribution forecast for Africa for October 2013". Africa Climate Conference, Arusha, Tanzania.

November 2013: Stone, D. "First contributions to the C20C Detection and Attribution Project". 6th Workshop of the International CLIVAR Climate of the 20th Century Project, Melbourne, Australia.

December 2013: Stone, D. "First contributions to the C20C+ Detection and Attribution Project". Fall Meeting of the American Geophysical Union, San Francisco, United States.

10.1.5 Posters

August 2012: Lawal, K. A. "The limit of predictability of South African seasonal climates: assessing the predictability of South African seasonal climate using HadRM3P". The workshop on Dynamics and Predictability of High-impact Weather and Climate Events, 6-9 August, Kunming, China

September 2012: Stone, D. "The weather risk attribution forecast for September 2012". Attribution of Climate and Weather Extremes: Assessing, Anticipating and Communicating Climate Risks, Oxford, United Kingdom.

September 2012: Wolski, P. "Attribution of floods in the Okavango Delta, Botswana". Attribution of Climate and Weather Extremes: Assessing, Anticipating and Communicating Climate Risks, Oxford, United Kingdom.

November 2012: Lawal, K. "Assessing the predictability of South African seasonal climate using HadRM3P ensemble spreads". National Global Change Conference, Boksburg.

December 2012: Stone, D. "The weather risk attribution forecast for December 2012". Attribution of Climate and Weather Extremes: Assessing, Anticipating and Communicating Climate Risks, Oxford, United Kingdom.

December 2012: Wehner, M. "First contributions to the Climate of the 20th Century Detection and Attribution Project". American Geophysical Union's Fall Meeting, San Francisco, California, United States.

April 2013: Lawal, K. "Assessing the variations in the predictability of South African seasonal climate with HadRM3P ensemble spreads". European Geophysical Union General Assembly, Vienna, Austria.

June 2013: Lawal, K. "Investigating the trends in the potential spread of seasonal predictability over South Africa provinces". 12th International Meeting on Statistical Climatology, Jeju, South Korea.

June 2013: Stone, D. "The weather risk attribution forecast for July 2013". 12th International Meeting on Statistical Climatology, Jeju, South Korea.

October 2013: Lawal, K. "On the relationship between South African seasonal climate predictability and climate indices". African Climate Conference, Arusha, Tanzania.

10.1.6 Interviews

February 2012: The Weather Risk Attribution Forecast being operated and studied in this project was featured in the article "Is this climate change?" in NCAR/UCAR's AtmosNews (https://www2.ucar.edu/atmosnews/attribution/attribution-demand).

November 2012: The Weather Risk Attribution Forecast being operated and studied in this project was featured and quoted in the article "Extremely bad weather" in ScienceNews (https://www.sciencenews.org/article/extremely-bad-weather).

June 2013: The Weather Risk Attribution Forecast being operated and studied in this project was featured and quoted in the article "Deadly heat waves intensify as summers sizzle" in livescience (http://www.livescience.com/37292-heat-waves.html).

10.2 Data and results arising from this project

- Output from climate model simulations performed under this project have been published on the Earth System Grid Federation under project "c20c" (http://portal.nersc.gov) and are freely accessible. The list of simulations is given at http://portal.nersc.gov/c20c/output_data/UCT-CSAG_HadAM3P-N96.pdf
- Output from climate model simulations performed under this project were distributed by USB stick to 22 African (including South African) researchers at the African Climate Conference, Arusha, Tanzania, October 2013.
- Monthly event attribution assessments performed under this project are posted on the Weather Risk Attribution Forecast (http://www.csag.uct.ac.za/daithi/forecast).

10.3 Input to international activities

- Experience from this project informed the assessment of the attribution of climate change risk in the upcoming Fifth Assessment Report of Working Group II of the Intergovernmental Panel on Climate Change, due for publication in March 2013.
- Experience in systematic event attribution developed through this project have informed event attribution plans of:
  - The International Detection and Attribution Group (see talks and posters listed in Section 10.1)
  - The Attribution of Climate-related Events activity (see talks and posters listed in Section 10.1)
  - The European Union FP7 EUCLEIA project, for which a member of this project is a scientific consultant
  - The U.S. Department of Energy CASCADE project
- The experimental design of the weather risk attribution system further developed and operated within this project has formed the basis for the experimental design of the World Climate Research Programme's International CLIVAR C20C+ Detection and Attribution Project.
- UCT is collaborating with other institutions throughout Africa, particularly the African Center of Meteorological Application for Development (ACMAD), to develop a continental event attribution activity, with a large focus on capacity development.

10.4 Student participation in the project

Two students were involved in aspects of this project.

- K. A. Lawal was fully funded from this project and lead the research on the "limits of predictability" component described in Sections 3, 4, and 5. He has two papers currently submitted to peer-reviewed journals, and has presented 8 talks and 5 posters at national and international meetings.
- O. Angélil, an M.Sc. student at ETH Zürich, Switzerland, was not funded by this project. However, his interaction with the project is notable in two respects. First, he is a South African citizen. Second, he analyzed the HadAM3P-N96 simulations generated under this project in collaboration with members of this project, and his analyses have had strong impacts on the event attribution analyses reported in Section 6 and 7. He has a successful M.Sc. thesis and one peer-reviewed paper in press describing these analyses.

Publications cited in this report

Allen MR and Stott PA. (2003) Estimating signal amplitudes in optical fingerprinting, part I: theory. Clim. Dyn., 21, 477-491.

Andersson L, Wilk J, Todd M, Hughes D, Earle A, Kniveton D, Layberry R and Savenije H. (2006) Impact of climate change and development scenarios on flow patterns in the Okavango River. J. Hydrol., 331, 43-57.

Annamalai H, Xie S-P, McCreary J-P and Murtugudde R. (2005) Impacts of Indian Ocean sea surface temperature on developing El Niño. J. Climate, 18, 302-319.

Boer G. (2000) A study of atmosphere-ocean predictability on long time scales. Clim. Dyn., 15, 419-434.

Browne NAK. (2011) Model evaluation for seasonal forecasting over Southern Africa, Ph.D. thesis, University of Cape Town.

Browne NAK, Abiodun B and Tadross M. (2011) Seasonal climate forecasting over southern Africa: evaluation of GCMs in simulating the inter-annual variability and impacts of SST. Int. J. Climatol., submitted.

Buckland ST. (1983) Monte-Carlo methods for confidence interval estimation using the bootstrap technique. Bulletin Applied Statistics, 10, 194-212.

Buckle C. (1996) Weather and climate in Africa, Longman, Malaysia.

Buhlmann P. (2002) Bootstraps for time series. Statistical Science, 17, 52-72.

Cerezo-Mota R, Favre A, Stone D, Jones R and Hewitson B. (2014) Impacts of land-scheme and integration domains on African precipitation. In preparation.

Enfield DB, Mestas-Nuñez AM, Mayer DA and Cid-Serrano L. (1999) How ubiquitous is the dipole relationship in tropical Atlantic sea surface temperatures? J. Geophys. Res. Oceans, 104, 7841-7848.

Essery RLH, Best MJ, Betts RA and Cox PM. (2001) Explicit representation of subgrid heterogeneity in a GCM land surface scheme. J. of Hydrometeorology, 4, 530-543.

Fauchereau N, Pohl B, Reason CJC, Rouault M and Richard Y. (2009) Recurrent daily OLR patterns in the southern Africa/southwest Indian Ocean region, implications for South African rainfall and teleconnections. Clim. Dyn., 32, 575-591.

Friederichs P and Paeth H. (2006) Seasonal prediction of African precipitation with ECHAM4-T42 ensemble simulations using a multivariate MOS re-calibration scheme. Clim. Dyn., 27, 761-786.

Giorgi F, Jones C and Asrar RG. (2009) Addressing climate information needs at the regional level: the CORDEX framework. WMO Bull., 58, 175-183.

González-Miranda JM. (1997) Predictability in the Lorenz low-order general atmospheric circulation model. Phys. Lett., 233A, 347-354.

Grimit EP and Mass CF. (2007) Measuring the ensemble spread-error relationship with a probabilistic approach: Stochastic ensemble results. Mon. Wea. Rev., 135-, 203-221.

Hargreaves GH and Samani ZA. (1985) Reference crop evapotranspiration from temperature. Appl. Eng. Agric., 1, 96-99.

Hegerl GC, Zwiers FW, Braconnot P, Gillett NP, Luo Y, Marengo-Orsini JA, Nicholls N, Penner JE, Stott PA and others. (2007) Understanding and attributing climate change, Climate Change 2007: The Physical Science Basis. Contribution of Working Group I to the Fourth Assessment Report of the Intergovernmental Panel on Climate Change, S. Solomon, D. Qin, M. Manning, Z. Chen, M. Marquis, K. B. Averyt, M. Tignor, and H. L. Miller, eds., Cambridge University Press, Cambridge, U.K., 663-745.

Hewitson BC and Crane RG. (2006) Consensus between GCM climate change projections with empirical downscaling: precipitation downscaling over South Africa. Int. J. Climatol., 26, 1315-1337.

Hoffman MT, Cramer MD, Gillson L and Wallace M. (2011) Pan evaporation and wind run decline in the Cape Floristic Region of South Africa (1974-2005): implications for vegetation responses to climate change. Clim. Change, in press.

Houghton JT. (1991) The physics of atmospheres, 2nd edition, Cambridge University Press, London.

Huggel C, Stone D, Auffhammer M and Hansen G. (2013) Loss and damage attribution. Nature Climate Change, 3, 694-696.

Hughes DA and Kingston DG. (2011) Uncertainty in water resources availability in the Okavango River Basin as a result of climate change. Hydrol. Earth Syst. Sci. Discuss., 15, 931-941.

Izumo T, Vialard J, Lengaigne M, de Boyer Montegut C, Behera SK, Luo J-J, Cravatte S, Masson S and Yamagata T. (2010) Influence of the state of the Indian Ocean Dipole on the following year's El Niño. Nature Geoscience, 3, 168-172.

Johnson RW. (2001) An introduction to the bootstrap. Teaching Statistics, 23(2), 49-54.

Johnston PA, Archer ERM, Vogel CH, Bezuidenhout CN, Tennant WJ and Kuschke R. (2004) Review of seasonal forecasting in South Africa: producer to end-user. Clim. Res., 28, 67-82.

Jones RG, Noguer M, Hassell DC, Hudson D, Wilson SS, Jenkins GJ and Mitchell JFB. (2004) Generating high resolution climate change scenarios using PRECIS, Technical report, Met Office Hadley Centre, Exeter, U. K., 40pp.

Jury M. (2012) A return to wet conditions over Africa: 1995-2010. Theoretical and Applied Climatology, 111, 471-481.

Kalnay E, Kanamitsu M, Kistler R, Collins W, Deaven D, Gandin L, Iredell M, Saha S, White G, Woollen J, Zhu Y, Leetmaa A, Reynolds R, Chelliah M, Ebisuzaki W, Higgins W, Janowiak J, Mo KC, Ropelewski C, Wang J, Jenne R and Joseph D. (1996) The NCEP/NCAR 40-year reanalysis project. Bull. Amer. Meteor. Soc., 77, 437-471.

Kanamitsu M, Ebisuzaki W, Woollen J, Yang SK, Hnilo JJ, Fiorino M and Potter GL. (2002) NCEP-DOE AMIP-II Reanalysis (R-2). Bull. Amer. Meteor. Soc., 83, 1631-1643.

Kaplan A, Cane M, Kushnir Y, Clement A, Blumenthal M and Rajagopalan B. (1998) Analyses of global sea surface temperature 1856-1991. J. Geophys. Res., 103, 18567-18589.

Kay AL, Crooks SM, Pall P and Stone DA. (2011) Attribution of Autumn/Winter 2000 flood risk in England to anthropogenic climate change: a catchment-based study. J. Hydrol., 406, 97-112.

Keenlyside NS, Latif M, Jungclaus J, Kornblueh L and Roeckner E. (2008) Advancing decadal-scale climate prediction in the North Atlantic sector. Nature, 453, 84-88.

Kinter J and Folland C. (2011) The International CLIVAR Climate of the 20th Century Project: Report of the Fifth Workshop. CLIVAR Exchanges, 16, 39-42.

Kumar A, Barnston AB, Peng P, Hoerling MP and Goddard L. (2000) Changes in the spread of the variability of the seasonal mean atmospheric states associated with ENSO. J. Climate, 13, 3139-3151.

Kumar A, Schubert SD and Suarez MS. (2003) Variability and predictability of 200mb seasonal mean heights during summer and winter. J. Geophys Res., 108.

Landman WA and Beraki A. (2010) Multi-model forecast skill for mid-summer rainfall over southern Africa. Int. J. Climatol., 32, 303-314.

Landman WA, Botes S, Goddard L and Shongwe M. (2005) Assessing the predictability of extreme rainfall over southern Africa. Geophys. Res. Lett., 32.

Landman WA and Goddard L. (2005) Predicting southern African summer rainfall using a combination of MOS and perfect prognosis. Geophys. Res. Lett., 32.

Lawal KA, Stone DA, Abiodun BJ, Rye C and Aina T. (2014a) On the relationship between South African seasonal climate predictability and climate indices. Clim. Dyn., submitted.

Lawal KA, Stone DA, Aina T, Rye C and Abiodun BJ. (2014b) Trends in the potential spread of seasonal forecasts over South Africa. Int. J. Climatol., submitted.

Li J and Ding R. (2011) Temporal-spatial distribution of atmospheric predictability limit by local dynamical analogs. Mon. Wea. Rev., 139, 3265-3283.

Liniger MA, Mathis H, Appenzeller C and Doblas-Reyes FJ. (2007) Realistic greenhouse gas forcing and seasonal forecasts. Geophys. Res. Lett., 34.

Lorenz EN. (1975) The physical bases of climate and climate modeling. Climate Predictability, GARP Publication Series, 16, 132-136.

Luo J, Behera SK, Masumoto Y and Yamagata T. (2011) Impact of global ocean surface warming on seasonal-to-interannual climate prediction. J. Climate, 24, 1626-1646.

Luo J, Masson S, Behera S, Shingu S and Yamagata T. (2005) Seasonal climate predictability in a coupled OAGCM using a different approach for ensemble forecasts. J. Climate, 18, 4474-4497.

Luo J, Masson S, Behera S and Yamagata T. (2007) Experimental forecasts of the Indian Ocean dipole using a coupled OAGCM. J. Climate, 20, 2178-2190.

Luo J. (2008) Extended ENSO predictions using a fully coupled ocean-atmosphere model. J. Climate, 21, 84-93.

Maraun D, Wetterhall F, Ireson Am, Chandler RE, Kendon EJ, Widmann M, Brienen S, Rust HW, Sauter T, Themeß M, Venema VKC, Chun KP, Goodess CM, Jones RG, Onof C, Vrac M and Thiele-Eich I. (2010) Precipitation downscaling under climate change: recent developments to bridge the gap between dynamical models and the end user. Rev. Geophys., 48, RG3003.

McCarthy TS, Cooper GRJ, Tyson PD and Ellery WN. (2000). Seasonal flooding in the Okavango Delta, Botswana — recent history and future prospects. S. Afr. J. Sci., 96, 25-33.

Meehl GA, Covey C, Delworth T, Latif M, McAvaney B, Mitchell JFB, Stouffer RJ and Taylor KE. (2007) The WCRP CMIP3 multimodel dataset: A new era in climate change research. Bull. Amer. Meteor. Soc., 88, 1383-1394.

Mitchell TD and Jones PD. (2005) An improved method of constructing a database of monthly climate observations and associated high resolution grids. Int. J. Climatol., 25, 693-712.

Molteni F, Buzzia R and Palmer TN. (1996) The ECMWF ensemble prediction system: methodology and validation. Q. J. R. Meteorol. Soc., 122, 73-119.

Murphy AH. (1988a) Skill score on the mean square error and their relationship to the correlation coefficient. Mon. Wea. Rev., 116, 2417-2424.

Murphy JM. (1988b) The impact of ensemble forecasts on predictability. Q. J. R. Meteorol. Soc., 114, 463-493.

Nester T, Komma J, Viglione A and Bloschl G. (2012) Flood forecast errors and ensemble spread — a case study. Water Resource Research, 48.

Nikulin G, Jones C, Giorgi F, Asrar G, Büchner M, Cerezo-Mota R, Christensen OB, Déqué M, Fernandez J, Hänsler A, van Meijgaard E, Samuelsson P, Sylla MB and Sushama L. (2012) Precipitation climatology in an ensemble of CORDEX-Africa regional climate simulations. J. Climate, 25, 6057-6078.

Pall P, Aina T, Stone DA, Stott PA, Nozawa T, Hilberts AGJ, Lohmann D and Allen MR. (2011) Anthropogenic greenhouse gas contribution to flood risk in England and Wales in Autumn 2000. Nature, 470, 382-385.

Parker DE, Jones PD, Folland CK and Bevan A. (1994) Inter-decadal changes of surface temperature since the late nineteenth century. J. Geophys. Res., 99, 373-399.

Pennell C and Reichler T. (2010) On the effective number of climate models. J. Climate, 24, 2358-2367.

Pielke RA, Matsui T, Leoncini G, Nobis T, Nair US, Lu E, Eastman J, Kumar S, Peters-Lidard CD, Tian Y and Walko RL. (2006) A new paradigm for parameterizations in numerical weather prediction and other atmospheric models. National Weather Digest , 30, 93-99.

Pope VD, Gallani M, Rowntree PR and Stratton RA. (2000) The impact of new physical parametrizations in the Hadley Centre climate model – HadAM3. Clim. Dyn., 16, 123-146.

Power S, Delage F, Chung C, Kociuba G and Keay K. (2013) Robust twenty-first-century projections of El Niño and related precipitation variability. Nature.

Rasmusson EG and Carpenter TH. (1982) Variations in the tropical sea surface temperature and surface wind fields associated with the Southern Oscillation / El Niño. Mon. Wea. Rev., 110, 354-384.

Rayner NA, Brohan P, Parker DE, Folland CK, Kennedy JJ, Vanicek M, Ansell T and Tett SFB. (2006) Improved analyses of changes and uncertainties in sea surface temperature measured in situ since the mid-nineteenth century: the HadSST2 data set. J. Climate, 19, 446-469.

Rayner NA, Parker DE, Horton EB, Folland CK, Alexander LV, Rowell DP, Kent EC and Kaplan A. (2003) Global analyses of sea surface temperature, sea ice, and night marine air temperature since the late nineteenth century. J. Geophys. Res., 108.

Reason CJC, Allan RJ, Lindesay JA and Ansell TJ. (2000) ENSO and climatic signals across the Indian Ocean Basin in the global context: Part I, inter-annual composite patterns. Int. J. Climatol., 20, 1285-1327.

Reason CJC and Jagadheesha D. (2005) A model investigation of recent ENSO impacts over southern Africa. Africa. Meteor. Atmos. Phys., 89, 181-205.

Reichler T and Roads JO. (2004) Time-space distribution of long-range atmospheric predictability. J. Atmos. Sci., 61, 249-263.

Reynolds RW, Rayner NA, Smith TM, Stokes DC and Wang WC. (2002) An improved in situ and satellite SST analysis for climate. J. Clim., 15, 1609-1625.

Reynolds RW and Smith TM. (1994) Improved global sea surface temperature analysis using optimum interpolation. J. Climate, 7, 929-948.

Rotunno R and Synder C. (20080 A generalization of Lorenz's model for the predictability of flows with many scales of motion. J. Atmos. Sci., 65, 1063-1076.

Rowell DP. (1998) Assessing potential seasonal predictability with an ensemble of multi-decadal GCM simulations. J. Climate, 11, 109-120.

Rudolf B, Becker A, Schneider U, Meyer-Christoffer A and Ziese M. (2010) On the most recent gridded global data set issued in fall 2010 by the Global Precipitation Climatology Centre (GPCC), Technical report, GPCC Status Report.

Stephenson DB and Doblas-Reyes FJ. (2000) Statistical methods for interpreting Monte-Carlo ensemble forecasts. Tellus, 52A, 300-322.

Stone DA. (2014) Boundary conditions for the C20C+ Detection and Attribution Project: the All-Hist/est1 and Nat-Hist/CMIP5-est1 scenarios, Technical report, Lawrence Berkeley National Laboratory.
http://portal.nersc.gov/c20c/input_data/C20C-DandA_dSSTs_All-Hist-est1_Nat-Hist-CMIP5-est1.pdf.

Stone DA and Allen MR. (2005) The end-to-end attribution problem: From emissions to impacts. Clim. Change, 71, 303-318.

Stott PA, Allen MR, Christidis N, Dole R, Hoerling M, Huntingford C, Pall P, Perlwitz J and Stone DA. (2013) Attribution of weather and climate-related extreme events, Climate Science for Serving Society: Research, Modeling and Prediction Priorities, G. R. Asrar and J. W. Hurrell, eds., Springer, 307-337.

Stott PA, Allen MR and Jones GS. (2003) Estimating signal amplitudes in optimal fingerprinting. Part II: application to general circulation models. Clim. Dyn., 21, 493-500.

Stott PA, Gillett NP, Hegerl GC, Karoly DJ, Stone DA, Zhang X and Zwiers F. (2010) Detection and attribution of climate change: a regional perspective. Wiley Interdisciplinary Reviews: Climate Change, 1, 192-211.

Stott PA, Mitchell JFB, Allen MR, Delworth TL, Gregory JM, Meehl GA and Santer BD. (2006) Observational constrains on past attributable warming and predictions of future global warming. J. Climate, 19, 3055-3069.

Stott PA, Stone DA and Allen MR. (2004) Human contribution to the European heatwave of 2003. Nature, 432, 610-614.

Straus DM and Shukla J. (2005) The known, the unknown and the unknowable in the predictability of weather, Technical Report 175, Center for Ocean-Land-Atmosphere Studies, 20pp.

Sylla MB, Giorgi F and Stordal F. (2012) Large-scale origins of rainfall and temperature bias in high-resolution simulations over southern Africa. Clim. Res., 52, 193-211.

Tang Y, Lin H and Moore AM. (2008) Measuring the potential predictability of ensemble climate predictions. J. Geophys. Res., 113.

Taylor KE, Stouffer RJ and Meehl GA. (2012) An overview of CMIP5 and the experiment design. Bull. Amer. Met. Soc., 93, 485-498.

Thompson DWJ and Wallace JM. (2000) Annular modes in the extratropical circulation. Part I: Month-to-month variability. J. Climate, 13, 1000-1016.

Tippett MK, Kleeman R and Tang Y. (2004) Measuring the potential utility of seasonal climate predictions. Geophys. Res. Lett., 31.

Tyson PD, Cooper GRJ and McCarthy TS. (2002) Millennial to multi-decadal variability in the climate of southern Africa. Int. J. Climatol., 22, 1105-1117.

Tyson PD and Preston-Whyte RA. (2000) The weather and climate of Southern Africa, 2nd edition, Oxford University Press South Africa, Cape Town.

Whitaker JS, and Loughe AF. (1998) The relationship between ensemble spread and ensemble mean skill. Mon. Wea. Rev., 126, 3292-3302.

Wilk J, Kniveton D, Andersson L, Layberry R, Todd M, Hughes D, Ringrose S and Vanderpost C. (2006) Estimating rainfall and water balance over the Okavango river basin for hydrological applications. J. Hydrol., 331, 18-29.

Wilks DS. (1995) Statistical methods in atmospheric sciences: an introduction, Geophys. Series, second edition, Academic Press Inc., California, 254-275.

Williams CJR, Kniveton DR and Layberry R. (2008) Influence of South Atlantic sea surface temperatures on rainfall variability and extremes over southern Africa. J. Climate, 21, 6498-6520.

Willmott CJ and Matsuura K. (19950 Smart interpolation of annually averaged air temperature in the United States. J. Appl. Meter., 34, 2577-2586.

Wilson D. (2000) The impact of a physically based microphysical scheme on the climate simulation of the meteorological office unified model. Q. J. R. Meteorol. Soc., 126, 1281-1300.

Wolski P. (2009) Assessment of hydrological effects of climate change in the Okavango Basin, Okavango Basin Transboundary Diagnostic Analysis Report , OKACOM, Maun, Botswana.

Wolski P, Coop L, Tadross M and Hewitson B. (2012a) Applicability of TRMM and RFE satellite rainfall products for statistical downscaling of GCM rainfall projections in Africa, Thirteenth WaterNet/WARFSA/GWP-SA International Symposium on Integrated Water Resource Management , 31 October-2 November 2012, Johannesburg, South Africa.

Wolski P, Stone D, Tadross M, Wehner M and Hewitson B. (2014) Attribution of floods in the Okavango Basin, Southern Africa. J. Hydrol., 511, 350-358.

Wolski P, Todd M, Murray-Hudson MA and Tadross M. (2012b) Multidecadal variability in hydro-climate of Okavango river system, southwest Africa, in the past and under changing climate. J. Hydrol., 475, 294-305.

Wolter K and Timlin MS. (2011) El/Niño Southern Oscillation behavior since 1871 as diagnosed in an extended multivariate ENSO index. Int. J. Climatol., 31, 1074-1087.

Zwiers FW. (1996) Interannual variability and predictability in an ensemble of AMIP climate simulations conducted with the CCC GCM2. Clim. Dyn., 12, 825-847.